Department of Precision and Microsystems Engineering

3D-printed multifunctional microfluidic AFM cantilever

Gijs van der Gugten

Report no : 2023.046
Coach : dr. M. K. Ghatkesar
: dr. ir. V. U. Shastri
: dr. W. M. van Weerden
: dr. F. Linke
Professor : dr. M. K. Ghatkesar
Specialisation : Micro and Nano Engineering
Type of report : Masters Thesis
Date : July 6th, 2023

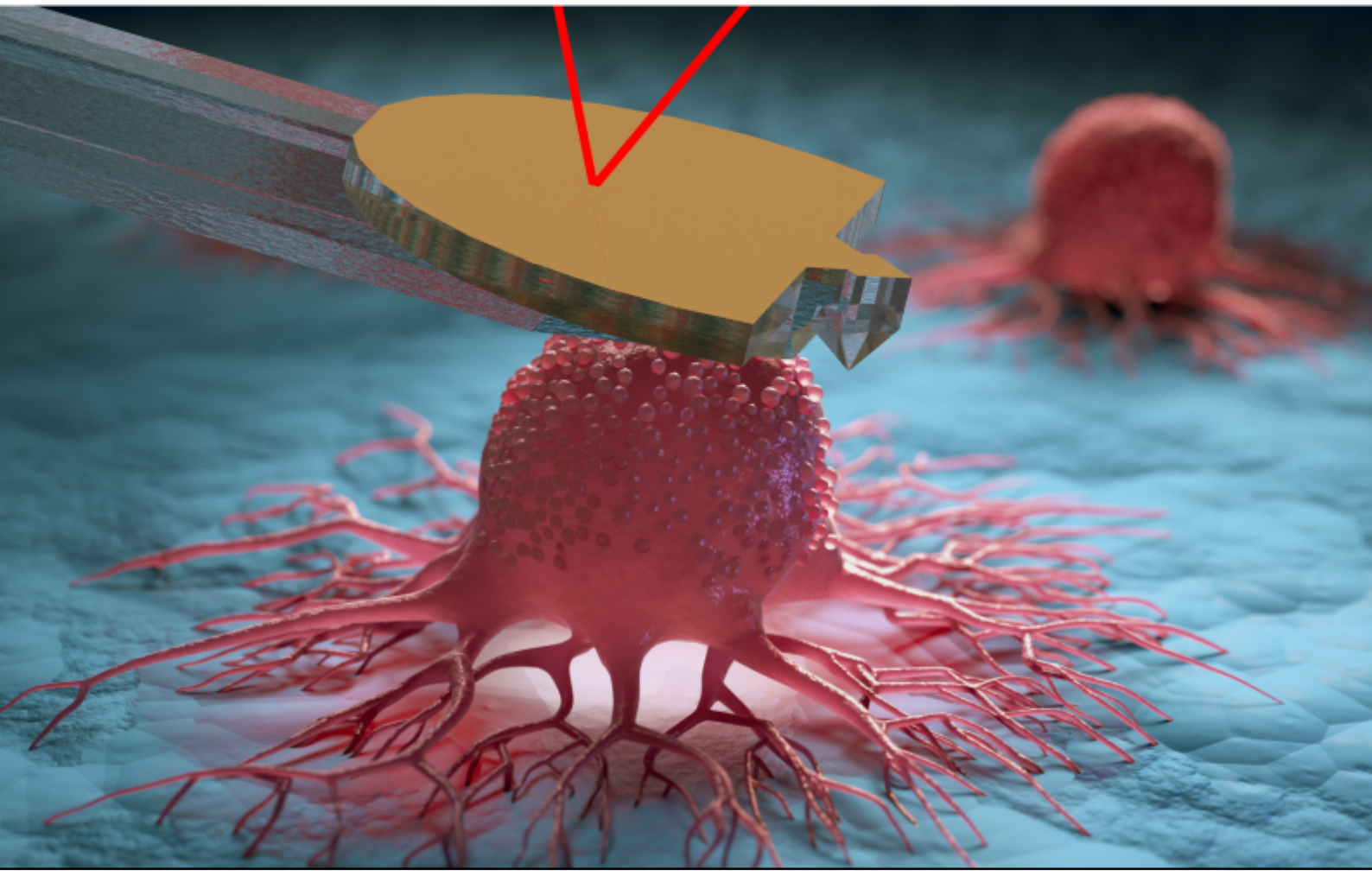

TU Delft Delft University of Technology

Challenge the future

3D-printed multifunctional microfluidic AFM cantilever

Gijs van der Gugten

to obtain the degree of Master of Science
Delft University of Technology,
to be defended publicly on Thursday July 20, 2023 at 10:00 AM.

Student number:	4163079		
Project duration:	February, 2022 – July, 2023		
Supervisors:	dr. M. K. Ghatkesar,	TU Delft,	Supervisor
	dr. ir. V. U. Shastri,	TU Delft,	Daily Supervisor
Collaborators:	dr. W. van Weerden,	Erasmus MC	
	dr. F. Linke,	Erasmus MC	
External:	dr. P. Boukany,	TU Delft	

TU Delft

Preface

Over the past year, I had the opportunity to work on a very interesting project with many facets. Throughout this journey, I acquired a wealth of knowledge in biology, fabrication techniques, and research in general. Learning about biology opened up an entirely new world for me. Although the project did not go as smoothly as I envisioned a year ago, I am immensely happy with and proud of our accomplishments.

I extend my gratitude to Murali, for giving me this opportunity and whose guidance and knowledge have been instrumental in shaping my understanding. I want to thank Vijay for his help and guidance, always making himself available to address my questions and problems. I would also like to thank our collaborators, Franziska and Wytske, from the Erasmus MC, for providing us engineers with their insights into the world of biology and facilitating our access to cells for experimentation. Additionally, I am grateful to the other lab members for their insights and perspectives. Pieter, for letting me draw upon his experience with 3D-printed cantilevers. I appreciate Ayman's contribution to the project by creating the hydrogel samples. Thanks to the technicians Gideon, Patrick, Spiridon and Rob for instructing me to use the tools and helping me find solutions to my technical problems.

I would also like to express my gratitude to my parents, Joan and Jacob for their patience and support. Lastly, my love goes to my girlfriend Hessel for her unwavering presence and support throughout this journey.

Gijs van der Gugten
Delft, July 2023

Abstract

Much research is conducted on the biomechanical properties of cells, particularly in cancer research. Cell stiffness and cell adhesion are two properties often studied, because they are important for the functioning of a cell. To study these properties, atomic force microscopy(AFM) is often used, using nanoindentation for stiffness analysis and fluid force microscopy(FluidFM) for adhesion analysis. However, these techniques often involve different cantilever probes, which complicates the measurement of both properties in a single cell. To make it possible to study cell stiffness and cell adhesion of a single cell, a multifunctional microfluidic AFM cantilever is developed in this research. This cantilever is equipped with a blunted pyramid-shaped tip for nanoindentation enabling the measurement of cell stiffness and imaging. Moreover, it features a channel running through its length, with an aperture on the tip, facilitating fluid force microscopy for determining cell adhesion. The multifunctional cantilever is fabricated using a multiscale 3d-printing technique, where stereo lithography is used for the larger parts, and two-photon polymerisation is used for the cantilever.

To demonstrate the capabilities of the cantilever, tests are conducted on various substrates. Nanoindentation is demonstrated on PDMS, hydrogel and endothelial cells to determine the Young's modulus of these materials. Fluid force microscopy is showcased by examining prostate cancer cells (PCA-3), removing the cells from the substrate while measuring the adhesion forces. The imaging capabilities of the cantilever were also demonstrated by generating a height map and a Young's modulus map through quantitative imaging of a hydrogel spheroid. This research shows that combining the properties of nanoindentation and FluidFM cantilevers into a single cantilever is possible. Integrating these functionalities into a single cantilever makes doing more mechanical measurements on a single cell possible.

Contents

Introduction

Investigating the mechanical properties of cells holds immense importance in biomedical research. Particularly in understanding diseases such as cancer. However, studying the mechanical properties of cells presents significant challenges, especially when it comes to analysing single cells. Traditional methods often struggle to provide comprehensive data on various mechanical properties in a single experiment, thereby limiting our understanding of cell behaviour. To address this need for better research methods, this report introduces the development of an Atomic Force Microscopy (AFM) cantilever specifically designed to investigate multiple mechanical properties of cells in a single experimental setup.

The report is split into three parts, the literature, the paper and the appendix. Part I. The literature, is a condensed version of the literature study conducted earlier this year. It provides background information on biology, measurement techniques for mechanobiological research and on atomic force microscopy in biological settings. Part II. The project, consist of the main research done in this study, it is written in the style of a scientific paper. It shows the process of designing fabricating and characterizing a multifunctional AFM cantilever. Part III. The appendix holds more measurements background information and a more extensive explanation of the fabrication methods used.

I

Literature

1

Biological background

1.1. Cells

All living things are built up of cells, some of single cells like bacteria and some of trillions of cells like humans [1]. There are many types of cells with many different functions, from bone to brain cells. Animals and plants are made up of cells called eukaryotic cells; these are cells with a nucleus. Cells are made up of several parts called organelles some of which can be seen in Figure 1.1. All organelles have their own functions in the cell. The organelles focused on in this literature survey are the *Nucleus*, the *Cytoplasm*, *Cytoskeleton* and, the *Cell Membrane*, there will also be information on the *Extracellular Matrix(ECM)*.

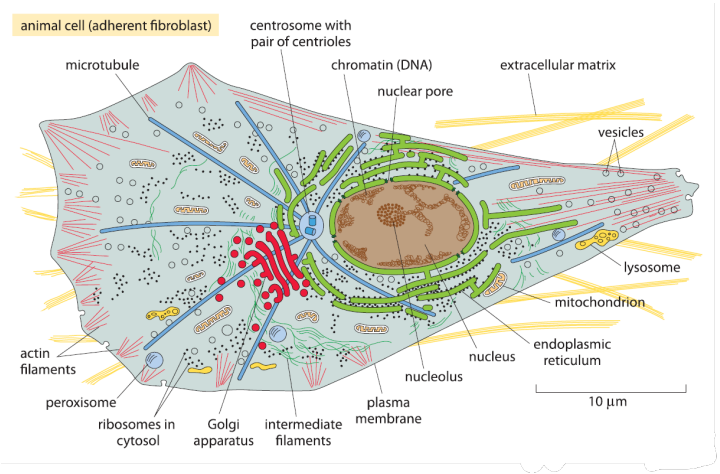

Figure 1.1: An image of an animal cell with all parts labelled [1]

- **Nucleus:** The cell nucleus is the cell's brain. The nucleus is a spherical organelle often found in the middle of a cell. The Nucleus is the part of the cell where DNA is store. Thee DNA holds all genomic information of the cell, all hereditary information is stored in the DNA [2]. Cells normally contain one Nucleus, often containing multiple copies of other organelles. It holds all information necessary for the growth and reproduction of the cells. The DNA is divided into genes, small parts of the DNA that describe specific functions of the cell.
- **Cytoplasm:** The cytoplasm is a gel-like substance which fills space in the cell outside the nucleus and inside the cell membrane. All organelles are inside the cytoplasm. The cytoplasm makes up most of the volume of a cell. Inside the cytoplasm is the cytoskeleton.
- **Cytoskeleton:** The cytoskeleton gives the cell its shape and physical properties, like stiffness and elasticity. It enables cells to maintain their shape and mechanical strength [3]. It is also part of

cell functions such as cell division and cell movement. The cytoskeleton is made of three groups of fibrous proteins, microtubules, actin filaments, and intermediate filaments.

- **Cell Membrane:** The cell membrane is the cell's outer layer. It divides the cytoplasm from the outside environment. The membrane consists of a lipid bilayer and several proteins which help with transportation and communication between the inside and outside of the cell. The cell membrane is also important for cell adhesion. On the surface of the cell membrane are focal adhesion points. These are points which the cell uses to attach itself to other cells of the ECM.
- **Extracellular matrix:** The extracellular matrix is a structure outside of the cells, giving the tissue its stiffness. Cells are attached to the ECM at multiple points called focal adhesion points.The ECM is made up of a set of proteins and minerals, like collagen and enzymes. There are two broad classes of ECM: basement membrane and interstitial matrix. Basement membranes are thin structures that provide a flat substrate onto which cells such as epithelial and endothelial cells adhere [3]. Interstitial matrices are 3d fibrous scaffolds which fill the space between cells [3]. The properties of the ECM depend on the type of tissue it is a part of. Cells connected to the ECM can change its properties. They can add or remove parts of the ECM or change the chemical composition [4]. How the ECM is affected depends on the type of cell. The ECM interacts with cells to regulate diverse functions, including proliferation, migration and differentiation [5]. Illnesses like cancer can also change the structure of the ECM.

1.1.1. Mechanobiology

Mechanobiology is the study of the effects of external physical forces on the development of cells [6]. Historically cell research has been focused on the chemical composition and interactions of cells. Over the last two decades, the importance of mechanical stimuli on cell development has become clearer. Mainly because new techniques to measure and apply forces on the cellular level have become available. These measurement techniques are discussed in chapter 2. Physical stimuli can result in multiple cell responses; examples are: changes in *cell adhesion*, *stiffness* or *differentiation*, these and more examples are shown in Figure 1.2a.

Cells actively sense the stiffness of their extracellular environment by exerting traction forces with

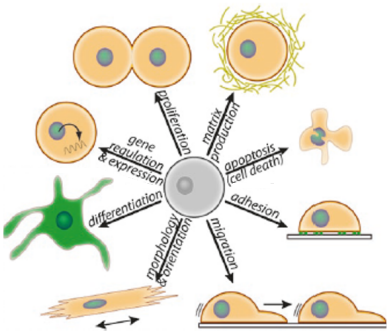

(a) Possible cell responses causes by physical stimuli [7]

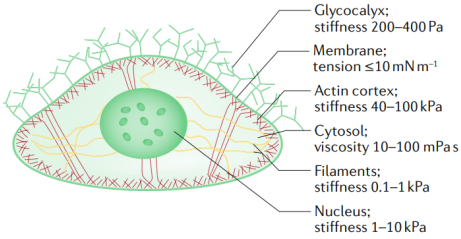

(b) Cell stiffness throughout the cell [8]

integrins [3]. This process of sensing mechanical signals and translating them to a cellular response is called *mechanosensing*. Integrins are proteins that pierce the cell membrane; they can signal two ways from the outside of the cell inward and from the inside out. Many fundamental aspects of cell behavior are *mechanosensitive*, including *adhesion*, *spreading*, *migration*, *gene expression* and *cell-cell interactions* [3]. Cells can normally sense stiffness up to a few microns from the cell membrane, but through the ECM the sensing distance can increase to 200μm [3].

The study of the mechanical properties of cells like cell *stiffness* is another focus of mechanobiology. The stiffness of a cell is a measure of how well a cell resists deformations. The stiffness of cells is relevant because the stiffness of individual cells and their surrounding ECM are critical for many biological processes [9].The cells get their stiffness from the *cytoskeleton*. Not all parts of the cell are equally rigid. The division of the stiffness can be found in Figure 1.2b. Cell stiffness can also be used as a

biomarker for illnesses. The stiffness of cancer cells, for example, is often lower than that of healthy cells [10].

Cell adhesion is a measure of how strongly a cell is connected to other cells, the ECM or biomaterials. It is essential in cell communication and cell regulation[11]. It helps regulate cell differentiation, cell cycle, cell migration, and cell survival. Cells monitor adhesion just like they monitor stiffness. Receptors and ligands communicate between the cell and the ECM [12]. Cell adhesion is governed by multiple systems, tight-adherens- and Gap Junctions, Desmosomes and integrins [13], which are focused on adhesion sites on the cell called focal adhesion points. Cell adhesion is also dependent on the topology and stiffness of the substrate [14], on substrates made of microfibres, there is more adhesion than their flat counterparts [15], and on substrates made of micropillars, the adhesion is highest when the pillars are placed the most dense [16].

1.2. Cancer

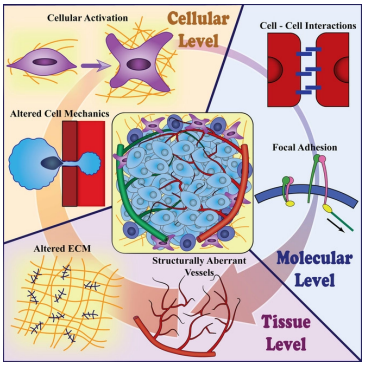

(a) A summary of the multiscale biophysics of cancer. Looking at the tumour microenvironment at the tissue level, the ECM is altered. At a cellular level, cancer cells are often softer than healthy cells [17]

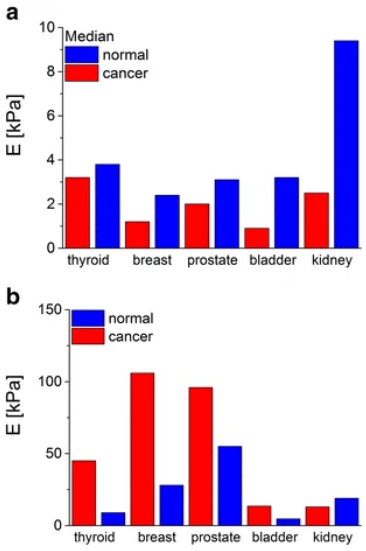

(b) A comparison of the stiffness of cancer cells and healthy cells in the top graph, and a comparison of the stiffness of cancer tissue and healthy tissue in the bottom graph [18]

Figure 1.3

Cancer is the second most common cause of death in the western world [19].It is a disease of uncontrolled cell growth which starts in one tissue and can spread through the body. Cancers start as tumours, a lump of abnormal cell growth. A tumour becomes cancerous when it is *malignant* when the primary tumour produces secondary growths, which can spread through the body. If the tumour does not spread, it is called a *benign* tumour [20].

Cancer cells have different *physical properties* compared to healthy cells. The cells are often softer than healthy cells a lack of actin fibres can cause this [18]. How much the cells have changed compared to healthy cells depends on the type of cancer. A comparison of healthy and cancerous cells and healthy and cancerous tissue can be found in Figure 1.3b. Paradoxically tumours can be up to 10 times stiffer than the healthy tissue; a stiffer ECM causes this. The higher tumour stiffness is correlated with tumour cell survival and enhanced proliferation [3]. As seen in Figure 1.3a, tumours affect tissue on all levels, from individual adhesion bonds to multi-cellular tissue, the behaviour changes.

These changes are often more pronounced in more aggressive types of cancer. The *physical properties* of metastatic cancer cells are different from benign cancer cells [21]. Metastatic cells are usually softer than benign cells and have less cell adhesion. The Young's modulus is regarded as a biomarker of cell motility and movement, it has been shown that cancerous cells have a lower Young's modulus

than benign cells [22] [23]. This can be useful when metastatic cells invade foreign tissue since the cancer cell can deform more easily and move through narrower passages. Adhesion is also *lower* in metastatic cells, this is necessary to disconnect from the primary tumour. Adhesive proteins such as E-cadherin, which is important in cell-cell adhesion, get downregulated [24]. Cancer cells also detach from the ECM [20].

2

Biomechanical Measurement Techniques

The mechanical properties of cells are an interesting research topic because they are very important for the behaviour of cells. Also, illnesses like cancer change the mechanical properties of cells, and the surrounding tissue, which changes how a cell acts, as discussed in section 1.2. Two of the main properties that can be changed by cancer are the stiffness of the cell and the surrounding tissue and the adhesion of cells.

To study the effects of cancer on the biomechanical properties of cells, a in vitro method is needed with which it is possible to do high-precision measurements of the cell adhesion and cell stiffness where a cancer cell can be added or removed. Single-cell experiments are preferred since more information can be extracted from these experiments. The goal is to find a method to measure the stiffness and adhesion of a single cell. Over the years many techniques to measure these properties of cells have been developed. In this chapter, the state-of-the-art in biomechanical measurement techniques is discussed.

2.1. Cell stiffness

The cell stiffness or elastic modulus measures the rigidity of a cell, and how well the cell keeps its shape under external forces. It is also a biomarker for cancers which makes it an important research topic. There are a few methods for measuring cell stiffness discussed in this section, *nanoindentation, optical tweezers, Acoustic microscopy and microfluidic methods*.

Nanointentation

One of the most used methods for measuring cell stiffness is nanoindentation. With nanoindentation a probe is used to make an indentation in a cell, the forces are monitored and with a mathematical model, the stiffness of the cell can be determined, in Figure 2.1a this process is shown [9]. This is often done using an Atomic force microscope (AFM).

Nanoindentation can be used to measure the stiffness locally but it can also be used for mapping the stiffness over the whole cell surface [25]. This depends on the type of probe that is used and the mode of the AFM. You can also use it to measure the stiffness of the substrate or ECM. Nanoindentation is a precise method where forces in the order of tens of pico-Newton to hundreds of nano-Newton are possible [9]. Tens of cells can be measured in one experiment but they have to be done one by one. A downside is that you can get artefacts if the indentation is more than 5% of the thickness of the cell, another challenge is that cells can only be approached from the top [26].

Optical tweezers

Another method for measuring the cell stiffness is using optical tweezers [27]. Optical tweezers are a technique where a focussed laser is used to apply a small(pN range) but very precisely controlled force.

Optical tweezers are used to trap single cells and other small particles. When a cell is trapped the it deforms slightly, this deformation can be used for calculating the stiffness [28], a sketch of a trapped cell is seen in Figure 2.1b. Similar techniques exist where magnetic tweezers are used [29]. These techniques have high precision but a low throughput.

Acoustic microscopy

Acoustic microscopy is a microscopy technique which uses ultra high-frequency ultrasound [30]. The soundwaves produced by the acoustic microscope penetrate the subject and can be used to define its mechanical properties such as density, stiffness and the thickness of the material. Acoustic microscopes can also be used in biological settings [31]. They can measure the stiffness of a cell but also monitor the changes in cell stiffness over time. A downside to acoustic microscopy is that it has relatively low resolution and its measurement changes when the size and shape of the cells change [32].

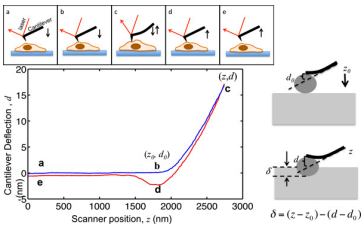

(a) A figure of the process of nanoindentation with an AFM and the produced force curve. [9]

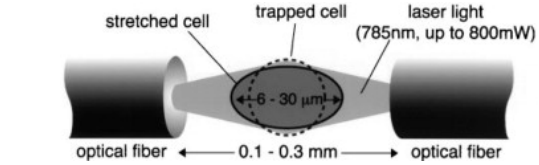

(b) Trapping a cell with lasers, from which the stiffness can be derived. [33]

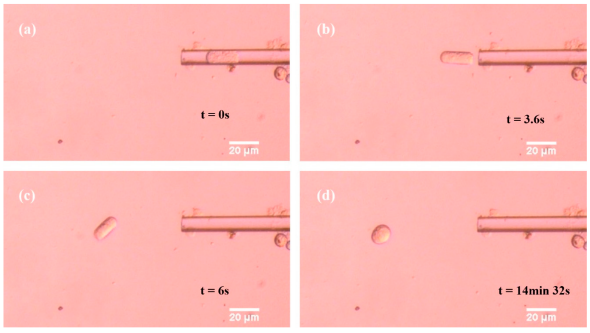

(c) Photos of the spheroidization of a cell when it is deposited from a pipette, from this process, the stiffness can be derived [34]

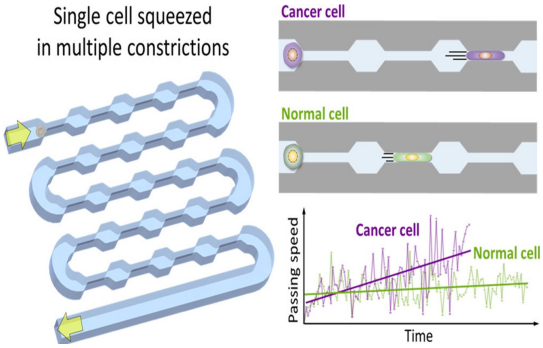

(d) An image of a channel with constrictions, the time it takes a cell to pass through the channel is a measurement of its stiffness [35]

Figure 2.1: Methods for finding the stiffness of a cell

Fluidic techniques

In research by Li et.al, a chip is designed to measure the stiffness of cells using a series of small channels as shown in Figure 2.1d, the time a cell takes to pass through the channels is measured, and flexible cells move quicker than stiff cells, the chip only measures relative values, but it can have a very high throughput [35].

The spheroidization of cells can also be used to determine the stiffness of a cell [35]. To do this, single cells are deposited from a micropipette into oil when the cells exit the pipette they are cylindrical in shape, in the oil they become spherical over time, the time this takes is related to the stiffness of the cell. The process is shown in Figure 2.1c. With a mathematical model, the cell stiffness can be calculated. It is an easy method with good potential throughput, but the precision needs to be determined.

2.2. Cell adhesion

Cell adhesion plays a role in cellular growth, differentiation, pattern formation and migration. Lower cell adhesion is also one of the most explicit mechanical properties of metastatic cancer cells. There are multiple ways to measure cell adhesion, they can be categorised into four groups: *shear measurements*, *micropipette manipulation*, *Single Cell Force Spectroscopy* (SCFS) and *cell traction microscopy*

and *FRET* force instruments [36]. These techniques are discussed and compared in this section.

Shear tests

Shear adhesion tests are the oldest technique to measure cell adhesion. For these tests, a force is applied to cells and it is measured when cells detach and how many cells detach. Usually, these experiments are done with large quantities of cells(hundreds). There are two techniques used to apply forces on cells, one is using centrifugal forces [37] [38][39], the other is using fluid flow [40][41][42], images of these techniques can be seen in Figure 2.2.

In *centrifugal experiments* a platform, well plate or cylinder, is spun very quickly to apply a centrifugal force on cells, there are a few configurations possible. In some studies [37][39], a flat disk with cells on top is spun, as seen in Figure 2.2a. Another approach is to place a closed well plate in a centrifuge with the cells aimed outward [43], as seen in Figure 2.2b. A third option is a cup with cells at the bottom, it is centrifuged upside down, then the cup is frozen and the cells are counted [38].

In *flow experiments*, a flow of water is used to flush away cells from a surface. The cells that stay attached to the surface are counted. So the adhesion is measured as a function of the flow. For flow experiments, there are multiple varieties used. The simplest type of flow experiment is done with a laminar flow between two glass plates as shown in Figure 2.2c, where the flow flushes away cells [42][41]. A different approach to flow experiments is using a radial flow chamber, where you have a circular chamber with a flat bottom, cells are placed at the bottom, and water enters from the centre and flows outward, as seen in Figure 2.2d [43]. A more sophisticated type of flow experiment is done by Kwon and colleagues, they fabricated a chip with four parallel microfluidic channels, each channel has a different structure to which the cell adheres, as imaged in Figure 2.3a. With this test setup, they could compare cell adhesion on multiple surface textures and the difference in adhesion of cancerous and healthy cells more easily [40].

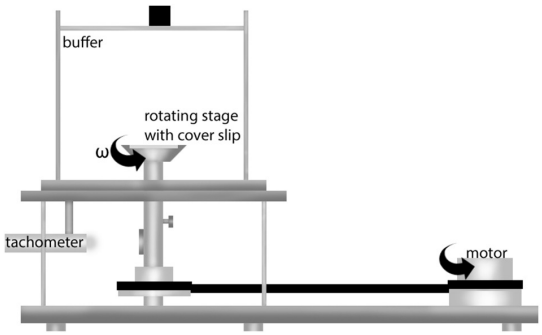

(a) An example of a spinning cell adhesion experiment [36] based on [37]

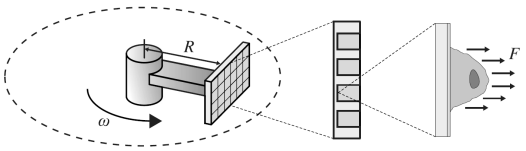

(b) A typical centrifugal experiment where a well plate is placed in a machine which spins it around [43]

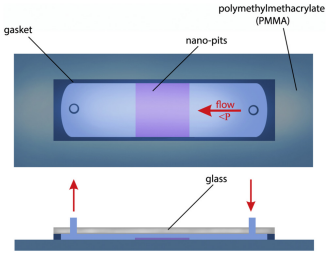

(c) An example shear flow experiment, between two plates a laminar flow is created, cells are placed in the nanopits, the adhesion is measured as a function of the flow [36] based on [42]

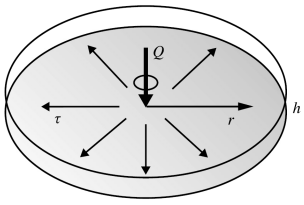

(d) A simple radial flow experiment, cells are placed at the bottom and water flows from the center outward [43]

Figure 2.2: Four different types of shear tests, image a and b are centrifugal set ups and image c and d are flow set ups

Shear experiments are relatively easy to do but a downside to shear experiments is that they can't be used for single-cell experiments. Another downside especially for flow experiments is that the force is dependent on cell size and cell shape. Since cells are heterogenic, their sizes differ a little so the measured adhesion is only an average. Measured shear force are usually in the 1-200Pa range.

Another method for measuring shear forces is cytodetachment, Figure 2.3b, in this technique an

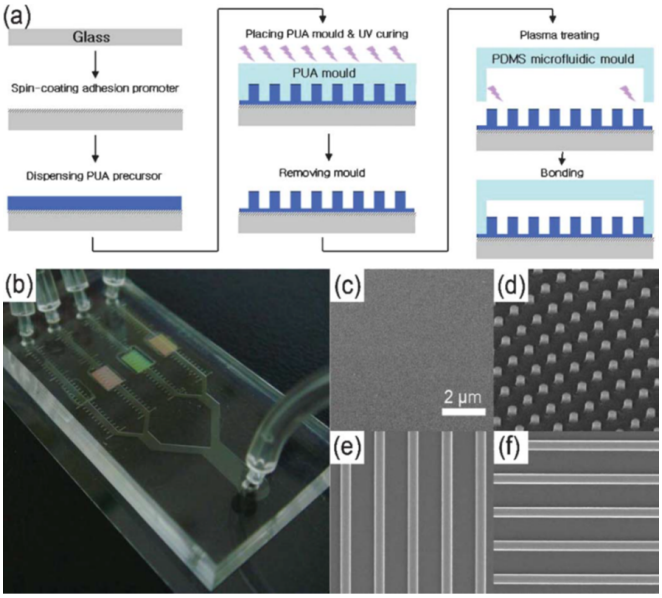

(a) Image of a four-channel flow experiment. Image a. shows the soft lithography production process of the microfluidic channels, image b. is a photo of the set-up where the four channels can be seen clearly, image C. to f. are the different structures of the channels where cell can adhere to. [40]

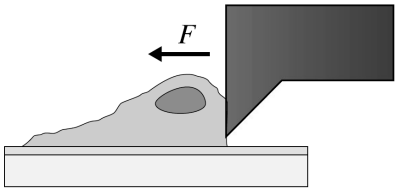

(b) cytodetachment, a cell gets pushed loose by an AFM [43]

AFM Probe is used to push loose a cell [43]. This way the shear forces for a single cell can be measured with a very high precision but with a lower throughput.

Micropipette manipulation

Micropipette manipulation is a collection of techniques that use micropipettes(pipettes with an aperture diameter measured in the micrometres, usually 5-10 μm) to do adhesion measurements. There are two ways to measure cell adhesion using micropipettes, micropipette *aspiration* and micropipette *suction*. With the aspiration technique, a negative pressure is applied to the cell in order to attach the pipette to the cell. With the suction technique, a negative pressure is used to detach a cell from its surface and suck it in completely.

Cell-cell adhesion studies can be done with the step pressure technique using two pipettes, Figure 2.4a. In this technique two pipettes are attached to two cells using the aspiration method, the two cells are then brought in contact with each other for an amount of time, next one of the pipettes is moved away slowly, if the cell detaches from the pipette the adhesion force is higher than the aspiration force, if not, it is lower [44][45]. A variant of this technique is one where one of the cells is sucked in completely when it detaches. One of the cells can also be replaced by a bead to measure the adhesion between the cell and the beads material.

In the cell suction technique, a cell is completely sucked into a pipette, shown in Figure 2.4b. The cell suction technique can be used to measure adhesion between a cell and its surface when the suction force is known exactly [46]. This process can be automated to measure many cells in a short amount of time(100s in 30min [36]). A downside to this technique is that the suction force is dependent on the size and shape of a cell.

Micropipette techniques can measure adhesion forces in the 0-10pN but the resolution is often not very high. Also moving the pipettes can sometimes be a problem [36]. The throughput of micropipettes is acceptable, depending on the technique it can be between 10 cell pairs for the step pressure technique and 100s of cells per experiment for the automated suction technique, each experiment can last for about 30 minutes until cells start to deteriorate.

Single Cell Force Spectroscopy

An AFM can also be used for adhesion measurements. In an adhesion measurement, the cantilever of the AFM is attached to the top of a cell, the cantilever then gets pulled upwards until it detaches while

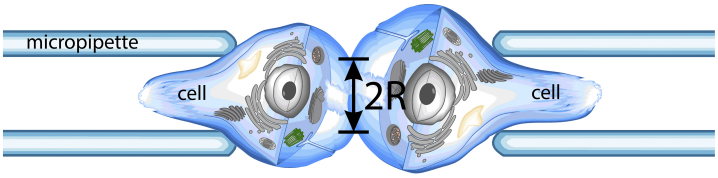

(a) An image of the step pressure technique, both pipettes are attached to a cell with a known negative pressure, the cells are brought together for some time to attach, then one of the pipettes is moved to the side, if the cell detaches from the pipette the adhesion force is higher than the pressure force. [36]

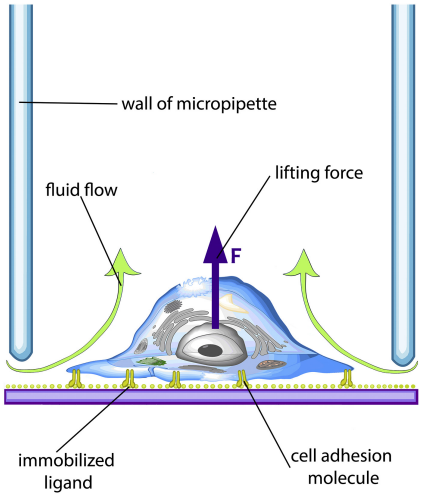

(b) An image of a pipette sucking in a cell, the suction force is known, and the cell adhesion force can be determined. [36]

Figure 2.4: Two types of micro-pipette experiments

the pulling forces are monitored, this method is called *single-cell force spectroscopy*(SCFS) [47]. The workflow can be seen in Figure 2.5 A, where a cell is attached to a cantilever and is brought in contact with a surface in order to measure the adhesion forces between the surface and the cell. Since the AFM can measures forces very precisely, high resolution detachment graphs can be made like Figure 2.5 B, in these graphs the stages of the cell detachment can be found. The detachment curve in the graph is not completely smooth, each ripple in the curve is caused by the detachment of a part of a cell, information about the adhesion strength and energy of specific focal adhesion points can be extracted from the curve. Adhesion measurements with the AFM are precise with a pN resolution and ”objective” you do direct measurements on the cell and are not dependent on cell size and shape. There is also a large force range for which AFMs can be used, from 500pN to 1.6muN adhesion forces [48].

A downside to SCFS is that it is a slow method. With a conventional AFM cantilever, only one cell can be measured per experiment, after each measurement the cantilever needs to be cleaned to remove the cell.

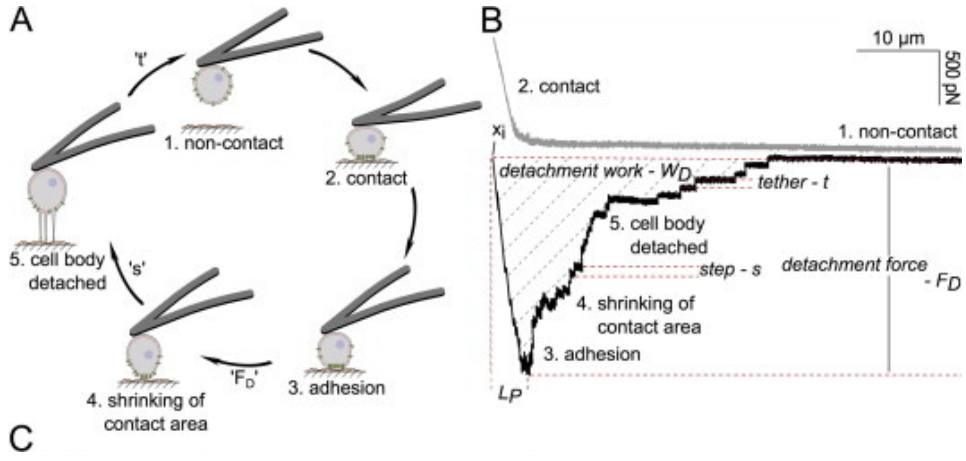

Figure 2.5: An example of single cell force spectroscopy. In image A the measurement method is shown. In Image B a typical force curve produced by the AFM is shown. [49]

A few methods for increasing the efficiency of SCFS have been developed [50]. *Fluid Force Microscopy*(FluidFM)is the most popular [51][52], a schematic image of the workflow can be found in Figure 2.6. For FluidFM a hollow AFM cantilever with a channel for aspiration is used. In this method,

the cell is attached to the cantilever by applying negative pressure through the hollow cantilever on the cell, like an aspirated micropipette. Conventional SCFS needs a few minutes to attach a cell to the cantilever, with FluidFM this can be cut down to a few seconds. A measurement with FluidFM is done in the same way as with conventional force spectroscopy, by pulling a cell upward until it detaches, when a measurement is finished the cell can be simply removed by putting positive pressure on the cell. The use of FluidFM can increase the speed of measurements to about 10 cells per experiment(30min) [48].

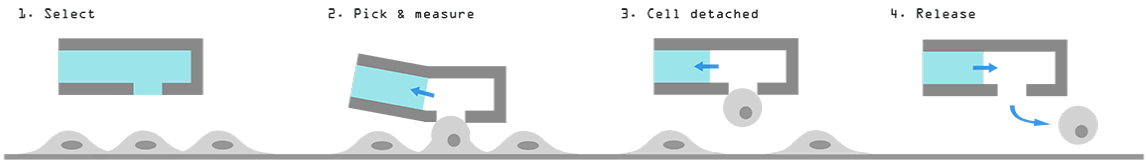

Figure 2.6: A schematic representation of FLuidFM [52]

Another novel way to increase the speed of Cell adhesion measurements is using 2 AFM cantilevers as tweezers. Which then are used to pick up cells [53] as shown in Figure 2.7. This is a relatively complex process because two cantilevers need to be aligned independently. Also, the two cantilevers produce a separate measurement which has to be combined, this makes this an interesting but impractical technique.

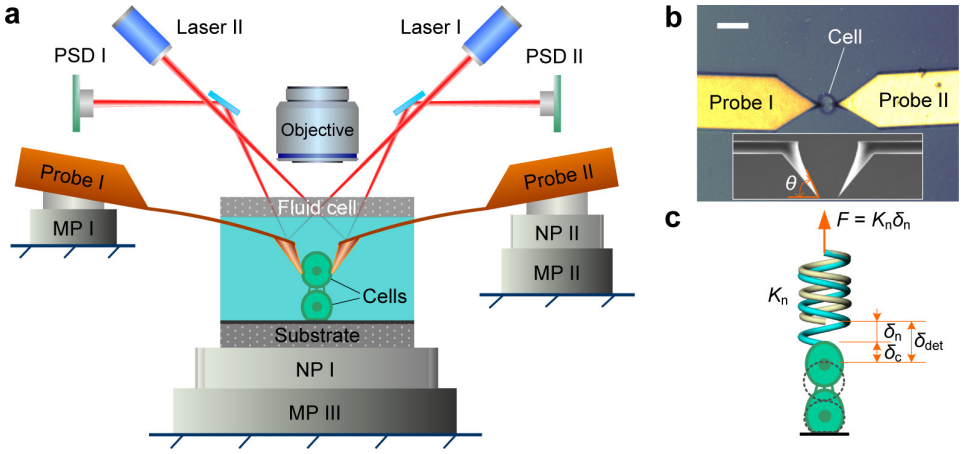

Figure 2.7: A figure of a set up where two AFM cantilevers are used as a tweezer for single cell force spectroscopy [53]

Single cell force spectroscopy is a slow but useful technique for measuring cell adhesion forces.

Cell Traction Force Microscopy and FRET force sensors

Cell traction force microscopy and FRET force sensors are instruments that measure cell adhesion by monitoring the deformation of the substrate beneath the cell. These are versatile techniques because all measurements are done from the bottom. These techniques can be used in combination with an AFM for more complex experiments. A downside is that they can not be used for cell experiments with more than one cell layer.

In Cell traction force microscopy(CTFM) the substrate is flexible and is embedded with fluorescent beads. The substrate deforms when a cell is placed on top. The location of the beads is monitored with a fluorescence microscope. The monitoring creates a displacement field, Figure 2.8a. From this displacement field, the traction field can be reconstructed by an elastic computational model [36]. 3D versions of this method are also available.

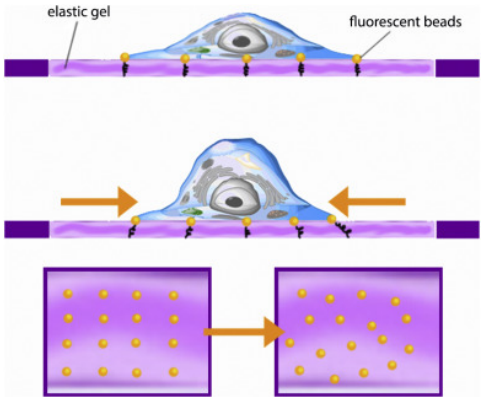

(a) Schematic image of traction force microscopy with fluorescent beads [36]

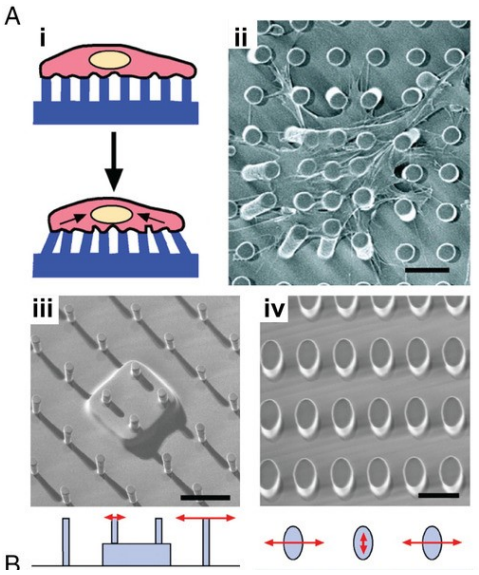

(b) Traction force microscopy with microneedles [54]

Figure 2.8: Two methods for traction force microscopy

Another way to monitor the traction is to use a substrate with microneedles [54], as seen in Figure 2.8b. A PDMS substrate is used with many needles on it, the needles have a diameter of one micrometre. The cells are placed on top of the microneedles, and they deform the needles slightly. The bending of the needles is monitored, since the stiffness of the needles is known the traction can be calculated.

Förster resonance energy transfer(FRET) force sensing is a technique to measure the individual binding forces between fluorescent molecules. With this technique, the forces of individual adhesion molecules can be monitored. since individual bonds can be monitored this is a very precise technique with a pN resolution [36]. This technique is mainly applicable to cell-substrate adhesion measurements. Also, it is also not appropriate for measuring complete cell adhesion because only one adhesion molecule type can be measured in each experiment.

2.3. Combined measurement techniques

There are a few methods where both cell stiffness and adhesion can be measured simultaneously, they are discussed in this section.

In a paper by Luo et. al, a new method is shown to determine both the stiffness and the cell adhesion of a cell in one measurement [55]. For this, a FluidFM tipless hollow cantilever is used and a confocal microscope. The cell adhesion is measured using SCFS as discussed in subsection 3.2.1. The stiffness is calculated by a model which uses the adhesion surface between the cell and the cantilever and the stress relaxation curve. The cells were stained with dye to make the adhesion surfaces more visible. An image of the adhesion surface of the cell and cantilever can be seen in Figure 2.9. In this research, it is used to find a relation between adhesion force and adhesion energy MCF-7 breast cancer cells, for which it seems that there is a linear relation. It is not clear how well this technique would work with multiple cells close together.

Another method for measuring adhesion and stiffness at the same time is using a combination of a surface sensor such as an optical biosensor to measure adhesion and an AFM for nanoindentation [56]. Or to use a traction force microscope in combination with an AFM. These methods have the potential for very high-resolution measurements but are limited to single-cell layer experiments.

A combination of an AFM with SCFS and a side-mounted microscope could be another way to mea-

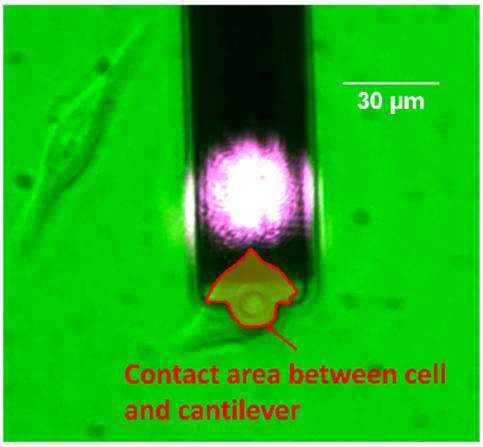

Figure 2.9: An image of the cantilever tip in and adhesion measurement with its contact area with the coloured, this contact area is used for calculating the cell stiffness [55]

sure cell adhesion and stiffness [57]. In this method, the AFM removes the cell from a substrate, while the microscope monitors the deformation of the cell. The deformation of the cell is related to the stiffness of the cell so the stiffness can be calculated. For this method, a new cell model must be developed.

Using a single AFM to measure both cell stiffness and cell adhesion is possible theoretically. To be able to do nanoindentation on a cell to find its stiffness and then use single-cell force spectroscopy to find the adhesion would be a valuable tool, because of the high precision of both methods. At this moment this is not possible because the cantilever the AFM uses would need to be changed mid-experiment since the cantilevers for nanoindentation and SCFS have different properties. A cantilever with properties of both is not available presently and would need to be developed. Since it is impractical to have glue on the cantilever for cell attachment this cantilever should need the properties of FluidFM, which would also improve its throughput.

2.4. Conclusion

There are several methods for measuring cell adhesion and cell stiffness. Not all techniques can be used for single-cell experiments. Also, it is desired that stiffness and adhesion can be measured in one experiment.

For stiffness studies nanoindentation and optical tweezers are the most precise. Nanoindentation can also be used in combination with other techniques and is quicker. Acoustic microscopy is also an interesting technique although it is less precise.

For cell adhesion studies, SCFS and CTFM have the highest precision. Shear stress and micropipettes can have the highest throughput but they are less precise and not always usable for single-cell experiments.

There are a few techniques available to measure both adhesion and stiffness in a single experiment. Using nanoindentation in combination with a surface measurement like CTFM can be interesting but is limited to single-cell layer experiments. Analysing the cell shape and the adhesion curve during SCFS is also a good option although this is not a proven technique. Ideally, both nanoindentation and SCFS are done on a single cell. Since this gives a high resolution and can be used with complex experimental setups. Therefore it is chosen to develop a new AFM cantilever which can be used for both SCFS and nanoindentation.

3

State-Of-The-Art: Cantilever Design

In chapter 2 it is shown that atomic force microscopy can be used to measure cell adhesion and cell stiffness, by using single-cell force spectroscopy and nanoindentation. For both measurement techniques, different types of AFM cantilevers are used. In this chapter, the working principle of AFM is discussed. The properties of the different types of cantilevers are discussed. The state-of-the-art for AFM cantilever production methods is discussed. And this knowledge is used for a state-of-the-art cantilever design.

3.1. Atomic Force Microscopy

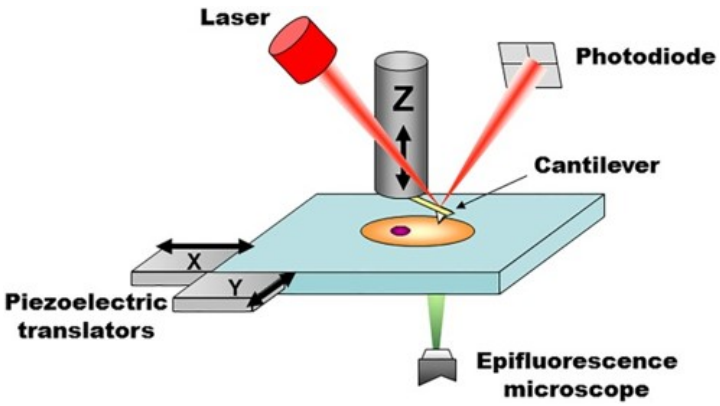

Figure 3.1: An image of an atomic force microscope with a inverted camera[58]

Atomic force microscopy (AFM) is a high-resolution microscopy method, it can have a sub-nanometer resolution [59]. It is used to image objects and surfaces smaller than what would be possible with conventional optical microscopes. Optical microscopes are diffraction limited atomic force microscopes use a mechanical cantilever to interact with a surface and are not limited by the wavelength of the light. A comparison of the resolution range of the AFM and other imaging techniques is made in Figure 3.2. AFMs were invented in the 1980s as an evolution of the stylus profiler and the scanning tunnelling microscope[60]. Although originally developed as a microscope the AFM gained many functions over time and is now used in many fields of research such as semiconductor science and technology, chemistry, physics, cell biology, and medicine[59]. A schematic AFM set-up as is often used in biological experiments can be seen inFigure 3.1. The main AFM parts are the cantilever or probe which is doing the actual measuring.The laser and photodiode which are used for monitoring the deflection of the cantilever, piezoelectric translators are the actuators which move the experiment in the x/y-direction, and an actuator which moves the cantilever in the z-direction, in some AFMs all actuators are used to move the cantilever and the experiment stays stationary. The parts mentioned so far are present in some form on all models of AFM, the AFM in the image also has an inverted epifluorescence microscope.

Inverted microscopes are often used in biological AFM experiments, for monitoring the cells on a larger scale.

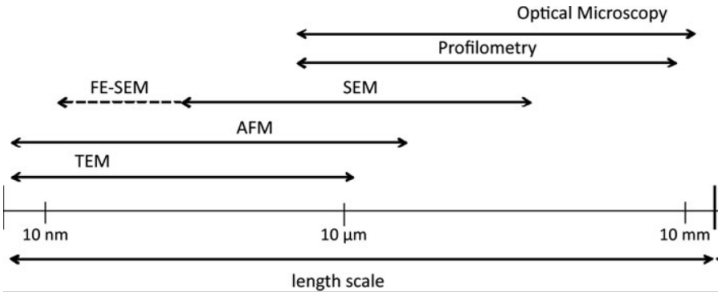

Figure 3.2: A comparison of the usability range of different imaging techniques [59]

The working principle of an AFM is relatively simple. An AFM uses a flexible cantilever with a sharp tip for imaging instead of the light in optical microscopes. The tip is dragged over a surface which causes deflections in the cantilever. These deflections are measured and from this, an image can be constructed. The deflection of the cantilever needs to be measured precisely. A few measuring methods that are used are: a reflected laser a Scanning Tunneling Microscope(STM) tip, a capacitance measurement or an interference measurement, these can be seen in Figure 3.3[61]. Most commonly a laser is used to measure the deflection, a laser is reflected off the cantilever to a detector, and the movement of the laser on the detector is monitored from this the movement of the cantilever is calculated. This method can also be used in biological applications such as cell experiments. Cell experiments are often done in a wet environment, in this case, the cantilever operates in the water. The laser gets refracted by the water and reflected of the cantilever as seen in image (f) of Figure 3.3.

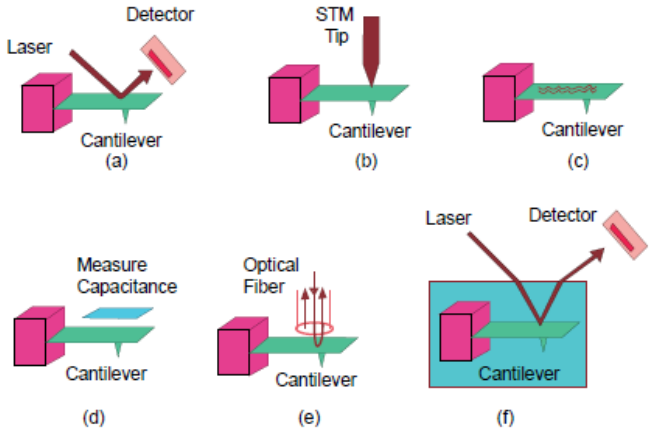

Figure 3.3: Some methods that are used for measuring the deflection of an AFM cantilever [61]

AFMs can be used in two modes, contact mode and non-contact mode. In contact mode, the tip of the cantilever physically touches the surface that is measured. In non-contact mode the tip does not touch the surface, the cantilever tip interacts with the local atomic forces such as magnetic, electrostatic and van der Waals forces which deflect the cantilever.

AFM can not only be used for imaging, it can also be used for force spectroscopy, direct measurements of the force interactions between the tip and the substrate. This can be done by measuring the deflection of the cantilever and using Hookes law, Equation 3.1, to calculate the forces. The stiffness of the cantilever is known very precisely. Because an AFM is a very high precision instrument forces in the nN range can be measured.

$$Hookes\ law: \ F = -k \times D \tag{3.1}$$

Where F is the force(N), k is the probe force constant/stiffness(N/m) and D the deflection distance(m).

AFMs can operate in dynamic and static modes, in dynamic mode, the cantilever is vibrating and tapping the subject, in the static mode the cantilever is not vibrating and is only moved by the actuators.

AFM is useful in biological applications because it can be used in warm and wet environments no specific sample preparation is needed, no conductive coatings for example which are needed for Scanning Electron Microscopy (SEM) and Tunnelling Electron Microscopy (TEM) images. AFM can also be combined with optical instruments for example an inverted or a side-view microscope to monitor the cells during experiments, or an optical biosensor to measure cell adhesion [57][59][56].

The functionality of an AFM is largely determined by the properties of the cantilever used. Mainly the stiffness and tip shape are important but also the eigenfrequencies, eigenmodes and quality factor.

3.2. Cantilever properties

In this section, the properties of Adhesion and stiffness measurement cantilevers are discussed and a design with the properties of both is proposed. As discussed before the most important properties of an AFM cantilever are the stiffness, the tip shape, the eigenfrequency, the eigenmode and the quality factor. The stiffness defines how much force is needed to deflect the cantilever in N/m. The tip shape is the physical shape of the point of the cantilever where it interacts with the measured subject. The eigenfrequency is the frequency at which the cantilever will vibrate when excited, measured in Hz. The eigenmodes are the shapes of the vibrations at the eigenfrequencies. The eigenfrequency and eigenmode are mainly important when the AFM is operated in the dynamic mode. The quality factor of an AFM cantilever is a measure of the energy dissipation of the cantilever.

3.2.1. Adhesion measurements

As seen in section 2.2 an AFM can be used for determining cell adhesion with single-cell force spectroscopy(SCFS); both Cell-Cell adhesion measurement and Cell-substrate measurements can be done. The working principle for cell-substrate measurement is as follows: a cell is attached to the tip of the cantilever, then the tip is moved upward and it pulls the cell loose from the substrate while the force is monitored. For cell-cell adhesion measurements first, a cell is attached to the cantilever. The cantilever is then moved to another cell where the cells are brought in contact for a certain amount of time(30sec-90min). There are a few methods to attach a cell to a cantilever, originally glue was used to attach the cell to the cantilever. This has a downside that the cell can not be removed easily, the cantilever must be washed after each measurement. Which makes this a slow process. A faster way to do these measurements is to use a FluidFM. In this method a small channel and a small hole, the aperture, are added to the cantilever. These are used to apply negative pressure on the cell with which the cell is attached. Also, it can be used to apply a positive pressure to detach the cell again. The under-pressure can also be used for immobilising cells. A benefit of FLuidFM is that cells generally survive the experiment and can be used for further experiments[62]. A cantilever design that can be used for FluidFM also needs a fluidic interface to attach it to a pressure controller.
The adhesion force in FluidFM can be calculated with Equation 3.2, where F_{ad} is the adhesion force[N], A is the adhesion area m^2, p is the pressure[Pa] and d is the diameter of the aperture.

$$\begin{matrix} Adhesion\,Force \\ F_{ad} = p \cdot A = p \cdot \frac{1}{4}\pi D^2 \end{matrix} \tag{3.2}$$

AFM cantilevers used in SCFS are usually *tipless*, they have a flat surface where they interact with the cell. For FluidFM cantilevers also an aperture is added to the probe. The aperture diameter lies in the 2-8μm range depending on the size of the cells that are picked up[52]. A wedge can be added to the tip so the tip and the substrate surface will be more parallel, because the force is aligned better there will be less lateral displacement of the cell [63], an example can be found in Figure 3.4. To have a high resolution, the cantilever spring constants should be as soft as possible. In the ideal case, the cantilever stiffness should come as close as possible to that of the animal cell investigated(10–60mN/m)[49]. FluidFM cantilevers with such low stiffnesses are not commercially available currently, the lowest stiffness commercially available is 0,3N/m[52].

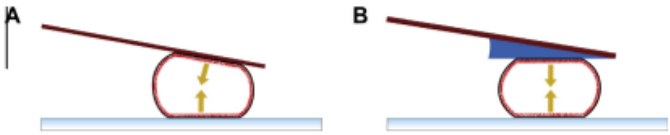

Figure 3.4: An image of a cantilever pushing on a cell without a wedge (A) and a cantilever with a wedge (B), in the cantilever with a wedge the forces align better and there will be less lateral displacement of the cell [63]

3.2.2. Stiffness measurements

The stiffness of a cell can be measured by using an AFM probe to make an indentation into the cell and measuring the resistance created. This creates a force-distance curve, from which the cell's stiffness can be calculated. To find the stiffness from an indention measurement a contact model is needed. The most common model used is the Herz model, which uses the tip geometry the force and the displacement to calculate the stiffness value. The Herz model for a probe with a spherical tip is shown in Equation 3.3 and for a probe with a blunted pyramid shape in Equation 3.4. Alternative calculation methods exist that are more accurate or take into account other properties such as the stiffness of the substrate and substrate adhesion[26][8].

$$Herz\ Model\ for\ a\ Sphere$$

$$F = E_{eff} \cdot \left[\frac{a^2}{R_p^2} \cdot ln\frac{R_p + a}{R_p - a}\right] \tag{3.3}$$

$$Herz\ Model\ for\ a\ Blunted\ Pyramid$$

$$F(\delta) = E_{eff} \cdot \left[\delta a - \frac{\sqrt{2}}{\pi}\frac{a^2}{tan(\theta)}\left(\frac{\pi}{2} - arcsin\left(\frac{b}{a}\right)\right) - \frac{a^3}{3R_p} + \sqrt{(a^2 - b^2)} \cdot \left(\frac{\sqrt{2}}{\pi}\frac{b}{tan(\theta)} + \frac{a^2 - b^2}{3R_p}\right)\right] \tag{3.4}$$

$$\delta = \frac{a}{2} ln\frac{R_p + a}{R_p - a}$$

$$Effective\ Stiffness$$

$$E_{eff} = \frac{E}{1 - \nu^2} \tag{3.5}$$

In these equations, F is the measured force, δ is the indentation, E is the Young's modulus, ν is the Poisson ratio, a is the contact radius, b is the transition radius of a blunt probe, the width of the probe at the point where the rounded tip ends, θ is the angle of the probe.

The stiffness of the cantilevers used for indentation should be about the same stiffness as the sample, the stiffness is in the kPa range for soft mammalian cells[48]. If the cantilever is much stiffer than the sample, the deflection becomes too small and the measurement imprecise, whereas cantilevers that are too soft do not sufficiently deform the sample leading to difficulties in estimating the sample stiffness[8][58]. The stiffness is commonly between 0.01N/m and 0.6 N/m.

The tips most commonly used for indentation measurements are *pyramid-shaped* with a blunted tip (>100nm radius), see Figure 3.5. Cantilevers with pyramid-shaped tips are commonly used for obtaining high-resolution images of living cells[64]. The blunted or rounded tip reduces the stress experienced by the probed cell, in comparison to sharp tips[58]. Blunted pyramid tips can still be used for mapping the cell membrane and the structures in the cellular cortex. Another tip shape that is used for indentation measurements is a colloidal tip, these are tips with a large spherical radius(10 µm diameter). Colloidal tipped cantilevers are mostly used to measure the effect of mechanical stimuli on the cell and to apply a mechanical force on a cell. The blunted pyramid-tipped cantilever is the tip shape most applicable for measuring cells. Because it can do nanoindentation without influencing the cell too much and can also be used for making images, which would not be possible with a colloidal-tipped probe.

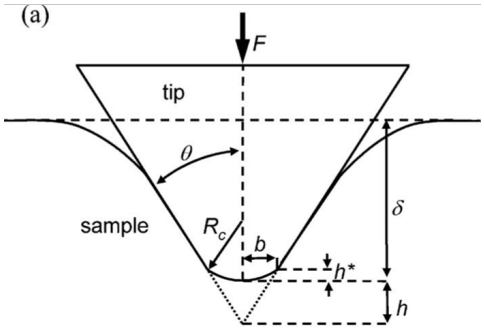

Figure 3.5: An image of a cantilever tip with a blunted pyramid shape [64]

3.2.3. Conclusion cantilever properties

For doing Fluid FM and nanoindentation in a single experiment a cantilever with the properties of both methods is needed, this can be done in two ways. One option is to have two cantilevers on one chip like in image Figure 3.6, this has an upside that it is relatively easy to produce, a downside is that the laser needs to be aligned again every time the measurement type is changed. The second option is to combine the properties of the two cantilevers into one cantilever design.

The second option would be the easiest to use. TO achieve this the properties of both cantilever types

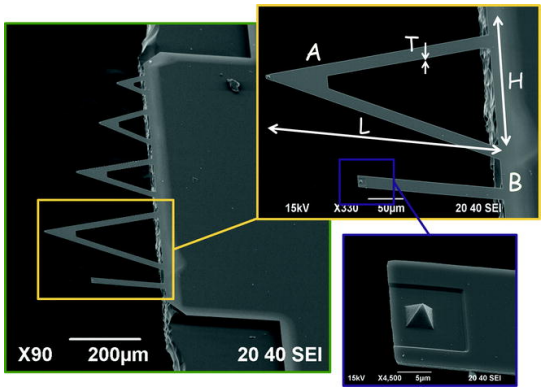

Figure 3.6: Multiple cantilevers with different properties on one chip [65]

must be combined into one design. For the final design, the optimal stiffness needs to be determined. And a tip design needs to be made with a blunted pyramid and a tipless part with an aperture; on the other end, the cantilever is connected to a fluidic interface.

3.3. Fabrication methods

Fabricating AFM cantilevers is a precise process, the geometry of the cantilever needs to be fabricated very precisely to do the ultra-precise AFM measurements. AFM cantilevers have features in the nanometer range. There are two methods to fabricate AFM cantilevers, one is using *photo-lithography* techniques and the other is using additive manufacturing. Photo-lithography is a proven method that is widely used in the semiconductor industry and is used in the fabrication of commercial AFM cantilevers. Cantilever fabrication with *additive manufacturing* is a newer method that is developed over the last decade, it is very promising for custom cantilevers because it provides much design freedom. There also exists a *hybrid* of these two methods which is also very promising. All of these techniques are discussed in this section.

3.3.1. Photo-Lithography

Photo-Lithography is the most common fabrication method for AFM cantilevers. It is the technique fabrication method that is also used for chip fabrication. Photo-Lithography can be used to make very small structures with nanometer feature sizes.Photo-Lithography is a 2.5D fabrication process, it is

mostly a 2D process with relatively small and simple 3D features.

The basic working principle of Photo-Lithography is the following: 1.The process starts with a wafer. 2. On the wafer photoresist is applied. 3. A mask is placed above the wafer. 4. The mask is lighted. 5. The photoresist reacts with the light and polymerises partly. 6. The mask is removed and part of the photoresist gets washed off; the lighted or unlighted part depends on the type of resist. 7. The wafer is etched, the remaining photoresist acts as a mask for the etchant. Then the remaining photoresist gets washed off, and the process is repeated.

In reality this process is much more complicated with different types of etchant, deposition of other materials, doping the wafer. But the basic principles stay the same.

For a hollow cantilever, this process needs to be repeated 13 times, for each repetition a new mask is needed[66]. The steps needed to fabricate a hollow AFM probe can be seen in Figure 3.10.

This makes the production of hollow cantilevers with Photo-Lithography an inefficient process, especially during prototyping since for each iteration of the design a new set of masks needs to be made.

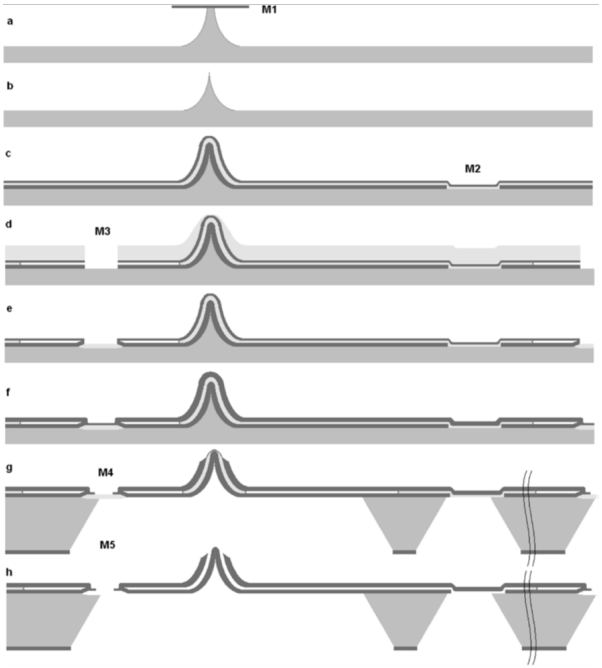

(a) An overview of the lithographic process steps needed to create a silicon hollow cantilever [66]

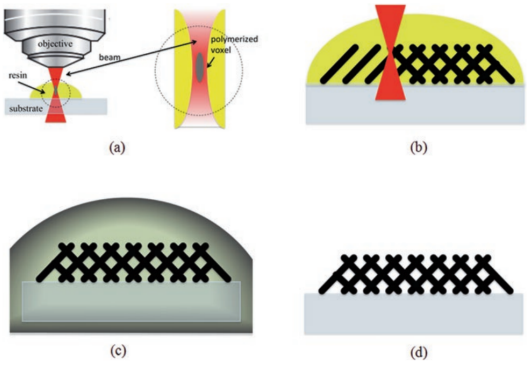

(b) Schematic images of the two photon polymerisation process [7]

Figure 3.7: Potential production processes for AFM cantilevers

Most commercial cantilevers are made of silicon or silicon oxide, the base material of most wafers. Research has also been done on polymer cantilevers which use SU-8 photoresist as the cantilever material[67]. Both conventional AFM cantilevers and microfluidic hollow cantilevers have been produced from SU-8[67]. The SU-8 polymer cantilevers have the advantage that they are easier to produce since no etchant is needed where fewer steps are needed than in Figure 3.7a. Also, polymer cantilevers can be more sensitive than their silicon counterparts, because of the lower Young's modulus of the material[68]. But they are also more sensitive to drift caused by environmental factors such as fluids and vacuum[68].

Photo-Lithography can be used to produce many cantilevers at once in batches, many cantilevers fit on a single wafer, the base material of the cantilever. The main drawbacks of using photo-lithography for the production of cantilevers are:

- That it is a lot of work to make a batch, and many steps need to be done.
- It is not easy to make small adjustments to the design, a new set of masks needs to be designed and fabricated for each design change.

- It is hard to make unconventional 3d shapes, such as unconventional cantilever tips, with Photo-Lithography because it is a 2.5d production method.

3.3.2. Additive Manufacturing

Additive manufacturing is a collection of fabrication techniques that add material to create an object, compared to most other fabrication techniques such as photo-lithography where the material is removed. There are many types of additive manufacturing, extrusion printing, stereo Lithography, inkjet printing, selective laser sintering, two-photon polymerisation and many more. Out of these techniques, only *two-photon polymerisation*(2PP) currently has the required sub-micron precision for the production of AFM cantilevers [69]. Another additive technique is SLA which has a lower resolution but is much faster. For all additive manufacturing methods, a design is made on the computer, this design is then translated to code which controls the 3d printer which produces the object.

Two-photon Polymerisation: Two-photon Polymerisation is a relatively new additive manufacturing technique with a very high precision and therefore, also many possible applications [70]. Because of its accuracy can be used as an alternative for photo-Lithography in low-volume applications such as scientific research.

Two-Photon Polymerisation is a resin printing process where a laser is used for locally polymerising the resin, as shown schematically in Figure 3.7b. Resin is a fluid that polymerises when hit by light of the right wavelength. The main parts of resin are monomers (the building blocks of polymers), a photo activator (A chemical which starts the polymerisation process under the influence of light) and a solvent. What makes two-photon polymerisation special is that the resin only polymerises when two photons hit a photo activator molecule in the resin simultaneously, compared to stereo lithography where the resin polymerises when a single photon hits it. Two photons can only hit the same spot in the focal point of a laser, the voxel. Since the voxel of a laser can be very small it is possible to achieve very a small feature size with this technique, in the order 100nm [71].

The voxel diameter is calculated with Equation 3.6 where lambda is the wavelength of the laser and N.A. stand for the numerical aperture of the objective used to focus the laser [7]. The voxel is moved through the resin in three dimensions to locally polymerise the resin, the laser is guided by a computer. 2PP makes structures on a layer-by-layer basis. The laser used in 2PP is a fast (femtosecond pulse time) laser with a wavelength of 800 or 780nm [7]. 2PP is a slow production method, making structures with dimensions in the mm range can take hours.

$$d \cong \frac{2\lambda}{\pi \times N.A.} \tag{3.6}$$

Stereolithography and digital light processing: Stereolithography (SLA) and digital light processing (DLP) are layer-by-layer based additive manufacturing processes. The base material used in SLA is a resin, the resin polymerises when it is hit with a single photon of the right wavelength. SLA and DLP are very similar processes, the difference is that SLA uses a laser with a moveable mirror to polymerise the resin and DLP uses a projector. SLA and DLP have a bed on which the structure is built, the bed has a small layer of resin on it. This resin layer gets partly polymerised by a scanning laser or a projector. Then a new layer of resin is applied to the bed and the process is repeated until the process is finished. In Figure 3.8 an example of SLA printing is shown. SLA and DLP printers can produce structures with a relatively high resolution feature sizes of up to 35 μm are possible [72]. The DLP and SLA printing speed can be 20mm/hour in the z-direction, depending on the layer thickness.

Additive manufacturing of AFM cantilevers: Additive manufacturing has been used before for the production of AFM cantilevers. Although this was always in low production research applications. In research by Alsharif et. al, AFM cantilevers were produced using two-photon polymerisation [74]. It was found that they functioned effectively for AFM. They were even better than their silicon counterparts when used in intermittent contact mode because of the higher quality factor.

A combination of DLP and 2PP is used by Kramer et. al to fabricate hollow AFM cantilevers [75]. In this research, 2PP is used to fabricate the hollow cantilever. This cantilever is printed on top of a connecting piece made with a DLP printer, this piece can be installed in the AFM and it has a connection point for a tube, Figure 3.9b. In order to get a good leak-free connection between the DLP and the cantilever, a dome is made at the end of the cantilever which covers the exit hole for the fluids in the

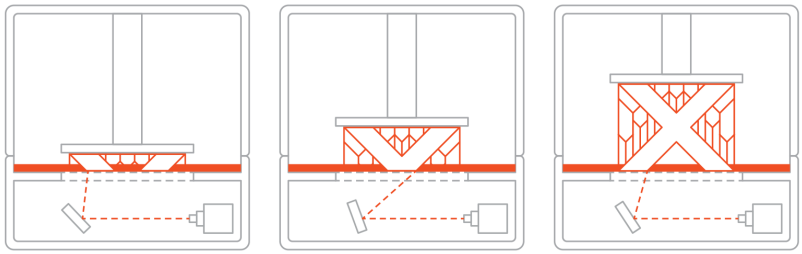

Figure 3.8: Schematic image of the stereo lithography process [73]

DLP piece. Images of his design can be found in Figure 3.9a where the different cantilever designs and the dome connector can be seen clearly.

In the thesis work of van Blankespoor [76], he improved on the fabrication method by using a laser cutter to drill a small channel in the fluid connector piece instead of printing the channel with the DLP printer. Since this channel is could be smaller than what can be achieved with the DLP printer a smaller 2PP printed dome is needed. This decreased the printing time greatly. This is a very promising production method but it is also sensitive to drift [77].

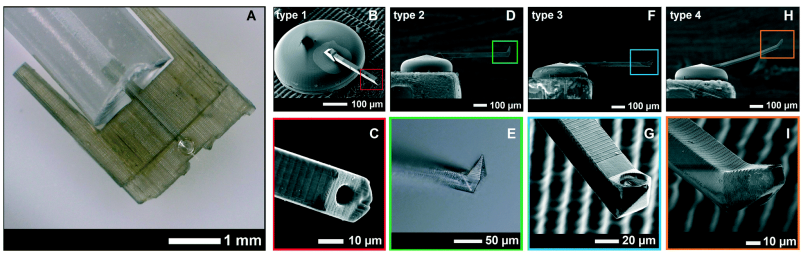

(a) The 3d printed cantilevers created by Kramer et. al [75]

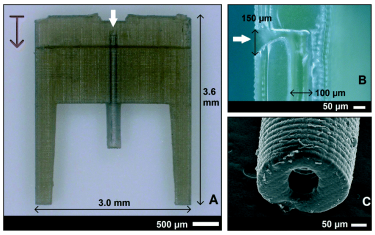

(b) The fluid interface printed with the stereo lithography technique by Kramer et. al [75]

Figure 3.9: Images of 3d printed cantilevers and fluidic interfaces [75]

Using additive manufacturing to fabricate AFM cantilevers is very promising because it provides much design freedom and is relatively quick for low production numbers. A downside is that it is a new technique which still has some drift problems and can only be used for the production of polymers.

3.3.3. Hybrid manufacturing

Combining lithography and additive manufacturing fabrication techniques can be an alternative to focusing on either of them. This can have the upside of combining the positive points of both fabrication techniques, the reliability of lithography and some of the design freedom of 3d printing.
In research by Goering et. al 2PP is used to add custom structures to silicon AFM cantilevers [78] . For example, tips with unconventional shapes are added to the cantilevers, to give the cantilevers new functions. A schematic drawing of the printing process and examples of interesting printed tip shapes can be seen in Figure 3.10a.Another modification that can be made to the silicon cantilever is scaffolds, they are added to the cantilever to ”tune” the eigenmodes of the cantilever as seen in Figure 3.10b. A challenge with this technique is that it has not yet been used for hollow cantilever designs, so some experimenting would be needed to optimise the process for that.

3.3.4. Conclusion

Manufacturing methods are discussed for the multi-functional hollow cantilever design. A combination of stereo lithography and two-photon polymerisation as used by Kramer et. al [75] is the best for this application. Because with this technique there is much design freedom which is needed for the multifunctional cantilever design. Because it is also a relatively quick fabrication process it is ideal for prototyping.Also, 3D printing has the benefit that in later designs more features can be added to the cantilever easily, features such as waveguides for depositing small amounts of liquid [76]. Hybrid

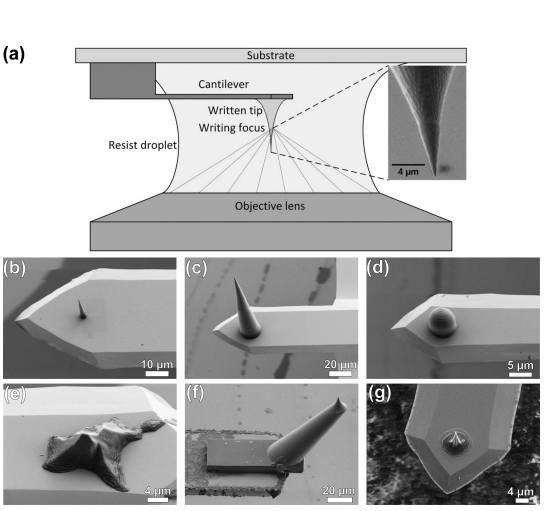

(a) The 3d printed tips on commercial silicon cantilevers [78]

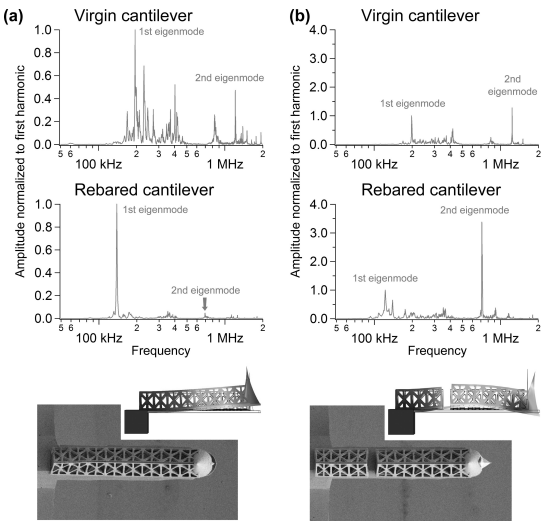

(b) 3D printed rebar on silicon cantilevers to tune the eigenmodes [78]

Figure 3.10: Images of the hybrid cantilevers [78]

cantilever production might be a nice alternative, but a downside is that the commercially available hollow cantilevers are only available in a few stiffnesses, which limits the design freedom. A downside to the additive manufacturing process is that it is still a new process which hasn't been perfected, solutions for expected problems such as cantilever drift need to be found.

4

Research Question

In earlier chapters, it is shown that there is a need to research cell mechanics and mechanobiology, especially cell adhesion and cell stiffness. Studying the mechanics of single cells remains difficult. A method which is used to study single cells is atomic force microscopy. This method can be used to study adhesion and cell stiffness individually. But, it is not possible to study both cell properties in a single experimental setup because different cantilevers are needed. Which makes the research question for this project://

How to combine indentation and fluid force microscopy in a single atomic force microscopy cantilever using multiscale additive manufacturing?

The sub-questions for this research are:

- What is the tip geometry of a multifunctional AFM cantilever?
- What is the optimal stiffness for an AFM cantilever for cell adhesion and cell stiffness measurements?
- Can nanoindentation be done with a multifunctional cantilever?
- Can Fluid force spectroscopy be done with a multifunctional cantilever?
- How to improve the signal to noise ratio of a 3d printed cantilever?
- Is it possible to do both nanoindentation and force spectroscopy on a single cell?

Bibliography

[1] Ron Milo and Rob Phillips. *Cell Biology by the Numbers*. en. Google-Books-ID: 9NPRCgAAQBAJ. Garland Science, Dec. 2015.

[2] *nucleus | Definition, Function, Structure, & Facts | Britannica*. URL: https://www.britannica.com/science/nucleus-biology (visited on 04/21/2022).

[3] Karin A. Jansen et al. "A guide to mechanobiology: Where biology and physics meet". In: *Biochimica et Biophysica Acta (BBA) - Molecular Cell Research*. Mechanobiology 1853.11 (Nov. 2015), pp. 3043–3052.

[4] Prem Kumar Viji Babu et al. "Nano-mechanical mapping of interdependent cell and ECM mechanics by AFM force spectroscopy". In: *Scientific Reports* 9.1 (Aug. 2019), p. 12317.

[5] Caroline Bonnans, Jonathan Chou, and Zena Werb. "Remodelling the extracellular matrix in development and disease". In: *Nature Reviews Molecular Cell Biology* 15.12 (Dec. 2014), pp. 786–801.

[6] Jeroen Eyckmans et al. "A Hitchhiker's Guide to Mechanobiology". en. In: *Developmental Cell* 21.1 (July 2011), pp. 35–47.

[7] Jasper Van Hoorick et al. *Polymer and photonic materials towards biomedical breakthroughs*. Springer, 2018.

[8] Michael Krieg et al. "Atomic force microscopy-based mechanobiology". en. In: *Nature Reviews Physics* 1.1 (Jan. 2019), pp. 41–57.

[9] Gawain Thomas et al. "Measuring the Mechanical Properties of Living Cells Using Atomic Force Microscopy". In: *Journal of Visualized Experiments : JoVE* 76 (June 2013), p. 50497.

[10] Sarah E. Cross et al. "Nanomechanical analysis of cells from cancer patients". en. In: *Nature Nanotechnology* 2.12 (Dec. 2007), pp. 780–783.

[11] Amelia Ahmad Khalili and Mohd Ridzuan Ahmad. "A Review of Cell Adhesion Studies for Biomedical and Biological Applications". en. In: *International Journal of Molecular Sciences* 16.8 (Aug. 2015), pp. 18149–18184.

[12] Chase E. Orsello, Douglas A. Lauffenburger, and Daniel A. Hammer. "Molecular properties in cell adhesion: a physical and engineering perspective". en. In: *Trends in Biotechnology* 19.8 (Aug. 2001), pp. 310–316.

[13] Tracey A. Martin et al. *Cancer Invasion and Metastasis: Molecular and Cellular Perspective*. Landes Bioscience, 2013.

[14] Dennis E Discher, Paul Janmey, and Yu-li Wang. "Tissue cells feel and respond to the stiffness of their substrate". In: *Science* 310.5751 (2005), pp. 1139–1143.

[15] Ana Sancho et al. "Cell Adhesion Assessment Reveals a Higher Force per Contact Area on Fibrous Structures Compared to Flat Substrates". In: *ACS Biomaterials Science & Engineering* 8.2 (Feb. 2022), pp. 649–658.

[16] Mahdiyeh Nouri-Goushki et al. "3D-Printed Submicron Patterns Reveal the Interrelation between Cell Adhesion, Cell Mechanics, and Osteogenesis". In: *ACS Applied Materials & Interfaces* 13.29 (July 2021), pp. 33767–33781.

[17] Peter E. Beshay et al. "The Biophysics of Cancer: Emerging Insights from Micro- and Nanoscale Tools". en. In: *Advanced NanoBiomed Research* 2.1 (2022), p. 2100056.

[18] Małgorzata Lekka. "Discrimination Between Normal and Cancerous Cells Using AFM". eng. In: *BioNanoScience* 6 (2016), pp. 65–80.

[19] Jacques Ferlay et al. "Cancer statistics for the year 2020: An overview". In: *International Journal of Cancer* 149.4 (2021), pp. 778–789.

[20] *cancer | Definition, Causes, Types, & Treatment | Britannica*. en.

[21] Valentin Gensbittel et al. "Mechanical Adaptability of Tumor Cells in Metastasis". en. In: *Developmental Cell* 56.2 (Jan. 2021), pp. 164–179.

[22] Qing Luo et al. "Cell stiffness determined by atomic force microscopy and its correlation with cell motility". en. In: *Biochimica et Biophysica Acta (BBA) - General Subjects* 1860.9 (Sept. 2016), pp. 1953–1960.

[23] Sarah E. Cross et al. “Nanomechanical Analysis of Cells from Cancer Patients”. In: Jenny Stanford Publishing, 2020.

[24] Ramin Omidvar et al. “Atomic force microscope-based single cell force spectroscopy of breast cancer cell lines: An approach for evaluating cellular invasion”. In: *Journal of Biomechanics* 47.13 (Oct. 2014), pp. 3373–3379.

[25] Andrew Wang et al. “Fast Stiffness Mapping of Cells Using High-Bandwidth Atomic Force Microscopy”. In: *ACS Nano* 10.1 (Jan. 2016), pp. 257–264.

[26] Jinju Chen and Guoxing Lu. “Finite element modelling of nanoindentation based methods for mechanical properties of cells”. en. In: *Journal of Biomechanics* 45.16 (Nov. 2012), pp. 2810–2816.

[27] Emad Moeendarbary and Andrew R. Harris. “Cell mechanics: principles, practices, and prospects”. In: *Wiley Interdisciplinary Reviews. Systems Biology and Medicine* 6.5 (Oct. 2014), pp. 371–388.

[28] Sylvie Hénon et al. “A New Determination of the Shear Modulus of the Human Erythrocyte Membrane Using Optical Tweezers”. en. In: *Biophysical Journal* 76.2 (Feb. 1999), pp. 1145–1151.

[29] A. R. Bausch, W. Möller, and E. Sackmann. “Measurement of local viscoelasticity and forces in living cells by magnetic tweezers”. eng. In: *Biophysical Journal* 76.1 Pt 1 (Jan. 1999), pp. 573–579.

[30] T. Kundu, J. Bereiter-Hahn, and K. Hillmann. “Measuring elastic properties of cells by evaluation of scanning acoustic microscopy V(Z) values using simplex algorithm”. en. In: *Biophysical Journal* 59.6 (June 1991), pp. 1194–1207.

[31] Esam T. Ahmed Mohamed and Nico F. Declercq. “Giga-Hertz ultrasonic microscopy: Getting over the obscurity- A short review on the biomedical applications”. en. In: *Physics in Medicine* 9 (June 2020), p. 100025.

[32] Nadja Nijenhuis et al. “Combining AFM and Acoustic Probes to Reveal Changes in the Elastic Stiffness Tensor of Living Cells”. en. In: *Biophysical Journal* 107.7 (Oct. 2014), pp. 1502–1512.

[33] Jochen Guck et al. “The optical stretcher: a novel laser tool to micromanipulate cells”. In: *Biophysical journal* 81.2 (2001), pp. 767–784.

[34] Yaowei Liu et al. “A Cell’s Viscoelasticity Measurement Method Based on the Spheroidization Process of Non-Spherical Shaped Cell”. en. In: *Sensors* 21.16 (Jan. 2021), p. 5561.

[35] Pengyun Li et al. “Automated Cell Mechanical Characterization by On-Chip Sequential Squeezing: From Static to Dynamic”. In: *Langmuir* 37.27 (July 2021), pp. 8083–8094.

[36] Rita Ungai-Salánki et al. “A practical review on the measurement tools for cellular adhesion force”. In: *Advances in Colloid and Interface Science* 269 (July 2019), pp. 309–333.

[37] Jason A. Wertheim et al. “BCR-ABL–induced adhesion defects are tyrosine kinase–independent”. en. In: *Blood* 99.11 (June 2002), pp. 4122–4130.

[38] B Angres, A Barth, and W J Nelson. “Mechanism for transition from initial to stable cell-cell adhesion: kinetic analysis of E-cadherin-mediated adhesion using a quantitative adhesion assay.” In: *Journal of Cell Biology* 134.2 (July 1996), pp. 549–557.

[39] Andrés J García, François Huber, and David Boettiger. “Force required to break $\alpha 5 \beta 1$integrin-fibronectin bonds in intact adherent cells is sensitive to integrin activation state”. In: *Journal of Biological Chemistry* 273.18 (1998), pp. 10988–10993.

[40] Keon Woo Kwon et al. “Label-free, microfluidic separation and enrichment of human breast cancer cells by adhesion difference”. en. In: *Lab on a Chip* 7.11 (Oct. 2007), pp. 1461–1468.

[41] George A. Truskey and Timothy L. Proulx. “Relationship between 3T3 cell spreading and the strength of adhesion on glass and silane surfaces”. en. In: *Biomaterials* 14.4 (Jan. 1993), pp. 243–254.

[42] E. Martines et al. “A parallel-plate flow chamber to study initial cell adhesion on a nanofeatured surface”. In: *IEEE Transactions on NanoBioscience* 3.2 (June 2004), pp. 90–95.

[43] Kevin V. Christ and Kevin T. Turner. “Methods to Measure the Strength of Cell Adhesion to Substrates”. In: *Journal of Adhesion Science and Technology* 24.13-14 (Jan. 2010), pp. 2027–2058.

[44] Kuo-Li Sung et al. “Determination of Junction Avidity of Cytolytic T Cell and Target Cell”. In: *Science* 234.4782 (Dec. 1986), pp. 1405–1408.

[45] Jin-Yu Shao, Gang Xu, and Peng Guo. “Quantifying cell-adhesion strength with micropipette manipulation: principle and application”. In: *Front Biosci* 9.2183-2191 (2004), pp. 23–24.

[46] Weibin Rong et al. “A vacuum microgripping tool with integrated vibration releasing capability”. In: *Review of Scientific Instruments* 85.8 (Aug. 2014), p. 085002.

[47] Jonne Helenius et al. “Single-cell force spectroscopy”. eng. In: *Journal of Cell Science* 121.11 (June 2008), pp. 1785–1791.

[48] Orane Guillaume-Gentil et al. “Force-controlled manipulation of single cells: from AFM to FluidFM”. en. In: *Trends in Biotechnology* 32.7 (July 2014), pp. 381–388.

[49] Jens Friedrichs et al. “A practical guide to quantify cell adhesion using single-cell force spectroscopy”. en. In: *Methods*. Nanoimaging Methods for Biomedicine 60.2 (Apr. 2013), pp. 169–178.

[50] Mi Li et al. “Advances in atomic force microscopy for single-cell analysis”. en. In: *Nano Research* 12.4 (Apr. 2019), pp. 703–718.

[51] André Meister et al. “FluidFM: Combining Atomic Force Microscopy and Nanofluidics in a Universal Liquid Delivery System for Single Cell Applications and Beyond”. In: *Nano Letters* 9.6 (June 2009), pp. 2501–2507.

[52] *Speed up single cell adhesion measurements with FluidFM*. en-US.

[53] Hui Xie et al. “In Situ Quantification of Living Cell Adhesion Forces: Single Cell Force Spectroscopy with a Nanotweezer”. In: *Langmuir* 30.10 (Mar. 2014), pp. 2952–2959.

[54] John L. Tan et al. “Cells lying on a bed of microneedles: An approach to isolate mechanical force”. In: *Proceedings of the National Academy of Sciences* 100.4 (Feb. 2003), pp. 1484–1489.

[55] Ma Luo et al. “Simultaneous Measurement of Single-Cell Mechanics and Cell-to-Materials Adhesion Using Fluidic Force Microscopy”. In: *Langmuir* 38.2 (Jan. 2022), pp. 620–628.

[56] Milan Sztilkovics et al. “Single-cell adhesion force kinetics of cell populations from combined label-free optical biosensor and robotic fluidic force microscopy”. en. In: *Scientific Reports* 10.1 (Jan. 2020), p. 61.

[57] Ovijit Chaudhuri et al. “Combined atomic force microscopy and side-view optical imaging for mechanical studies of cells”. eng. In: *Nature Methods* 6.5 (May 2009), pp. 383–387.

[58] Núria Gavara. “A beginner’s guide to atomic force microscopy probing for cell mechanics”. en. In: *Microscopy Research and Technique* 80.1 (2017), pp. 75–84.

[59] Peter Eaton and Paul West. *Atomic Force Microscopy*. eng. Oxford: Oxford University Press, 2010.

[60] G. Binnig, C. F. Quate, and Ch. Gerber. “Atomic Force Microscope”. In: *Physical Review Letters* 56.9 (Mar. 1986), pp. 930–933.

[61] Chin Wee Shong, Chorng Haur Sow, and Andrew T. S. Wee. *Science at the Nanoscale: An Introductory Textbook*. en. Google-Books-ID: jnr3YMNxAjMC. Pan Stanford Publishing, 2010.

[62] Linda Hofherr, Christine Müller-Renno, and Christiane Ziegler. “FluidFM as a tool to study adhesion forces of bacteria - Optimization of parameters and comparison to conventional bacterial probe Scanning Force Spectroscopy”. en. In: *PLOS ONE* 15.7 (July 2020), e0227395.

[63] Martin P. Stewart et al. “Wedged AFM-cantilevers for parallel plate cell mechanics”. en. In: *Methods*. Nanoimaging Methods for Biomedicine 60.2 (Apr. 2013), pp. 186–194.

[64] Félix Rico et al. “Probing mechanical properties of living cells by atomic force microscopy with blunted pyramidal cantilever tips”. In: *Physical Review E* 72.2 (Aug. 2005), p. 021914.

[65] Bruno Torre, Davide Ricci, and Pier Carlo Braga. “How the Atomic Force Microscope Works?” en. In: ed. by Pier Carlo Braga and Davide Ricci. Methods in Molecular Biology. Totowa, NJ: Humana Press, 2011, pp. 3–18.

[66] N. Moldovan, Keun-Ho Kim, and H.D. Espinosa. “Design and fabrication of a novel microfluidic nanoprobe”. In: *Journal of Microelectromechanical Systems* 15.1 (Feb. 2006), pp. 204–213.

[67] Vincent Martinez et al. “SU-8 hollow cantilevers for AFM cell adhesion studies”. en. In: *Journal of Micromechanics and Microengineering* 26.5 (Apr. 2016), p. 055006.

[68] Maria Tenje et al. “Drift study of SU8 cantilevers in liquid and gaseous environments”. en. In: *Ultramicroscopy*. 11th International Scanning Probe Microscopy Conference 110.6 (May 2010), pp. 596–598.

[69] Andres Diaz Lantada and Pilar Morgado. “Rapid Prototyping for Biomedical Engineering: Current Capabilities and Challenges”. In: *Annual review of biomedical engineering* 14 (Apr. 2012), pp. 73–96.

[70] Kwang-Sup Lee et al. “Recent developments in the use of two□photon polymerization in precise 2D and 3D microfabrications”. In: *Polymers for Advanced Technologies* 17 (Feb. 2006), pp. 72–82.

[71] Zahra Faraji Rad, Philip D. Prewett, and Graham J. Davies. “High-resolution two-photon polymerization: the most versatile technique for the fabrication of microneedle arrays”. en. In: *Microsystems & Nanoengineering* 7.1 (Sept. 2021), pp. 1–17.

[72] *SLA vs. DLP: Guide to Resin 3D Printers*. en.

[73] .

[74] Nourin Alsharif et al. “Design and Realization of 3D Printed AFM Probes”. en. In: *Small* 14.19 (2018), p. 1800162.

[75] Robert C. L. N. Kramer et al. “Multiscale 3D-printing of microfluidic AFM cantilevers”. en. In: *Lab on a Chip* 20.2 (Jan. 2020), pp. 311–319.

[76] M.B. Blankespoor. “Liquid dosing on the micro-scale”. MA thesis. Delft University of Technology, 2022.

[77] P.F.J. van Altena. “Multiscale 3D printed polymer probes for single cell experiments”. MA thesis. Delft University of Technology, 202.

[78] Gerald Göring et al. “Tailored probes for atomic force microscopy fabricated by two-photon polymerization”. In: *Applied Physics Letters* 109.6 (2016), p. 063101.

II

Project

3D-printed multifunctional microfluidic AFM cantilever

Abstract

Much research is conducted on the biomechanical properties of cells, particularly in cancer research. Cell stiffness and cell adhesion are two properties often studied, because they are important for the functioning of a cell. To study these properties, atomic force microscopy(AFM) is often used, using nanoindentation for stiffness analysis and fluid force microscopy(FluidFM) for adhesion analysis. However, these techniques often involve different cantilever probes, which complicates the measurement of both properties in a single cell. To make it possible to study cell stiffness and cell adhesion of a single cell, a multifunctional microfluidic AFM cantilever is developed in this research. This cantilever is equipped with a blunted pyramid-shaped tip for nanoindentation enabling the measurement of cell stiffness and imaging. Moreover, it features a channel running through its length, with an aperture on the tip, facilitating fluid force microscopy for determining cell adhesion. The multifunctional cantilever is fabricated using a multiscale 3d-printing technique, where stereo lithography is used for the larger parts, and two-photon polymerisation is used for the cantilever.

To demonstrate the capabilities of the cantilever, tests are conducted on various substrates. Nanoindentation is demonstrated on PDMS, hydrogel and endothelial cells to determine the Young's modulus of these materials. Fluid force microscopy is showcased by examining prostate cancer cells (PCA-3), removing the cells from the substrate while measuring the adhesion forces. The imaging capabilities of the cantilever were also demonstrated by generating a height map and a Young's modulus map through quantitative imaging of a hydrogel spheroid. This research shows that combining the properties of nanoindentation and FluidFM cantilevers into a single cantilever is possible. Integrating these functionalities into a single cantilever makes doing more mechanical measurements on a single cell possible.

4.1. Introduction

There is a lot of interest in studying the mechanical properties of cells. This fairly new research field has come up over the last two decades. Until then, most cell research was focused on the chemical processes of cells. The physical properties of cells are important for cell behaviour, if there are changes in the cell properties, cell behaviour will change dramatically. Cells also monitor their surroundings and react to changes in the physical properties of their surroundings. The physical properties of its surroundings also change how cells develop over time. Generally, cells do not undergo significant physical changes throughout their lifespan, but it can happen. One of the main causes of changes in cells is disease. Especially cancers can change cell properties significantly. Therefore, cancer researchers dedicate a lot of effort to studying the physical properties of cells. Some of the observations of these researchers are that tumours have a higher stiffness than healthy tissue of the same type, and individual cancer cells are softer than their healthy counterparts also cell adhesion is lower [1]. These changes are even more pronounced for metastatic cancers. Cell stiffness and adhesion are two of the most important cell properties and are often the focus of cancer studies. The cell stiffness or elastic modulus measures the rigidity of a cell, and how well the cell keeps its shape under external forces. Measuring cell adhesion and cell stiffness is challenging, especially for individual cells. Measuring both the adhesion forces and Young's modulus of a single cell is nearly impossible.

4.1.1. Device specifications

A tool that is often used for single-cell research is the atomic force microscope(AFM), it can be used for studying cell adhesion and cell stiffness. An AFM uses microscopic cantilevers to examine the

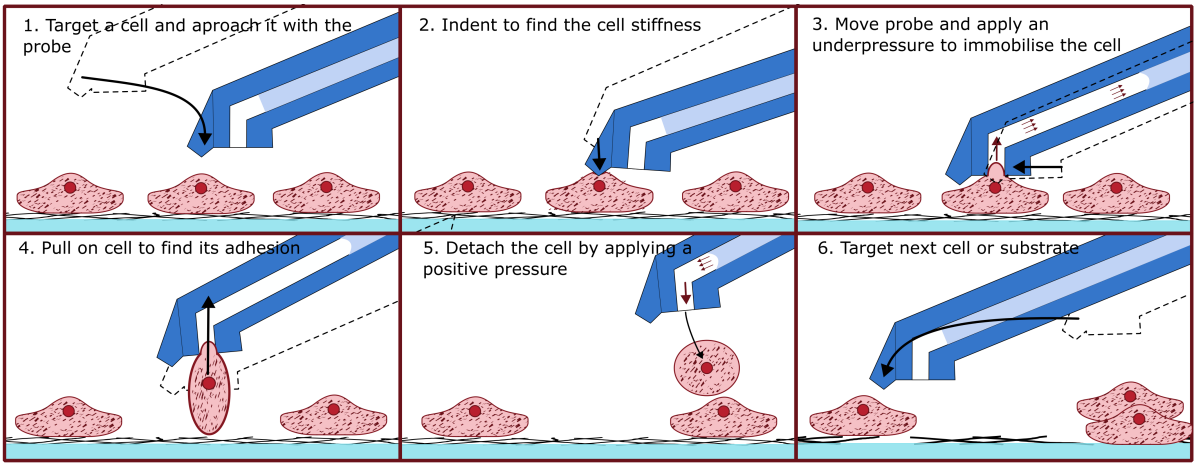

Figure 4.1: An experiment which would be made possible with a multifunctional cantilever. First, nanoindentation is done on a cell, then a fluid force microscopy measurement is done.

surface of a sample and conduct measurements. It can image and measure forces with an extremely high resolution. The functionality of the AFM depends in large part on the type of cantilever used. Studying both cell adhesion and cell stiffness with an AFM is done regularly, but it takes a lot of time and effort because a different cantilever is needed for the two measurements, the cantilever must be changed between a stiffness and an adhesion measurement, this makes it impractical to do both measurements on a single cell [2][3]. In practice, multiple experiments are done with different sets of cells. Having a cantilever which can do both measurements and does not need to be replaced in between would speed up research greatly and would also make it possible to measure the adhesion and stiffness of a single cell, this would help with finding relations between the two. Currently, a cantilever like this does not exist. In this project, a cantilever is developed to do both nanoindentations on cells to find the cell stiffness and Single Cell Force Spectroscopy(SCFS) with FluidFM to find the cell adhesion. It is able to do the experiment depicted in Figure 4.1, where a nanoindentation measurement is conducted on the cell, followed by a force spectroscopy measurement.

4.2. Theory

4.2.1. Atomic Force Microscopy

Atomic force microscopes are incredibly precise instruments which can image sub-nanometer structures and measure piconewton forces. The main working principle of an AFM is the following: a microcantilever physically cantilevers a surface where it interacts with local forces while the cantilever deflection is monitored. The monitoring is most often done by reflecting a laser on the cantilever and measuring the deflection angle change caused by tip interactions.

Scanning the cantilever over a surface can construct an image of the topography. Since the physical properties of the cantilever are known, properties like the stiffness and sensitivity, forces acting on the tip of the cantilever, can be determined very precisely using Hookes law, $F = -k \times D$, where F is the force k is the stiffness and D is the deflection. The functionality of the AFM depends on the type of cantilever used. The stiffness, natural frequencies, quality factor, and tip shape of the cantilever are all important for AFM measurements. Using the force measurement properties of the AFM, cell properties can be found.

The Young's modulus contributes to the cell stiffness and can be measured with *nanoindentation*. In this method, a cantilever is pressed into a cell for a small distance (100s of nm) and is retracted again, all the while the forces acting on the cantilever are recorded. This creates a force-distance curve. With a mathematical model, the Young's modulus can be derived from this curve.

Single Cell Force Spectroscopy *Single Cell Force Spectroscopy*(SCFS) is an AFM technique in which a cell is attached to the tip of a cantilever and pulled loose from its surroundings while the forces are monitored. During the experiment, the cantilever moves towards the cell until it makes contact and immobilises it. It retracts until the cell detaches from its surroundings, measuring the forces working on it during each step. This process generates a force-distance curve, which provides information about adhesion.

The immobilisation of the cell is historically

done with adhesives on the cantilever. Using adhesives has a downside in that cells are permanently fixed to the cantilever. After each measurement, the cantilever must be removed from the AFM and cleaned to detach the cell. This makes SCFS a slow and cumbersome method. Over the last decade, hollow cantilevers have been developed with a small aperture that can apply a negative pressure on the cell to immobilise it. This technique is called *FluidFM*. After the Force Spectroscopy measurement is done, positive pressure can be applied to detach the cell from the cantilever [4].FluidFM can test more cells in a single experiment without replacing the cantilever. Fluid FM can also be used to pick and place cells. A downside is that commercial FluidFM cantilevers are expensive and only a few variants exist.

FluidFM tip The properties of cantilevers for SCFS are different than those used for nanoindentation. AFM cantilevers used for SCFS are generally soft (<1N/m) to get the highest sensitivity, although, for some specific techniques, stiffer cantilevers are used[5]. These cantilevers are usually tipless; they have a flat surface where the measured cell can attach. Ideally, tipless cantilevers compensate for the approach angle of the AFM, so the cells touched will only be touched from the parallel with the substrate. No lateral forces will work on the cell; this can be achieved by creating a wedge at the tip [6].

To do fluid force microscopy, some more features are needed. There must be a channel running through the cantilever. The cantilever tip needs an aperture from which pressure can be applied to the sample. Also, the cantilever needs to connect to an external pressure source.

4.2.2. Quantative Imaging

There are a few methods for imaging cells with atomic force microscopy. In contact mode imaging, the cantilever tip is in direct contact with the surface, it scans the area that is imaged. The downsides are that it does not work well with living cells because they often move and are too soft to image this way. Also, the contact mode method wears down the tip quickly.

A second imaging method is Quantitative Imaging™(QI™). In QI™ mode, many indentations are made on a grid. The indentations are shallow and are made in milliseconds. Therefore QI™ can be used on cells without disturbing them. A complete force-distance curve is created for each pixel. An image is constructed by combining many indentations between the 126 and 2500 points on both X and Y axis. Since each pixel is a complete indentation, much information can be derived from a QI image. For example, the image can show the measured substrate's height, Young's modulus or adhesion force. This makes it a practical method to study cells and their properties because the local differences in elasticity can be mapped in high resolution.

4.2.3. Calculation of elastic modulus

Nanoindentations are used to find the stiffness of a sample by creating a force-distance curve. The apparent stiffness of a sample found by a force-distance curve is $k_{app} = \delta F/\delta$, where k_{app} is the apparent stiffness δF is the force acting on the sample and δ is the deformation [7]. The apparent stiffness depends on several factors, such as the contact area, indentation depth, surface interactions, and indentation speed. The sample deformations are modelled to find the Young's modulus, and the mechanical stress on the sample is calculated.

The basic contact models are the Hertz, Johnson–Kendall–Roberts(JKR) and Derjaguin–Müller–Toporov(DMT) models. The JKR and DMT models take into account the surface forces like adhesion where the Hertz model doesn't, the cell experiments in this research are done with water, and the surface forces are deemed low therefore, the focus in this research is on the Hertz contact model. The indentation models assume that the material is continuous and the strains are small. The indentations shouldn't be deeper than 20% of the substrate height to get reliable data.

The most basic Hertz model models the interactions of a sphere and a flat surface Equation 4.1. Derived models for different shaped tips exist(pyramid, conical). The blunted pyramid is spherical at its tip and pyramid shaped deeper. A model that changes from a spherical to a pyramid model when the indentation gets deeper is needed; the Hertz model for blunted pyramid is suitable for this, shown in Equation 4.2 [8][7].

$$
\begin{aligned}
&Hertz\,Model\,for\,a\,Sphere \\
&F = E_{eff} \cdot \left[\left(a^2 + R_p^2\right) \cdot ln\left(\frac{R_p + a}{R_p - a}\right) - 2aR_p \right] \\
&\delta = \frac{a}{2} ln \frac{R_p + a}{R_p - a}
\end{aligned}
\tag{4.1}
$$

$$Hertz\,Model\,for\,a\,Blunted\,Pyramid$$

$$F(\delta) = E_{eff} \cdot \left[\delta a - \frac{\sqrt{2}}{\pi}\frac{a^2}{tan(\theta)}\left(\frac{\pi}{2} - arcsin\left(\frac{b}{a}\right)\right) - \frac{a^3}{3R_p} + \sqrt{(a^2 - b^2)} \cdot \left(\frac{\sqrt{2}}{\pi}\frac{b}{tan(\theta)} + \frac{a^2 - b^2}{3R_p}\right)\right] \tag{4.2}$$

$$Effective\,Young's\,modulus$$

$$E_{eff} = \frac{E}{1 - \nu^2} \tag{4.3}$$

In these equations, F is the measured force, δ is the indentation,E_eff is the effective Young's modulus also known as the plain strain modulus, E is the Young's modulus, ν is the Poisson's ratio, a is the contact radius, b is the transition radius this is the point where the blunted pyramid goes from spherical to pyramid-shaped, θ is the angle of the pyramid, R_p is the tip radius of the pyramid. The Hertz model assumes the probe is axisymmetrical, a pyramid is not axisymmetrical, and the cross-section of the pyramid is modelled as a circle. In Equation 4.2 the effective Young's modulus is found from the indentation, to find the true Young's modulus Equation 4.3 is used. To get accurate values from this model the tip radius R_p, the transition radius b and the pyramid angle θ of the tip needs to be known. If an indentation with a blunted pyramid is less deep than the radius of the tip the simplest Hertz model for spheres, Equation 4.1, can be used.

A typical force-distance curve from an indentation is shown in Figure 4.2.a. The indentation model is fitted to the extension curve. The contact point, the point where the cantilever touches the surface, the baseline, the neutral deflection of the cantilever are indicated. From the retraction curve, the surface adhesion can be found.

4.2.4. Adhesion strength

Force-distance curves are created when removing a cell from a surface with force spectroscopy. Information about the adhesion between the cell and substrate can be derived from these curves. The total adhesion force can be measured. This is the entire force needed to release a cell from its environment. It can be found by measuring the distance between the minimum of the retraction curve and the baseline, Fmax in Figure 4.2.b. Also, the total adhesion energy can be found, which is needed to release a cell from its environment. It can be found by measuring the area between the retraction curve and the baseline, the green area in Figure 4.2.b. Also, adhesion forces of individual focal adhesion points can be derived from the force-distance curve, jumps in the retraction curve characterise these, indicated with arrows in Figure 4.2.b. The height of each jump corresponds with the adhesion force of that adhesion point. Combined with optical microscopy techniques, the adhesion forces can be correlated with specific focal adhesion points of the cell.

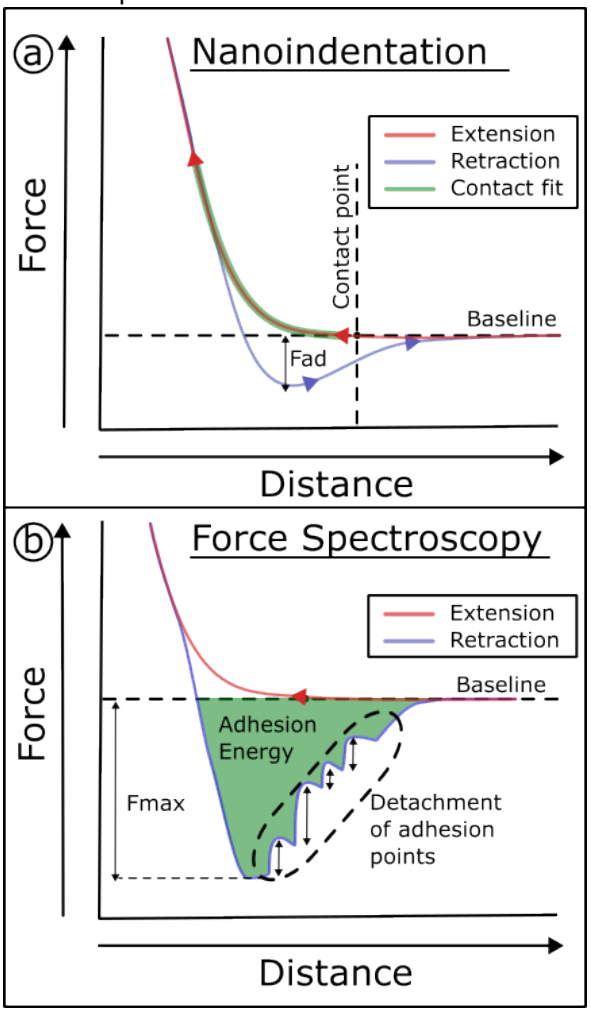

Figure 4.2: Examples of typical AFM force-distance curves, the extension of the cantilevers are shown in red, the retraction in blue. Figure (a) shows a curve from a nanoindentation measurement, the contact model fit in green, and the surface adhesion Fad is shown. The baseline and contact points are indicated. Figure (b) shows a Force spectroscopy curve. From the retraction curve the adhesion energy and adhesion force can be found.

4.2.5. Fabrication methods

Fabricating a multifunctional cantilever as suggested in Figure 4.1 would be very challenging with conventional fabrication methods. Traditionally AFM cantilevers have been manufactured us-

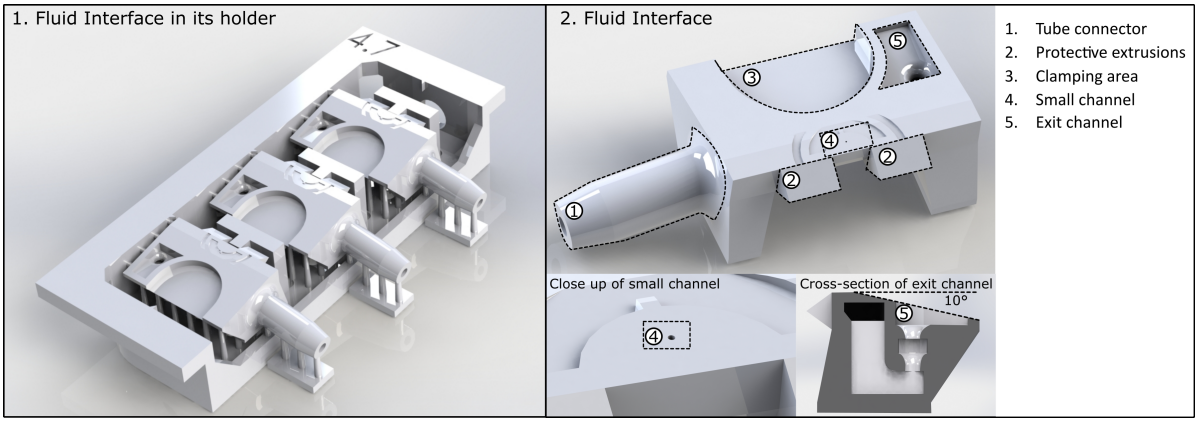

Figure 4.3: Figures of the fluid interface design. 1. Shows the fluid interfaces in its holder, the connecting pillars are also shown. 2. Shows an overview of the fluid interface with some parts highlighted. (1) The tube connector where an external tube for water or air is connected. (2) Protective extrusion, to prevent bumping the cantilever. (3) The clamping area for the cantilever holder. (4) The small channel where the cantilever is connected. (5) The exit channel. Once the fabrication process is completed, the exit channel, which aids fabrication, will be closed.

ing chip manufacturing methods like photolithography. Photolithography is a great method for large-scale high precision manufacturing. It has the downside that it is a 2.5D manufacturing method. It is not very suitable for producing complex 3-dimensional shapes. Also, it is difficult to customise designs since new masks need to be manufactured. Therefore manufacturing the multifunctional cantilever with photolithography is not ideal. Also, it typically takes weeks to manufacture a cantilever. Additive manufacturing is a more suitable method for manufacturing this cantilever, a novel multiscale additive manufacturing method for fluidic AFM cantilevers was developed by Kramer et al. [9][10]. In this process a combination of two additive manufacturing techniques is used for the fabrication of AFM cantilevers.With additive manufacturing, it is possible to make complex shapes. It is also faster than conventional methods, fabricating a new design takes a few days. Because of the added flexibility designs can be iterated upon quickly. A downside of the additive manufacturing method is that there is less experience with this technique for cantilever development. Also, the maximum resolution is slightly lower compared to conventional methods.

The cantilevers made with additive manufacturing in earlier research have a low laser sum (<0,5V) in comparison to commercial cantilevers (1V - 3V), this is bad for signal-to-noise ratio and must be improved for cantilevers to be practical [9][10].

4.3. Design

The design is split into two parts, the fluidic interface and the cantilever, which are produced with different methods and have different design considerations.

4.3.1. Fluid Interface design

The multifunctional cantilever is small and fragile. It is mounted on the fluid interface to handle and connect it to the outside world. The fluid interface has a channel for fluids or air to move through, which finishes in a small channel ($\varnothing 40 \mu m$) on top of the interface where the cantilever dome attaches. Also, there is a connection to mount a tube(Masterflex Transfer Tubing, Tygon® ND-100-80 Microbore, ID 1.02mm, OD 1.78mm). The fluid interface is designed to fit on the JPK cantilever holder(JPK Instruments), to make alignment and mounting easy, it is saddle-shaped, demonstrated in Figure 4.4a.

The surface on top of the holder is tilted 10 degrees to compensate for the 10-degree angle of the cantilever, this is done to make the cantilever parallel with the AFM cantilever holder as seen in Figure 4.4b. The fluid interface is as thin as possible, to counteract the distance effects of the AFM laser, 0,8mm total. The fluidic channels of the fluid interface and the cantilever can be seen in Figure 4.4b. The bottom edge of the part has a 45-degree taper to make it less likely to interfere with the AFM laser, Figure 4.4b.

The fluid interface has an exit hole to help development fluids move through the channels more easily, it has been positioned on top so it can be accessed easily. The channel can be closed by adding a small droplet of resin, surrounding the exit hole with a cavity for the resin to spread. The channel to the exit hole has a complicated geometry with several sharp edges to ensure the closing

resin won't flow through [11], Figure B.2.2.5. The top of the fluid interface has a few features to make it easier to find the print location of the cantilever in the 3d printer. The print platform is a semicircle with a protrusion from the centre which is aligned with the channel, there are concentric semicircles surrounding the print surface, which can help with finding the print area, as seen in Figure B.2.2.

The fluid interface has several features which help protect the fragile cantilever during handling. There is only one way for the cantilever to touch a surface. The main safety feature is the two extrusions from the front of the holder on the sides of the cantilever, the other feature is the 10-degree difference between the print surface and the clamping surface. Because of this angle, the holder can be put upside down while the cantilever stays suspended. The legs of the saddle on the front are aligned with the two extrusions so the holder can sit stably on its front without falling over and damaging the cantilever. The figures of the protected areas are in Figure B.2.2.

Three fluid interfaces are mounted in a basket connected with small breakaway pillars for fabrication. The basket is 24.80mm long and has a 0,80mm edge, Figure B.2.1 so it fits the multi-DiLL sample holder(NANOSCRIBE GmbH & Co. KG) which has 25mm x 25mm x 0,7mm spaces for substrates. The total height of the holder is 4mm so it fits in the NANOSCRIBE print slot. The interface is connected to the holder with thin $\varnothing 0,3mm$ pillars which become thinner where they attach to the fluid interfaces. To remove the fluid interfaces from the holder interfaces can be broken away from the pillars, seen in Figure B.2.1. The holders are aligned in such a way that the print surface for the cantilevers is horizontal. In front of the fluid interface, there is a T-shaped pillar. This pillar helps keep the NANOSCRIBE print resin in place, it sits 0,3mm lower than the print surface so it won't interfere with the printed cantilevers. The pillar is positioned such that there is a 150µm gap between it and the fluid interface this is small enough so there is no leakage of print resin.

4.3.2. Cantilever design

For the multifunctional AFM cantilever properties of nanoindentation cantilevers and FLuidFM cantilevers are combined. It will have a sharp tip to do indentations and a tipless part with an aperture where cells can be attached. The stiffness of the cantilever will be designed to be 0,6N/m, which is in the higher range for nanoindentation cantilevers but still useable for force spectroscopy.

Length is initially calculated analytically with the beam theory formulas for a one-sided fixed beam, with the second moment of area of a square tube, see Equation 4.4, the results are confirmed with Finite Element Modeling(COMSOL Multiphysics®).The cantilever should be a manageable length; a shorter cantilever will be better for QI imaging because of the higher natural frequencies. In QI mode the cantilever moves very quickly, which can cause resonations in the cantilever. Therefore the 2nd moment of inertia(I_z) should be as small as possible, so the cantilever should be as thin as possible. The cantilever Wall thickness is is 3,5µm with a 9µm channel, as shown in Figure 4.4d.

$$Spring\ constant\ and\ ideal\ length\ estimation$$

$$k_z = 3\frac{EI_z}{l^3}$$

$$I_z = \frac{w_o^3 h_o - w_i^3 h_i}{12}$$

$$L_{ideal} = \sqrt[3]{\frac{3EI_z}{k_{ideal}}} \tag{4.4}$$

$$Eigenfrequency$$

$$f \approx \frac{1.875^2}{\sqrt[3]{\frac{1}{3}}}\frac{\sqrt{\frac{k}{m}}}{2\pi} \tag{4.5}$$

Where k_z is the spring constant of the beam in the z-direction, I_z is the second-moment area, E is the Young's modulus of the material, l is the beam length, w_o and h_o are the width and height of the outside of a square beam, w_i and h_i are the width and height of the inside channel of a square tube, L_{ideal} is the length of the beam should to achieve desired stiffness k_{ideal} with the given parameters. In Equation 4.5, f is an estimation for the eigenfrequency, where k is the stiffness and m is the beam's mass.

The desired stiffness for the cantilever is 0,6N/m. With this stiffness, an ideal length of 430µm is found using Equation 4.4. The cantilever part of the cantilever is positioned at a 10-degree angle for optimal print results with smooth outer surfaces,Figure 4.4d.

The cantilever has an aperture with a diameter of 6µm, this is large enough to put an immobilisation force on a cell which is much greater than the adhesion forces, as calculated in Equation 4.6, where $F_{immobilise} \gg F_{adhesion}$ with an assumed negative pressure of p=800mbar [2]. The aperture is in the middle of a tipless area, which is tilted 10 degrees in relation to the cantilever, like a wedge, this is done to compensate for the tilt in the JPK

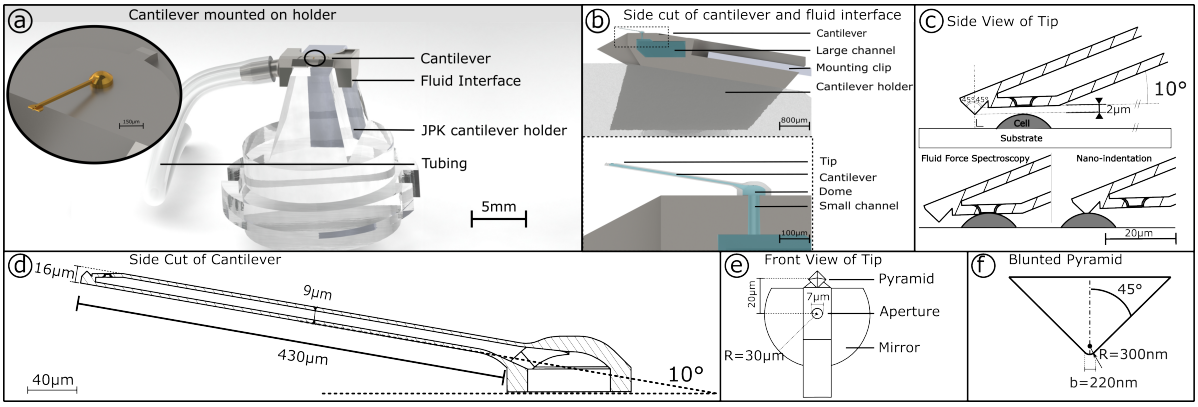

Figure 4.4: (a) Render of the cantilever on the cantilever holder with a tube connected. (b) Side cut of the cantilever and fluid interface, the channels are highlighted in blue. (c) Side view of the tip, the tip is shown with a cell and how it would be positioned when doing an indentation and force spectroscopy. The tip and aperture don't interfere with each other's measurements. (d) Side cut of the complete cantilever, the most important dimensions are shown. (e) Front view of the tip with some dimensions. (f) Figure of the side of the pyramid with the important dimensions.

cantilever holder, the tipless area will be parallel with the test substrate, as seen in Figure 4.4c.

$$
\begin{aligned}
&F_{immobilise} = p \times A = p \times \pi \times r^2 \\
&p = 800mbar \\
&r = 3\mu m \\
&F_{immobilise} = 1,41\mu N \\
&F_{adhesion} \approx 50nN \\
&F_{immobilise} \gg F_{adhesion}
\end{aligned}
\tag{4.6}
$$

The cantilever has a sharp tip at the front for indentation, it has the shape of a blunted pyramid with 45-degree edges and a tip radius of 300nm. It protrudes 2µm from the tipless area of the cantilever, as shown in Figure 4.4c. The pyramid is also tilted such that it faces the surface straight from the top, which commercial cantilevers don't do, this gives cleaner indentations with fewer lateral forces. The sharp tip and the aperture are spaced such that they won't interfere with each other's measurements. They are spaced for cells with a height of at least 2µm and a diameter of maximal 20µm, demonstrated in Figure 4.4c.

The movement of the tip of the cantilever is measured by reflecting a laser from the top of the cantilever and observing the movement of the reflected laser. To increase the reflectivity of the cantilever, the tip of the cantilever is made wider than the cantilever to reflect as much laser light as possible. The material used for the cantilever, IP-Dip, doesn't reflect light well and is transparent. To make the cantilever able to reflect the laser it is coated with gold. Gold is used because it is biocompatible, chemically inert and highly reflective.

The cantilever has a sharp tip and an aperture, during experiments it can be a challenge to align the right part of the cantilever with the desired part of the cell. To help with this, there are reference shapes on the side of the cantilevers at the height of the relevant features, a triangle for the pyramid and a half-circle for the aperture, which can be seen in Figure 4.4e. The widest part of the circle corresponds with the aperture and the corners of the pyramid correspond with the top.

The dome of the cantilever is the part that connects the cantilever to the fluid interface. It is shaped like a flattened hollow sphere. It has a 20µm thick wall which provides much surface area to adhere to the fluid interface. The sphere smoothly funnels the channel from the fluid interface into the cantilever to reduce resistance. The dome is not perfectly spherical, it is made flatter at the top to improve the printing time, it also is lifted 20µm at the bottom to make sure that the cantilever will be away from the surface, Figure 4.4c.

4.4. Materials and Methods

4.4.1. Fabrication methods

The cantilevers and the fluid interface are fabricated using additive manufacturing methods, for the cantilever Two Photon Polymerisation (2PP) and the fluid interface Stereolithography (SLA). The fabrication of the cantilever needs a few steps, they are summarised below.

1. SLA printing, printing and developing the fluid interface.

2. Laser Drilling, drilling a small channel in the fluid interface.

3. First gold coating, gold coat the fluid interface to assist the 2PP printing.

4. 2PP printing, printing and developing the cantilever on the fluid interface.
5. Second gold coating, coat the cantilever to make it reflective.

The parts are designed in a Computer-Aided Design (CAD) program, SOLIDWORKS (Dasault systems), and then processed with slicers to create a recipes for the 3d-printers.

Fabrication of fluid interface The fluid interface is manufactured with a stereolithography resin printer (Original PRUSA SL1S SPEED, Prusa Research) using photosensitive resin (Prusament Resin Tough Prusa Orange, Prusa Research) as the build material. This is a different printer and material than used in earlier research with the multiscale additive manufacturing approach, this printer has a higher pixel size (50µm VS 30µm) but is cheaper, quicker and easier to use [9]. The CAD file is processed with the PRUSA SLICER (V2.5.2 Prusa Research), using the 0.025 UltraDetail settings, which produces prints with a 25µm layer height. With this process, 16 holders, each holding three fluid interfaces, are printed in a single session. A printing session takes about 40 minutes. The prints are then developed in a bath of IPA (2-propanol, >99,5%, SIGMA-ALDRICH), for five minutes, twice. The prints are dried using a blow gun between baths, and extra attention is paid to clearing the channel.

Drilling of the aperture using LASER The desired channel diameter on top of the fluid interface is 40µm, which is smaller than achievable with the SLA printer. Therefore a laser cutter is used to drill the small channel. The laser cutter used is a LASEA (LS-Lab plus, LASEA SA), a 15W femtosecond laser cutter specialised for micromachining. To generate the smallest possible channel, the laser is operated in picture mode where the laser is pulsed in a single spot to drill a hole instead of drawing small circles to drill the channel Figure B.2.2.4. The settings used are described in Table 4.1.

Table 4.1: Settings LASEA LASER

Laser speed [µm/s]	800
Repetitions[#]	300
Power[%]	30
Pulse speed[Hz]	75018
Drawing	1µm circle
Working mode	Picture mode

Fabrication of microfluidic cantilever The multifunctional cantilever is fabricated with the NANOSCRIBE 3d printer (NANOSCRIBE Photonic Professional GT+, NANOSCRIBE GmbH & Co. KG). A state of the art 3d printer which uses a print technique called two-photon-polymerisation (2PP). This technique uses a focused laser beam to polymerise a negative photoresist (resin). The photoresist polymerises if two photons hit a monomer in the resin simultaneously. This can only happen when the light intensity is very high. This intensity is only reached in the most focused part of the laser, the voxel. The voxel position in the resin can be controlled and used to draw 3d structures. The thickness of the lines drawn is directly related to the size of the voxel. The voxel size is determined by the objective used; the higher the magnification of the objective, the smaller the voxel. Sub-micron features are desired for the multifunctional cantilever, so the highest magnification objective is used (63x /1.4 Oil Dic, Plan-APOCHROMAT, ZEISS). With this objective, a voxel size of roughly 300nm is produced.

The resin used for the cantilever is IP-Dip (NANOSCRIBE GmbH & Co. KG). IP-Dip is a biocompatible, non-cytotoxic photo-resist which can be used for sub-micrometre feature sizes [12]. The physical properties of the polymerised IP-Dip depend on the level of polymerisation. Not every part of the cantilever needs to have the same properties. The CAD model is split into three parts to optimise each part of the cantilever. Each part has different print settings to optimise its properties. The three parts are the *dome*, the *neck* and the *tip*. The three parts of the cantilever are sliced individually and are then combined again with the slicer (DeScribe NANOSCRIBE GmbH & Co. KG).

The dome is the part that attaches to the fluid interface, its print properties are optimised for maximal adhesion and print speed. The neck is the longest part of the cantilever with the fluidic channel, its print quality needs to be high so the surface can be used to reflect the AFM laser. Also, the properties need to be constant, and the detail needs to be high enough for the channel and aperture to be open. Finally, there is the tip, consisting of the blunted pyramid. It is the finest part of the cantilever, and its print properties are optimised for the maximum detail needed for the pyramid.

The material's properties are defined by the recipe used, the most important print properties are described in Table 4.2.

The cantilevers are printed with the NANOSCRIBE on top of the fluid interface. The fluid interface is loaded into the NANOSCRIBE and used as a substrate. The print is aligned to the small laser-drilled channel and started, printing takes

Table 4.2: The most important slicer settings for the NANOSCRIBE

	Laser Power [mW]	Laser Power [%]	Laser scanspeed [µm/s]	Slicing distance [µm]	Hatching distance [µm]	Galvo accerlation [V/ms^2]
Dome	37,5	75	90000	0.35	0.25	6
Cantilever	22,5	45	40000	0.2	0.2	6
Tip	25	50	50000	0.05-0.3	0.15	1

roughly 20 minutes. The printer is then aligned to the next holder, or the holder is removed from the printer. The sample needs to be developed after printing. The development consists of three steps: First the prints are put into a bath of PGMEA (Propylene glycol methyl ether acetate, SIGMA-ALDRICH) for 60 minutes. Then the print is put in a bath of IPA (2-propanol, >99,5%, SIGMA-ALDRICH) for 10 minutes and finally put in a bath of NOVEC™7100 (3M™) for 5 minutes. Between each step, the print is dried carefully with the air blower. A syringe is used to force development fluids in the channels during development.

Gold coating and post-processing The fluid interface and the cantilever are gold coated with a sputter coater (JEOL JFC-1300). The fluid interface is coated to help the NANOSCRIBE 3d printer locate the interface more easily, the top surface of the fluid interface is coated with a thin layer of gold (5̃nm). To make the cantilever reflective, the mirror side of the cantilever is coated with an 80nm layer of gold. The used settings for the sputter coater are in Table 4.3.

Table 4.3: Sputtercoater settings

	Fluid interface	Probe
Amperage [mA]	10	40
Time [s]	7	60
Layer height [nm]	4	80

After the 2PP printing is finished, the exit hole on the fluid interface is permanently closed, this is done by plugging the channel connector and adding a droplet of resin to the exit hole, the fluid interface is then cured for 8 minutes in the curing station (Photopol light curing unit, dentalfarm).

4.4.2. Cantilever characterisation and functional testing

Device characterisation The fabricated cantilevers are imaged with Keyence and Motic optical microscopes. A scanning electron microscope (SEM) is used (JEOL JSM-6010LA), operated with a 10kV electron acceleration for detailed images of the samples. The images created are analysed with Fiji(ImageJ 1.53t [13]).

An Atomic Force Microscope is used to characterise the fabricated cantilevers, the model used is the JPK Nanowizard 4 (JPK Instruments), with an inverted optical microscope (zeiss AxioObserver). It is used for all the AFM measurements, nanoindentation, Fluid FM, QI and contact imaging.

The JPK AFM has two methods for calibrating the spring constant and sensitivity of a cantilever, a contact-based and a non-contact method. The non-contact method is easier and faster than the contact method. It is not suitable to use for polymer cantilevers, because it relies on a high quality factor which can't be achieved easily with polymers.

For finding the stiffness of the cantilever, the contact mode calibration method of the JPK is used. This is a two-step method, first, a force curve is made on a hard surface, and second, a thermal noise measurement is done. The indentation creates a force-distance curve, the repulsive contact part of the graph is used for finding the sensitivity, in nm/V. In this part of the measurement, the movement of the piezo directly corresponds to the deflection of the cantilever.

In the thermal noise measurement, the vibrations caused by the thermal noise in the cantilever are measured. This results in a frequency amplitude graph with peaks around the natural frequencies of the cantilever. A fit is made around the eigenfrequency. From the thermal noise measurement, the spring constant is derived. A correction factor is needed to compensate for the difference in the bending shape of the cantilever between thermal noise and indentation [14], the correction factor is 0,817.This method determines the Quality factor, the natural frequency, the sensitivity and the spring constant.

Fluidic characterisation To check the fluidic capabilities and leakage water is pushed through the cantilever. Testing is done with filtered deionised water pushed with a 5ml syringe. Images are made using the ZEISS inverted microscope.

4.4.3. Imaging silicon reference chip

To demonstrate the imaging capabilities of the cantilever, a reference chip with 100nm deep patterns (SHS-0.1, Applied NanoStructures) is imaged, using contact mode imaging and QI imaging. The patterns are gratings and squares. The gratings are straight lines 2µm wide and repeated every 3µm, these are imaged in contact mode. The square holes are 2µmx2µm and are positioned in a grid 3µm apart, the squares are imaged in QI mode.

For both imaging methods the process is similar. The cantilever is calibrated as described in subsection 4.4.2, the sample is approached, and an image is started. The settings used in contact mode are: size 100µmx100µm, scanspeed 226µm/s, setpoint 28nN. The settings used in QI mode are: Z-length is 180nm, indentation speed 90µm/s, size 6µmx6µm, setpoint 30nN. The images created in both working modes are analysed in JPK SPM data processing (DP Version:8.0.45, JPK gwcl).

4.4.4. Method used for experiments with PDMS

The nanoindentation capabilities of the multifunctional cantilever are tested on a soft well-known material. The indentation tests are done on a commercial PDMS (Polydimethylsiloxane) sheet with an unknown Young's modulus. The Young's modulus for PDMS is between 1 and 6MPa depending on the amount of cross-linking and additives [15]. PDMS is used because of its relatively low stiffness. A reference is made to the AFM indenter with the multifunctional cantilever, using a known reliable indenter. For this, the Optics11 Life Piuma Nanoindenter with a cantilever with a 20µm spherical glass tip and a stiffness of 47.3N/m (Optics 11). The created force-distance curves are analysed with optics11 DataViewer V2.5.7 (Optics11).

The nanoindentation process with the AFM is as follows. First, the cantilever is calibrated as described in subsection 4.4.2. Then, a setpoint (10nN) and measurement length (5µm) and speed (3µm/s)are set. The AFM is programmed to make 16 indentations in a 4x5 grid where each point is spaced 10µm apart. The surface is approached with the cantilever and the measurements are started. The force-distance curves created are analysed with AtomicJ (version2.3.1 [16]), and further analysis is done in MATLAB (Mathworks).

4.4.5. Method used for experiments with hydrogel

A 3D-printed PNIPAM-based hydrogel half spheroid made to look like a cell is used to demonstrate the indentation and QI imaging capabilities on a soft cell-like material. The hydrogel is printed with the NANOSCRIBE 2PP 3d printer. The hydrogel is shaped like a half spheroid with a diameter of 45µm and a height of 12µm, an image of the CAD model is shown in Figure 4.9.4.

Nanoindentation is done in the same manner on the hydrogel spheroids as on the PDMS in subsection 4.4.4.

QI imaging is done on the hydrogel spheroids to make a height map and map the Young's modulus, the QI imaging is done similarly as in subsection 4.4.3. Some different settings are used: Z-length is 1,14µm, indentation speed 300µm/s, size 60µmx60µm, setpoint 3nN. The Young's modulus of the image is analysed with the JPK SPM data processing software(DP Version:8.0.45, JPK gwcl), used is the Hertz model for a spherical tip with a radius of 668nm, the spherical tip can be used because the QI indentations are only shallow.

4.4.6. Method used for experiments with cells

Experiments are done on endothelial cells(Human Umbilical Vein Endothelial Cells), and prostate cancer cells (PCA-3). Our collaborators at Erasmus MC in Rotterdam culture the cells in EBM2 medium(Lonza, Basel, Switzerland), supplemented with growth factors (EGM-2 SingleQuotsTM Sup-plements, Lonza). They use Petri dishes from TPP (Switzerland), which are compatible with the JPK Petri dish heater. To ensure the cells' safety during transport, they are placed inside a protective container for transportation from Rotterdam to TU Delft. At the TU Delft the cells are brought up to a temperature of 37°C with a portable incubator prototype. After the cells are brought up to temperature cell 1 ml of cell medium is added, to ensure that the cantilever and its holder are properly submerged. To keep cells alive during experiments they are mounted in the JPK Petri dish heater (JPK Instruments, Germany) which maintains a constant temperature of 37 °C.

Endothelial cells On the endothelial cells nanoindentations are performed to find the Young's modulus, this is done similarly to the hydrogel and PDMS substrates subsection 4.4.4.

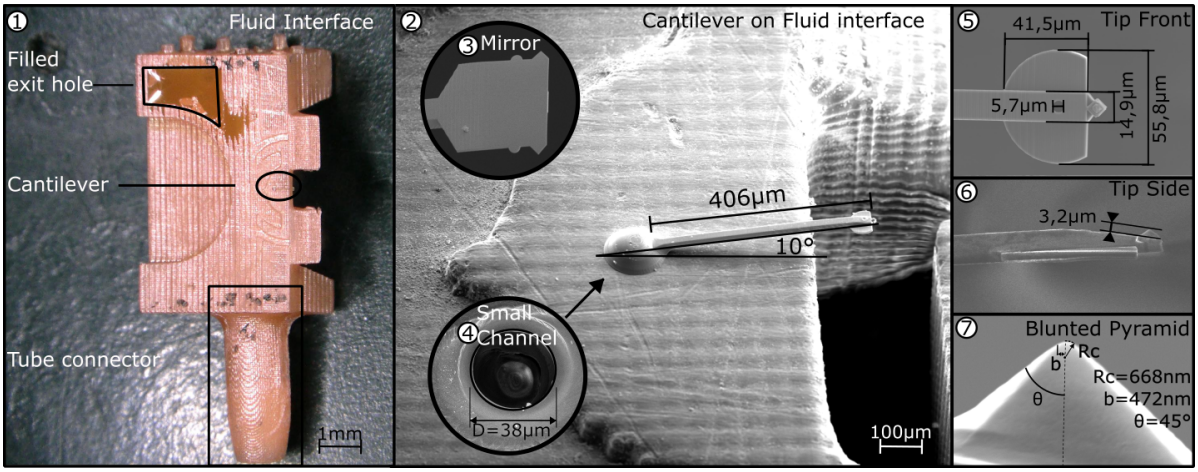

Figure 4.5: Microscope images of the fluid interface and cantilever. (1) Microscope image of fluid interface (orange) after fabrication. The exit hole is plugged, the cantilever is printed and the tube connector is ready. (2) SEM image of the cantilever on the fluid interface. (3) The mirror side of the cantilever (4) The small laser drilled channel, the cantilever is printed over this channel. (5) Detailed image of the front of the tip with dimensions. (6) Side of the tip, the offset between the tipless part and the tip is marked. (7) A closeup of the blunted pyramid tip with dimensions.

Prostate cancer cells On the prostate cancer cells, single-cell force spectroscopy is done to measure the cell-substrate adhesion, it is done using Fluid FM. For the SCFS, the CellHesion ®(JPK Instruments) module is installed on the AFM which extends the range of the piezos to 100µm. To control the air pressure during the SCFS experiments an Elveflow OB-1 pressure controller is used. For the experiment, a cell is selected. The cantilever is aligned with the cell so the aperture is on top of the nucleus. The cell is approached with the cantilever, a negative pressure of -800mbar is applied through the aperture. Then the cantilever is retracted for 50µm which removes the cell from the surface and a force-distance curve is created. The force-distance is analysed with the JPK data analysis software.

4.4.7. Reflectivity test

With earlier 3D-printed AFM cantilevers the laser signal was too small to be practical, to enhance the signal sum the multifunctional cantilever is equiped with a mirror. A cantilever is fabricated with a variable mirror-width to quantify the effects of the mirror's width on the laser signal sum. This mirror is tested in the AFM, the laser spot is aligned with different locations on the cantilever and the reflection sum is analysed.

4.5. Results and discussion

4.5.1. Fabricated cantilevers and interfaces

The dimensions of the cantilever are verified with the SEM shown in Figure 4.5. The length of the cantilever is 406µm, the tip radius of the cantilever is 668nm, 90-degree tip angle, and the transition radius is 472nm, the offset of the tip from the tipless area is 3,2µm,the aperture radius of the cantilever is 5.7µm, and the mirror surface of the cantilever is smooth.The found tip geometry(tip radius, pyramid angle, and transition radius, are important to know accurately for modelling the tip cell interactions with Equation 4.2. The hole drilled with the laser cutter in the fluid interface has a surface diameter of 38µm.

The dimensions of the cantilever are slightly smaller, ~5%, than their designed dimensions, except for the tip radius, which is more than twice the designed size, 668nm VS 300nm. The smaller dimensions might be caused by the curing process or an artefact of printing. The limited resolution of the 2PP printing process causes the larger tip radius.

4.5.2. Effect of tip width on the laser sum

The effect of the tip width on the laser sum is tested in an experiment In Figure 4.6, it is found that the laser sum becomes greater when the cantilever tip is wider, with an optimum around a width of 68µm. The reason for this effect might be that the laser is a focused beam and that the tip of the cantilever is not positioned in the voxel of the laser. This could be caused by the fluid interface, which is thicker than the conventional silicon chips used for AFM cantilevers (0,15mm against 0,8mm). A solution to this would be to make the fluid interface thinner, which is currently not possible with the SLA printer, or design a fluid interface for the CYTOSURGE

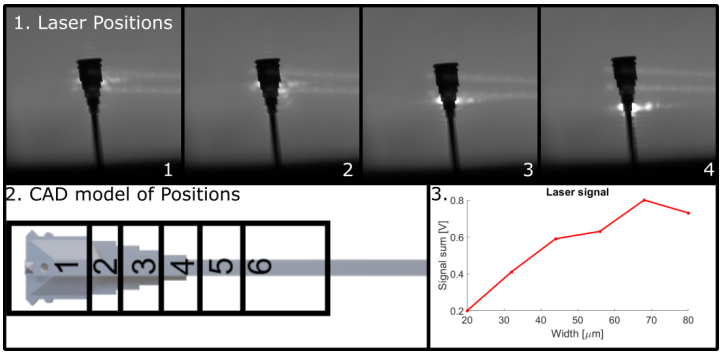

Figure 4.6: 1. shows the position of the laser spot on the cantilever. 2. Shows the CAD model of the cantilever with the variable width. 3. Shows the results in a width - laser sum graph

Table 4.4: Laser signal

Area	Width [µm]	Signal [V]
Widest	20	0,2
2	20	0,2
3	32	0,41
4	44	0,59
5	56	0,63
6	68	0,8
Further	80	0,73

JPK cantilever holder, which might provide more height.

4.5.3. Nanoindentation results

Nanoindentation measurements are done on PDMS, hydrogel spheroids and endothelial cells. Indentations on PDMS are done with two methods, with the multifunctional cantilever and with a commercial PIUMA indenter. On PDMS, an average Young's modulus of 2.86MPa is found with the PIUMA indenter over nine indentations, and an average Young's modulus of 2,77MPa is found with the multifunctional cantilever in the AFM over 18 indentations. Boxplots of the measurements and a typical force-distance curve are shown in Figure 4.7. The retraction curve made with the multifunctional cantilever, Figure 4.7a, shows a large downward peak, implying much adhesion between the tip and the substrate. Also, Figure 4.7a.1 shows an oscillating baseline where it should be flat. The oscillating effect is regularly observed in force-distance curves created with the multifunctional cantilever. The oscillation might be caused by interference in the AFM laser [17]. Although the absolute mean values of the commercial indenter and the multifunctional cantilever are similar, the data spread of the commercial indenter is smaller. Since the found values are similar, the multifunctional cantilever can be used for nanoindentations on soft surfaces.

The second indented surface is made of 3D-printed hydrogel, 20 indentations are done, and a mean Young's modulus of 30,77kPa is found. This is the range for this material [18]. The spread of the measurements is shown Figure 4.7b. The extension and retraction curve are shown in the Figure 4.7a.2. The retraction curve does not meet the extension, which it should do. This indicates that some force keeps the cantilever from relaxing completely, which might be surface adhesion, but it is most likely hydrodynamic drag [17]. Hydrodynamic drag would mean that the indentation is done too fast and that this misalignment disappears if done slower.

Indentations are also done on live endothelial cells. A box plot over 18 indentations is shown in Figure 4.7b, a mean Youngs's modulus of 2,85kPa is found which is a realistic value according to literature[19]. The typical force-distance curve of the endothelial cell is shown in Figure 4.7a.3, it is smooth with no peaks in both the extension and the retraction phase, which indicates low surface adhesion.

4.5.4. Imaging results

Imaging reference chip Imaging is initially done on a silicon test sample with a height of 100nm. The contact mode imaging is demonstrated on the linear gratings of the chip; the result is shown in Figure 4.8a. The shape and size of the gratings are visible. The average measured distance between each grating is 3,038µm, where it should be 3.00µm, this is relatively accurate considering the blunt tip. In Figure 4.8a, a cross-section of the grating is shown, the gratings can be seen clearly, but are not smooth, and the total height is not always 100nm.

A different part of the chip is imaged in QI mode. This part has a grid of squares recessed 100nm. A height map is shown in Figure 4.8b. The squares are seen clearly in this image, but the corners are rounded compared to the SEM image. No Young's modulus map could be made of the chip in QI mode because the Silicon is too hard to make an indentation. The reference sample is slightly damaged, which you can also see in SEM images, which might explain some irregularities.

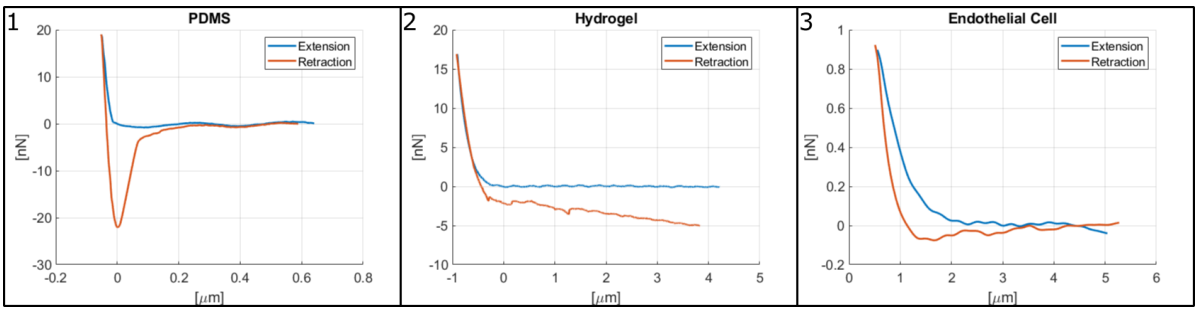

(a)

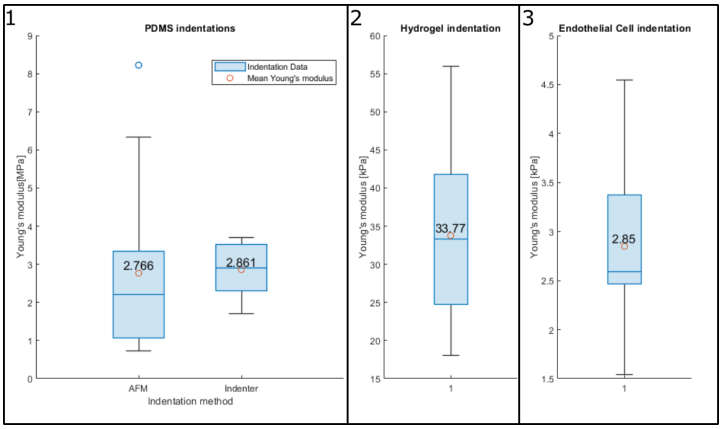

(b)

Figure 4.7: Indentation results. Figure (a) shows typical force-distance curves of nanoindentation done with the multifunctional cantilever on PDMS, hydrogel and living endothelial cells. Figure (b) shows boxplots with the resulting Young's moduli from the nanoindentations. For reference, nanoindentation is also done with a commercial indenter on PDMS.

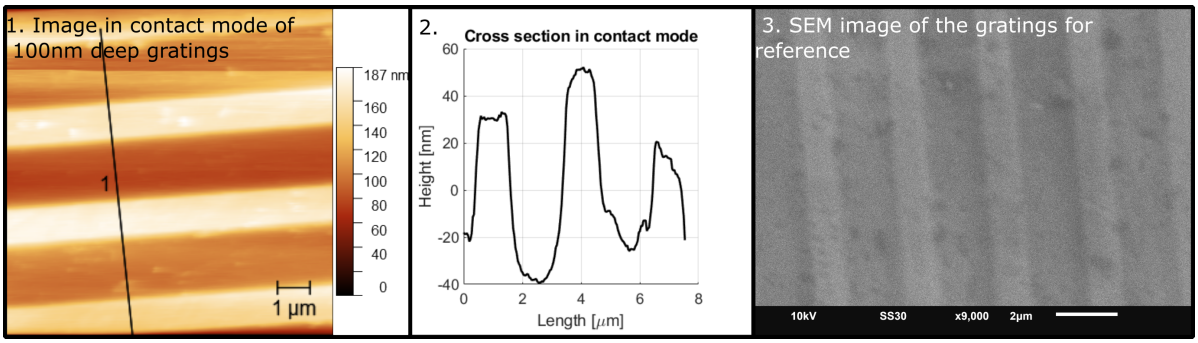

(a)

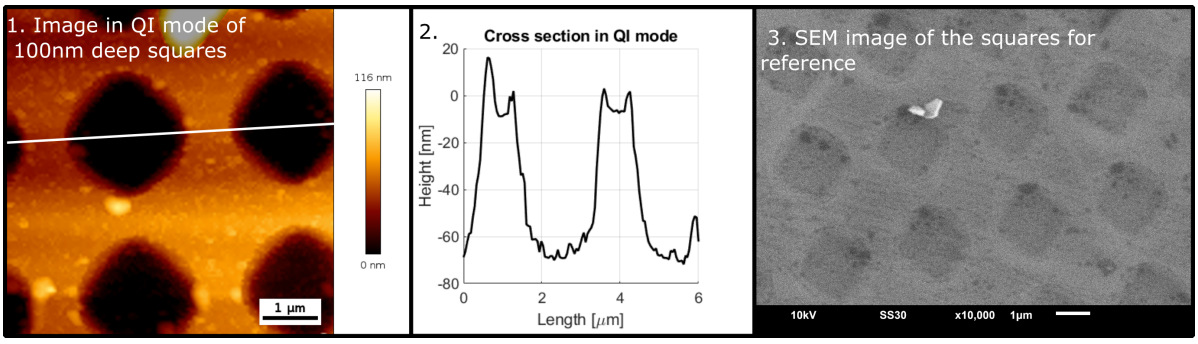

(b)

Figure 4.8: Imaging results, Figures (a) and (b) are images and a cross-section of gratings on the reference chip made in contact mode. Figure (c) is a QI image of squares on the reference chip. (d) are SEM images of the reference chip. The top are the squares and the bottom are the gratings.

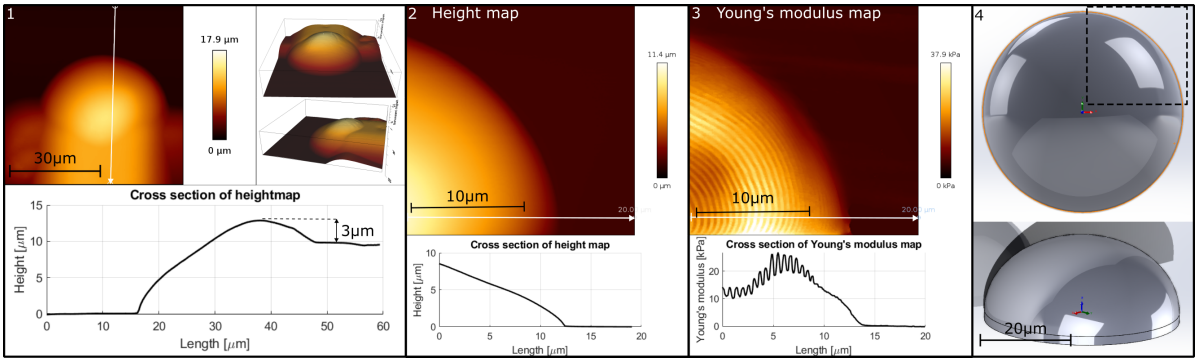

Figure 4.9: Images of a hydrogel half spheroid imaged in QI mode with the multifunctional cantilever. (1) Is a height map of the complete spheroid, the bottom is truncated. (2) Is a 3d image generated from image (1). (3) shows a cross-section of (1) where the truncated part can be seen clearly. (4) is a height map of the top right quadrant of the spheroid, and a crosssection. (5) It is the same image as in (4) analysed for the Young's modulus, also with a cross section. Periodic differences in the Young's are observed. (6) A top and side view of a CAD image of the spheroid, the top quadrant analysed in image (4) and (5) is marked with a dotted line.

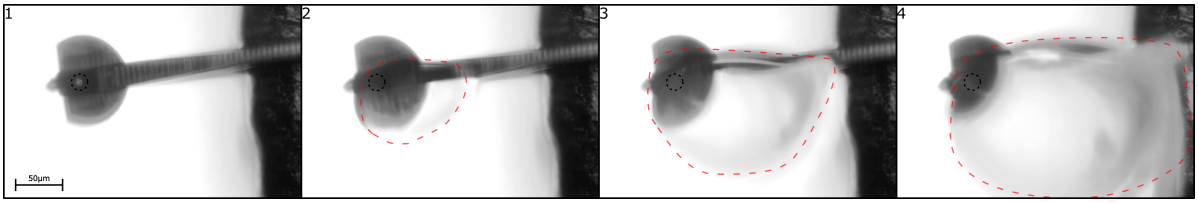

(a)

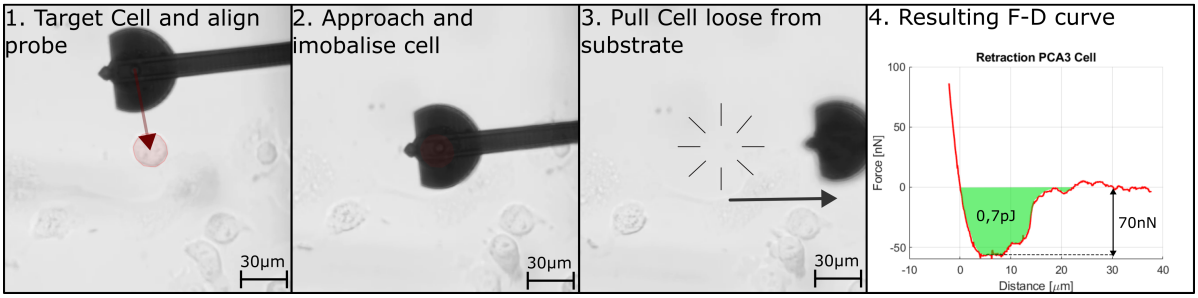

(b)

Figure 4.10: Fluid Force microscopy results. (a) Pushing fluid through the cantilever, the edge of the growing droplet is marked with red. (b) A cell, marked in red, is removed from a substrate using Fluid FM capabilities of the cantilever. In image 1, a cell(red) is targeted, and the cantilever is moved over it. In image 2, the cantilever approaches the cell and a negative pressure is applied to immobilise it. In image 3, the cantilever is moved upward until the cell is removed from the surface and the cantilever is moved away. Figure 4, shows the produced force-distance curve from the cell removal.

Hydrogel Hydrogel spheroids are the second substrate that has been imaged. A height map image is made of the whole spheroid, the result is shown in Figure 4.9 images 1 to 3. The top half of image 1 looks as expected, like a half sphere but slightly deformed, the bottom half of image 1 looks different. This is caused by the pyramid tip of the multifunctional cantilever which protrudes only 3µm from the tipless area of the cantilever and cannot reach all the way across the sphere. In Figure 4.9.3 a height graph is shown on the y-axis of image 1, in the graph, you can see clearly that the graph is truncated 3µm under the top, this is consistent with Figure 4.5.6 where a tip-height of 3,5µm is found.

Secondly, a QI image is made of the top right quadrant of the spheroid, the area marked with a dotted line in Figure 4.9.6. In Figure 4.9.4 the height map is shown with a graph, the graph is smooth. In Figure 4.9.5 a Young's modulus analysis of the same image is done. This image is not smooth, concentric circles are shown where the Young's modulus is slightly different. These rings suggest different levels of polymerisation in the hydrogel, likely an artefact of the 3d printing process used to create the hydrogel spheroid.

4.5.5. Fluid FM

The open fluidic channels of the cantilever are demonstrated in Figure 4.10a, where water is pushed through the cantilever and the aperture to create a droplet. Assuming the droplet is spherical a droplet with a volume of a few dozen picoliters is produced.

FluidFM is demonstrated in Figure 4.10b, where a PCA cell is targeted for removal is removed and a force-distance curve is made. The retraction force-distance curve is shown in Figure 4.10b.4 from which the adhesion forces can be derived. The total adhesion force of the cell to the substrate is 70nN and the total adhesion energy is 0,7pJ.The cantilever can do Fluid FM and remove single cells from a substrate. However, more tests are needed for complete validation.

4.5.6. Physical properties cantilever

The cantilevers are calibrated in the AFM using the contact mode calibration method. This method uses two measurements an indentation on a hard surface, and a thermal noise measurement, with these two measurements, the stiffness, natural frequency, sensitivity and Q-factor of the cantilever are determined, the values of these properties are shown in Table 4.5. The physical properties of the cantilever are modelled in two ways with back-of-the-envelope calculations Equation 4.4, and a FEM model, a Young's modulus of 3,1GPa is used. The results are in Table 4.5. The laser signal for this cantilever is on average 1V but up to 3V is observed. This improves the signal-to-noise ratio and reduces problems like drift, a big problem in earlier research.

Table 4.5: The physical properties of the multifunctional cantilever

Stiffness [N/m]	0,66	$\pm$ 0,1
Natural frequency (in air)[kHz]	23	$\pm$ 2000
Sensitivity [V/nm]	12	$\pm$ 36
Laser signal [V]	1	$\pm$ 0,5
Q-factor	15	$\pm$ 4
Length cantilever [µm]	406	
width [µm]	15	
height [µm]	15	
Channel wall thickness [µm]	3,5	
Aperture diameter [µm]	5,7	
Tip radius [nm]	668	
Transition radius [nm]	472	
Pyramid angle [°]	45	

4.6. Conclusion

In this project, a novel multifunctional AFM cantilever is designed and fabricated to do nanoindentation and Fluid force microscopy.

The cantilever tip has several features never combined before, an indentation tip and a Fluid FM tip for force spectroscopy. The indentation tip is blunted pyramid-shaped, it is placed such that it is perpendicular to a substrate for optimal indentations, it can also be used for imaging. The tipless part has an aperture from which an underpressure can be applied, or fluids can be dispensed, the aperture is placed on a wedge parallel to the substrate. The cantilever has a large mirror to improve the signal, with features that make alignment easy. The laser signal is much higher because of the large mirror than in earlier research, which improves the signal-to-noise ratio and eliminates earlier problems like drift.

The cantilever is hollow and the thinnest 3d printed hollow AFM cantilever ever printed, with a height and with of 16µm and a wall thickness of 3,5µm. It is printed on an angle for optimal print quality. The fluid interface is also angled to compensate for the cantilever print angle.

The multifunctional cantilever design is tested and verified to be used for nanoindentation, Fluid FM, and imaging soft surfaces. With this cantilever, the stiffness and adhesion of a single cell can be measured, which couldn't be done before.

Outlook

Thesis conclusion

In this project, a multifunctional cantilever has been developed, making it possible to combine several experiments into one. In the literature study, a research question is asked:

How to combine indentation and fluid force microscopy in a single atomic force microscopy probe using multiscale additive manufacturing?

The answers found are the following. The multifunctional cantilever needs a new tip shape. This multifunctional tip has a sharp tip for indenting and imaging and a tipless part for force spectroscopy. For nanoindentation it has blunted pyramid tip which can also be used for imaging. For FluidFM, it features a channel running through its length, with an aperture on the tip, facilitating fluid force microscopy. The cantilever needs a stiffness which works for both nanoindentation measurements and force spectroscopy, a stiffness of 0,55N/m works for both. Nanoindentation is demonstrated on PDMS hydrogel and endothelial cells. Fluid FM is demonstrated on PCA-3 cells, the results are promising but more research is necessary.

This research shows that combining the properties of nanoindentation and FluidFM cantilevers into a single cantilever is possible. Integrating these functionalities into a single cantilever makes doing more mechanical measurements on a single cell possible.

Main innovations

- Tip shape: Never before is a tipless FluidFM tip combined with a sharp pyramid tip.
- Mirror: A mirror is added to the cantilever tip to improve reflection. This increases the laser signal sum in the AFM to a much higher level than was possible before with 3d-printed cantilevers.
- Alignment features: The tip has distinctive features to make precise alignment easier.
- Experiment: Never has Fluid FM and Nanoindentation been done on cells with a single cantilever, which is made possible by the multifunctional cantilever.
- Size: The cantilever is thinner than the earlier cantilevers at the TU Delft.

Recommendations

In this section a few recommendations for further research are given.

Continuing this research:

More measurements Perform more measurements with the multifuntional cantilever to get more statistically significant results

Specialized cantilevers Design more specialised cantilevers for QI mode and Microrheology, the multifunctional cantilever is capable of doing both, but it isn't optimised.

Design improvements

Photonic crystal mirror Integrate the reflective mirror into the design of the cantilever so no gold coating is needed, this can be done with Photonic crystals such as a Bragg reflector, some literature is found in section D.5.

Other cantilever holder Redesign the fluid interface for the Cytosurge cantilever holder, with this you might be able to bring the cantilever closer to the laser voxel, and then you won't need an enlarged mirror.

Different fabrication techniques fluid interface Use a different fabrication technique for the fluid interface, something with more reliable properties than 3d printed resin.

Materials for fluid interface Test more materials for the fluid interface and the nanoscribe. The material used with the PRUSA printer was used because it was available and worked. But better materials must be out there, which might have a higher resolution, better bonding with the IP-DIP and might be easier to find automatically.

Parametric design of AFM cantilever Make an automated CAD program to easily customize cantilevers for specific applications. The user provides a desired stiffness and tip shape and a design is created automatically, a parametric design approach.

Automate the interface finding with NANOSCRIBE Use SERVERMODE to let a Python script automate the Nanoscribe printing, which could find the print location and make large-scale cantilever production possible.

Cantilever coatings Cells sometimes stick to the cantilever. A coating might solve this. Adding microstructures to the cantilever also works, making the cell hydrophobic by adding small lotus leaf-inspired hairs for example.

Improving testing.

Automated multifunctional testing AFM Make an automatic test script for the JPK AFM to do both nanoindentation and Fluid FM on a single cell. The user selects a target, and the tip is moved automatically and adjusts its position on the cell depending on the type of measurement.

Smart AFM test setups Develop smarter test setups in the AFM, for example, multiple cell wells where different cells can be cultivated. Fluid FM then moves cells from one location to the next to study the cell-cell interactions.

Add automated pressure control to AFM Add automatic pressure control to the JPK AFM software using a Python script to make Fluid FM easier.

Poisson ratio instruments Develop an easy method for measuring the Poisson ratio of a cell, in this study and most literature cells are assumed incompressible $\nu = 0,5$ but this is not always the case, currently it is challenging to measure the poison ratio of a cell.

With the multifunctional cantilever and some improvements, many new possibilities will open for cell research.

Bibliography

[1] Małgorzata Lekka. “Discrimination Between Normal and Cancerous Cells Using AFM”. eng. In: *BioNanoScience* 6 (2016), pp. 65–80.

[2] Livia Angeloni et al. “Fluidic Force Microscopy and Atomic Force Microscopy Unveil New Insights into the Interactions of Preosteoblasts with 3D-Printed Submicron Patterns”. en. In: *Small* 19.2 (2023), p. 2204662.

[3] Sharareh Jalali et al. “Regulation of Endothelial Cell Adherence and Elastic Modulus by Substrate Stiffness”. eng. In: *Cell Communication & Adhesion* 22.2-6 (2015), pp. 79–89.

[4] Orane Guillaume-Gentil et al. “Force-controlled manipulation of single cells: from AFM to FluidFM”. en. In: *Trends in Biotechnology* 32.7 (July 2014), pp. 381–388.

[5] Hui Xie et al. “In Situ Quantification of Living Cell Adhesion Forces: Single Cell Force Spectroscopy with a Nanotweezer”. In: *Langmuir* 30.10 (Mar. 2014), pp. 2952–2959.

[6] Martin P. Stewart et al. “Wedged AFM-cantilevers for parallel plate cell mechanics”. en. In: *Methods*. Nanoimaging Methods for Biomedicine 60.2 (Apr. 2013), pp. 186–194.

[7] Michael Krieg et al. “Atomic force microscopy-based mechanobiology”. en. In: *Nature Reviews Physics* 1.1 (Jan. 2019), pp. 41–57.

[8] Félix Rico et al. “Probing mechanical properties of living cells by atomic force microscopy with blunted pyramidal cantilever tips”. In: *Physical Review E* 72.2 (Aug. 2005), p. 021914.

[9] Robert C. L. N. Kramer et al. “Multiscale 3D-printing of microfluidic AFM cantilevers”. en. In: *Lab on a Chip* 20.2 (Jan. 2020), pp. 311–319.

[10] P.F.J. van Altena. “Multiscale 3D printed polymer probes for single cell experiments”. MA thesis. Delft University of Technology, 202.

[11] M.B. Blankespoor. “Liquid dosing on the micro-scale”. MA thesis. Delft University of Technology, 2022.

[12] *Nanoscribe photoresins specifically designed for Two-Photon Polymerization*. en-GB.

[13] Johannes Schindelin et al. “Fiji: an open-source platform for biological-image analysis”. en. In: *Nature Methods* 9.7 (July 2012), pp. 676–682.

[14] H.-J. Butt and M. Jaschke. “Calculation of thermal noise in atomic force microscopy”. en. In: *Nanotechnology* 6.1 (Jan. 1995), p. 1.

[15] Ronaldo Ariati et al. “Polydimethylsiloxane Composites Characterization and Its Applications: A Review”. In: *Polymers* 13.23 (Dec. 2021), p. 4258.

[16] Paweł Hermanowicz et al. “AtomicJ: An open source software for analysis of force curves”. In: *Review of Scientific Instruments* 85.6 (June 2014), p. 063703.

[17] JPK Instruments AG. *Nanowizard AFM Handbook Version 6.0*. JPK, 2018.

[18] Muhammad Abdul Haq, Yunlan Su, and Dujin Wang. “Mechanical properties of PNIPAM based hydrogels: A review”. en. In: *Materials Science and Engineering: C* 70 (Jan. 2017), pp. 842–855.

[19] R. Vargas-Pinto et al. “The Effect of the Endothelial Cell Cortex on Atomic Force Microscopy Measurements”. In: *Biophysical Journal* 105.2 (July 2013), pp. 300–309.

III

Appendix

A

Atomic force microscopy

A.1. Cantilever calibration

The JPK AFM has two methods for calibrating the spring constant and sensitivity of a cantilever, a contact-based and a non-contact method. The non-contact method is based on the method proposed by Sader [1], it is easier and quicker than the contact method. Shown in Equation A.1 it uses the thermal noise and properties of the medium and cantilever geometry to estimate the spring constant. Currently, it is not suitable to use directly for polymer cantilevers because it relies on high-quality factors that can't be achieved easily with polymers.

$$k = 0,1906\rho b^2 LQ\Gamma_i(\omega_R)\omega_R^2 \tag{A.1}$$

Where ρ the density of the medium L and b is the length and width of the cantilever, Q is the quality factor, Γ_i is a hydrodynamic function [2] and ω_R is the natural frequency of the cantilever.

The contact mode calibration method of the JPK is used to find the cantilever's stiffness. This method has two steps, first is making an indentation on a hard surface and the second is doing a thermal noise measurement. The indentation creates a force-distance curve, the repulsive contact part of the graph is used for finding the sensitivity, in nm/V. In this part of the measurement, the movement of the piezo directly corresponds to the deflection of the cantilever.

From the thermal noise measurement, the spring constant is derived. The method is based on work by Hutter [3], where the equipartition theorem is used to relate the fluctuations of the cantilever to the spring constant. Summarised, the thermal energy calculated from the absolute temperature should be equal to the energy measured from the oscillation of the spring [4]. The precise algorithm used by the software is not given but is based on the Sader method Equation A.1.

An example of calibration figures is shown in Figure A.1, where an indentation and a thermal noise measurement are seen.

A.2. Quantative imaging

Images of the settings used to image the hydrogel spheroids can be seen in Figure A.2.

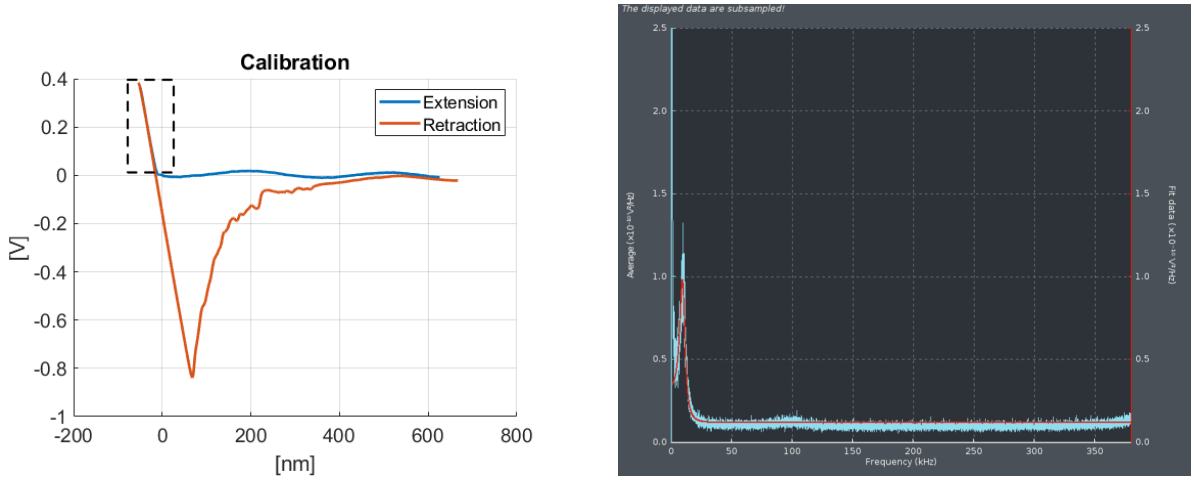

Figure A.1: Measurements used for calibration. Figure (a) shows an indentation on a hard surface used to find the sensitivity, the part of the curve used to find the sensitivity is marked. Figure (b) shows a thermal noise measurement of a cantilever in air, a high peak of 20kHz is seen a secondary lower peak is around 100kHz.

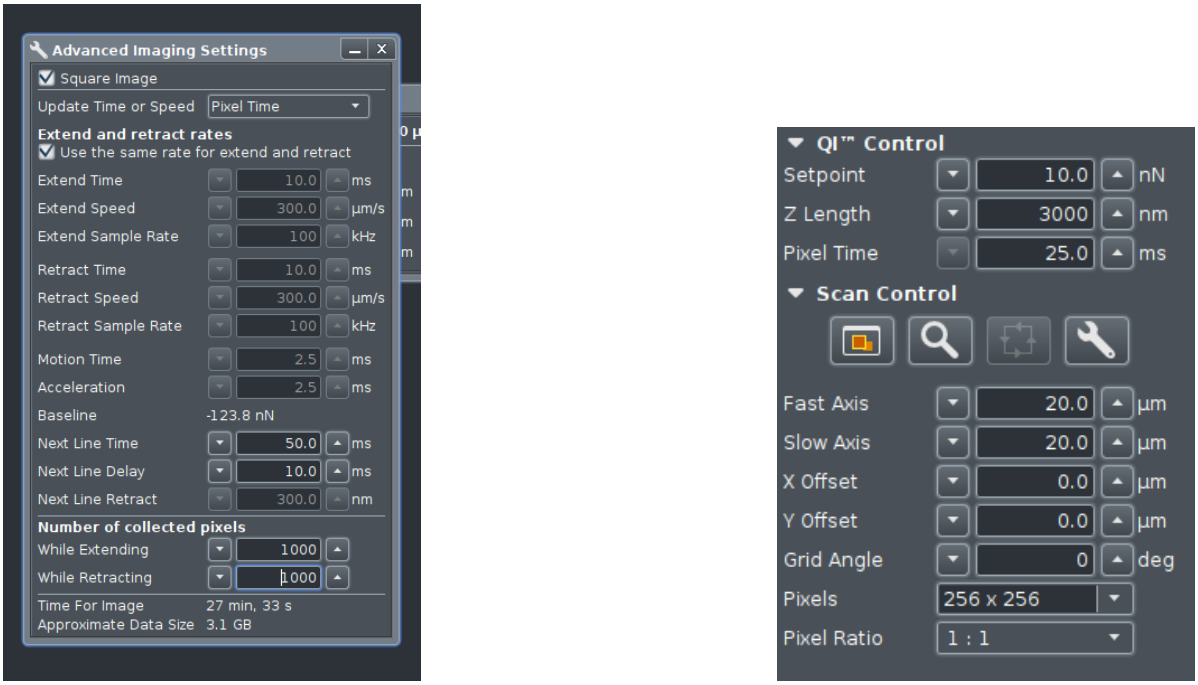

Figure A.2: The settings used for imaging hydrogel spheroids in QI mode

Figure A.3: A cantilever mounted on the JPK cantilever holder

B

Design

B.1. Cantilever

Technical drawings of the cantilever are seen in Figure B.1

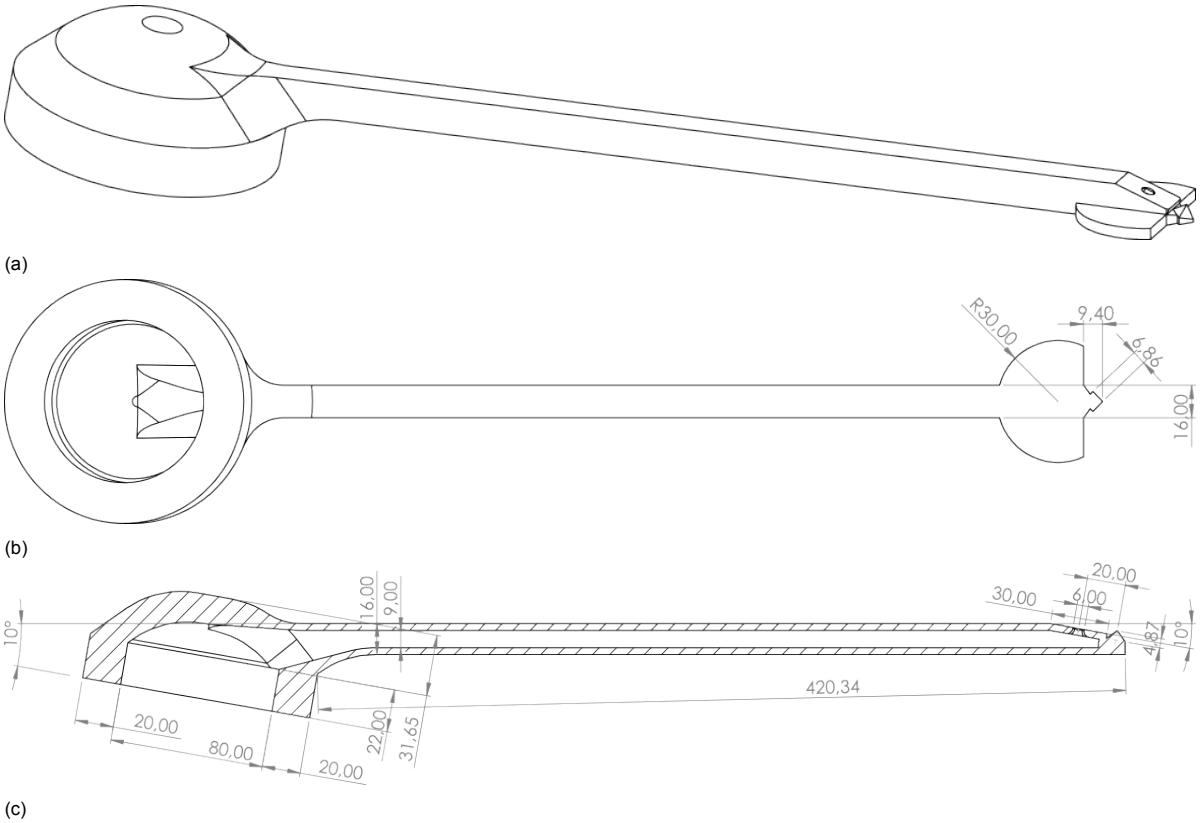

Figure B.1: Technical drawings of the multifunctional probe

B.2. Fluid interface

Technical drawings of the fluid interface and the basket can be found here in Figure B.2 and Figure B.3

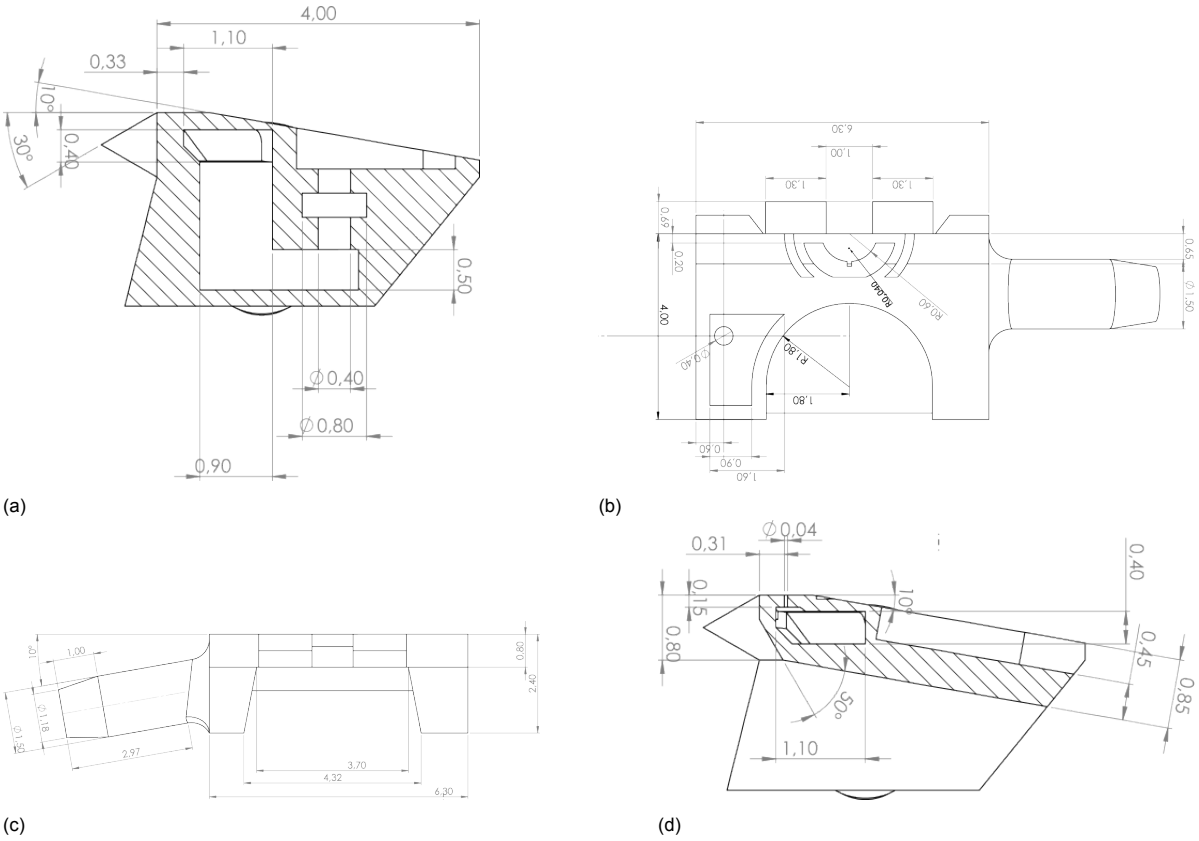

Figure B.2: Technical drawings of the fluidic interface

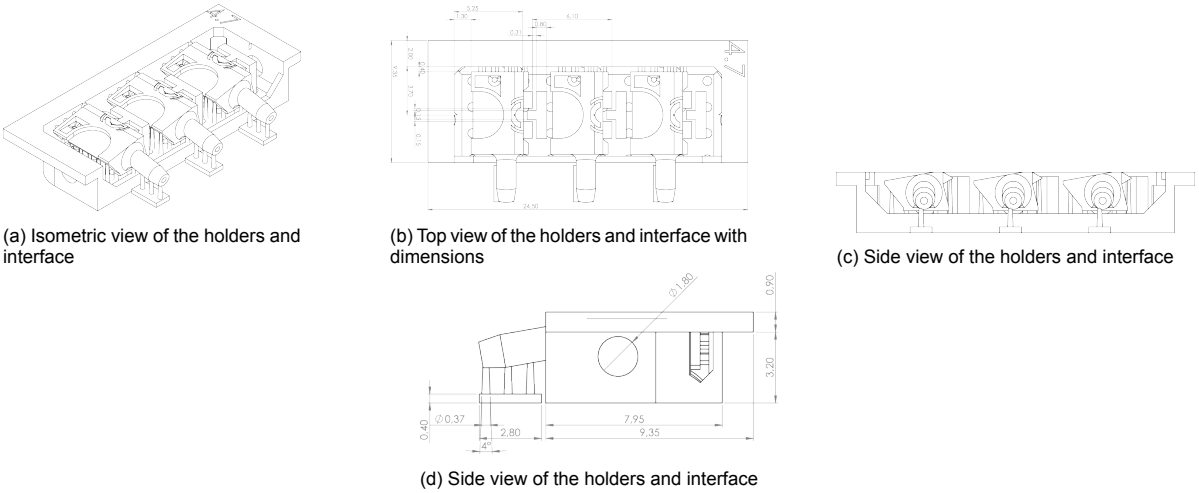

(a) Isometric view of the holders and interface

(b) Top view of the holders and interface with dimensions

(c) Side view of the holders and interface

(d) Side view of the holders and interface

Figure B.3: Technical drawings of the fluidic interface holder

C

Fabrication

The fabrication process of the multifunctional AFM cantilevers consists of several steps:

1. Print the fluidic interface with a resin printer, section C.1
2. Drill a channel in the fluidic interface with a laser cutter, section C.2
3. Coat the fluidic interface with a thin layer of gold, section C.3
4. Print the cantilever on top of the fluidic interface with the NANOSCRIBE
5. Close the exit hole of the fluidic interface, subsection C.4.4
6. Coat the cantilever with a thick layer of gold, section C.3

In this section, each step in the fabrication is explained.

C.1. Fluid Interface

For the fabrication process of the hollow cantilevers additive manufacturing is used. For the production of the cantilever two photon polymerisation is used, this is an additive manufacturing technique which can produce very small features up to 300nm. A downside to this technique is that it becomes slow when it is used for producing larger designs. Therefore, a different manufacturing method is chosen for the larger parts of the design. The methods chosen are Digital Light Processing(DLP) and Stereo lithography(SLA).

Two desktop resin printers are used to make the fluid interfaces: the EnvisionTEC Micro Plus HD plus HiRes printer(ETEC GmbH) and the PRUSA SL1S (Prusa Research) printer. Initially, the EnvisionTEC printer was used with 3DM tough resin. The specifications of the ENVISIONTEC printer are shown in Table C.1. This printer broke down throughout the project and was replaced by the PRUSA SL1S printer using Prusament Resin Tough Prusa Orange. The printers use similar print techniques but have some differences. The printers make an object on a layer-by-layer basis. The printers both use light to polymerise a thin layer of negative photoresist called resin. The printers polymerise a thin resin layer, which is moved upward, and a new photoresist layer is added below. This resist is then exposed, and the cycle continues.

Table C.1: The properties of the EnvisionTEC Micro Hi-res Plus

Envisiontec Specifications	
Build Envelope	45×28x100 mm
XY Resolution	30 µm
Dynamic Voxel Resolution in Z (Material dependent)	25 – 75 µm
Light Source	Industrial UV LED

The DLP printer is used to print the fluidic interfaces which can be mounted in the AFM, the fluidic interface has a connector for a 0.8mm tube with a channel attached. This tube can be used for regulating the pressure inside the cantilever. The cantilevers are later printed on top of the fluidic interfaces using the NANOSCRIBE.

The PRUSA printer has a lower resolution than the EnvisionTEC but is quicker and has a much larger build volume. The working principle is a bit different than the EnvisionTEC. The PRUSA SL1S printer uses a monochrome LCD screen to expose the resin. The rest of the specifications are in **??**. It then shakes to add a new resin layer below the build plate quickly. This greatly speeds up the printing process; with the PRUSA printer, the fluid interfaces can be printed in 25 minutes. Because of the larger build volume more fluid interface could be printed at a time, up to 16 holders with 3 fluid interfaces in a single batch. The printers have a similar but slightly different workflow described below.

Table C.2: The specifications of the Prusa Sl1S 3D printer [5]

Prusa SL1S	
Build Envelope	127×80×150 mm
LCD Resolution	5.96”, 2560×1620p
XY Resolution	50µm
Supported layer heights	0.025-0.1 mm

C.1.1. Process

EnvisionTEC process:

Slice with the software on the computer called…

1. Choose the right settings for the resin
2. 25µm is the highest precision for 3DM tough
3. Import .stl file
4. Align the design, make sure it is 2mm from the build plate and 1mm from the edge
5. Add supports
6. Copy the design and supports
7. Slice
8. Save the sliced pats on a USB stick

Fill the printer with the resin. Mostly 3DM Tough was used, I also experimented with HTM40 and e-glass. HTM40 did not work well in combination with the NANOSCRIBE and the e-glass couldn’t make the small channels needed.

Home the printer Load the USB stick with the print file

Load the print file

Start the print Print finished Remove the build plate and the resin bath from the printer Remove the print from the build plate. The easiest way to do this is to get a knife in between the first thin layer of material and cut the print loose from there.

PRUSA SL1S printer After the EnvisionTEC printer broke we used a Prusa SL1S printer. This printer prints PRUSAment Resin Tough Orange. The printing follows the same steps as the EnvisionTEC printer but is slightly different. Slicing The model is sliced in Prusa slicer 2.5.0(Prusa Research a.s). The standard settings for the SL1S SPEED are used. The SLA print setting is at 0.025 UltraDetail, the highest precision available. The .stl model is imported by clicking the add button. Align the model correctly, generally with the bottom down; for some prints, it can be advantageous to print at an angle to get better overhang quality or to align the print so that the surface with the highest needed quality is parallel with the build plate. Add supports, this is best done manually so there won’t be any supports which clog the channels or which make it impossible to remove the fluid interfaces. The supports are added roughly every 0,5mm, and the diameter of the support attachment is set to 0,4mm. After the

supports are added, more copies of the same model can be added with the add instance (+) button, up to 14 models can be printed at once. The arrange button can spread the models on the build plate. Sometimes the models must be moved slightly by hand to make them fit properly. Press the slice now button to slice the models, they can be saved on a USB stick. Starting the printer Insert the USB with the model in the machine and start the printer. Select the model and the machine will tell how much resin is needed. Before printing resin needs to be added. Remove the resin container from the printer and bring it to the dirty lab area. Add as much resin as is required, usually around 50If the resin is filled to the correct level the container can be installed in the printer. The print can be started.

Developing The resin print needs to be developed before it can be used, the development consists of the following parts:

1. Clean the print with IPA in an ultrasonic bath for 7 minutes to dissolve all the leftover resin from the print.
2. Remove the print from the cleaning bath.
3. Dry the print carefully with an airgun; try to clean all the channels by blowing air through them.
4. If there are still shiny areas on the print, the undeveloped resin is not completely washed away; repeat the cleaning step with the ultrasonic bath with a clean batch of IPA.
5. Cure the print in the UV Curing oven, turn on both the light and the oven on for 8 minutes for 3DM tough.

Cleaning the printer Clean the build plate with IPA

1. Remove the leftover Resin from the resin bath with a pipette and dispose of it in the recycle bottle
2. Clean the resin bath with a clean cloth, don't use any solvents because this can damage the print screen. Clean the corners thoroughly using a cardboard playing card to push the cloth in.
3. Place the build plate and the resin bath back into the printer enclosure.

C.2. Laserdrilling

The cantilever needs to be printed over a channel. Ideally, this channel should be as small as possible so the dome of the cantilever can be printed quickly, but so small that it will clog and give much resistance. A channel with a diameter of 30µm seems ideal. The smallest channel size that can be printed reliably with the resin printers has a diameter in the order of 100s of µm. This is too large. M. Blankespoor found in his research that it was possible to use an Optec laser cutter to drill the channels in the fluidic interface [6]. His recipe was used and improved upon for the initial channels. Later the Optec laser was replaced by the more precise and quicker LASEA laser cutter to drill the desired holes.

C.2.1. Optec

First, the Optec nanosecond laser cutter (OPTEC WS-STARTER, OPTEC SA) was used to drill channels; since the smallest channels didn't have the desired size and the process was slow, I switched to another laser cutter. Initially, I started with Blankespoor's recipe, which often resulted in cracked holes caused by overheating. Therefore I searched for new settings with better results, lower laser power, faster laser movement speeds and more repetitions gave better results. You'd ideally use low power, fast scan speeds and many repetitions for the cleanest cuts. If the number of repetitions were too high(over 500), the channel would become oval, probably caused by an accumulated alignment error. The final settings used can be found in table….. The Optec laser cutter can drill holes of 78µm in 3DM tough. For the Optec laser the workflow is as follows:

- First, the laser is started according to the manual, then it needs 25minutes to warm up properly. When it is ready it can be seen in the software.
- Now a drawing of a circle can be made in the Autocad software, a diameter of 10µm is used.
- Import the drawing in the main software

Table C.3: The used settings of the LASEA laser cutter in the KYLA software

LASEA Specifications	
Laser speed[µm/s]	800
Repetitions[#]	300
Power[%]	30
Pulse speed[Hz]	75018
Drawing shape	Circle
Diameter Drawing[µm]	1
Diameter Cut[µm]	38
Working mode	Picture mode

- Use the drill tool and set it to use the correct number of layers and other properties.
- Set the laser Amperage.
- Use tape to mount the sample on a silica plate.
- Set the silica plate in the laser cutter.
- Turn on the vacuum pump to fix the sample.
- Align the microscope with the sample
- Start the cut. this moves the sample stage from the microscope to the laser head where the actual cutting is done, this movement costs 30s. Then it cuts, which takes 4s. Then the stage moves back to the microscope
- The cut can be inspected with the microscope
- Repeat the alignment for the next hole.

(a)

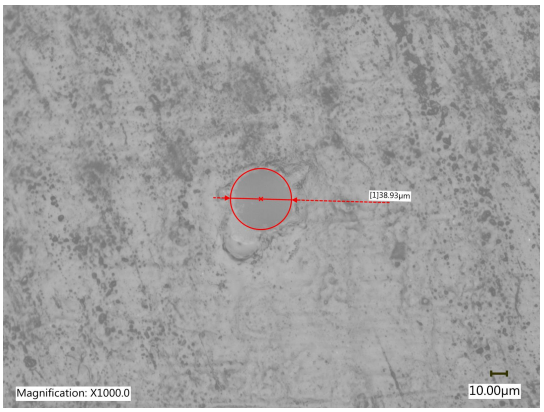

(b)

Figure C.1: Laser drilled holes. (a) A drilled hole by the optec laser cutter in 3DM tough clear material, it has a diameter of 78um (b) A typical drilled hole of the LASEA lasercutter in Prusament tough orange resin with a diameter of 38um

C.2.2. LASEA

The LASEA laser cutter (LASEA LS-Lab plus, LASEA SA) is a femtosecond lasercutter specialized for micromachining. The LASEA was used for drilling the connecting channel between the fluidic interface and the cantilever, into the fluidic interface. The LASEA laser is more practical for drilling the channels than the Optec laser for a few reasons. One it is faster because the stage doesn't move from the microscope to the laser lens. Two, it has a longer voxel so the laser doesn't need levels in the z-direction. The settings used by the LASEA lasercutter in the KYLA software, Table C.3.

C.3. Gold Coating

The cantilever needs to be reflective for the AFM to measure its position. A layer of gold is used to make it reflective. For this, the same sputter coater is used as for preparing the fluid interface, the JEOL. The cantilever with its fluid interface must be removed from the holder and put upside down on the holder plate. The holder plate is a small plate with a few spots where the fluid interfaces can lay upside down without damaging the cantilever; these spots need a piece of tape to keep the cantilevers still, this is shown in Figure C.2. The plate is put in the sputter coater at 25mm from the top with the gold filament. The settings used are 50mA for 60 seconds, resulting in a gold coat of roughly 80 nm. The layer height is verified with an experiment with the AFM where a microscopic glass slide is gold coated and imaged, the result is shown in Figure C.3.

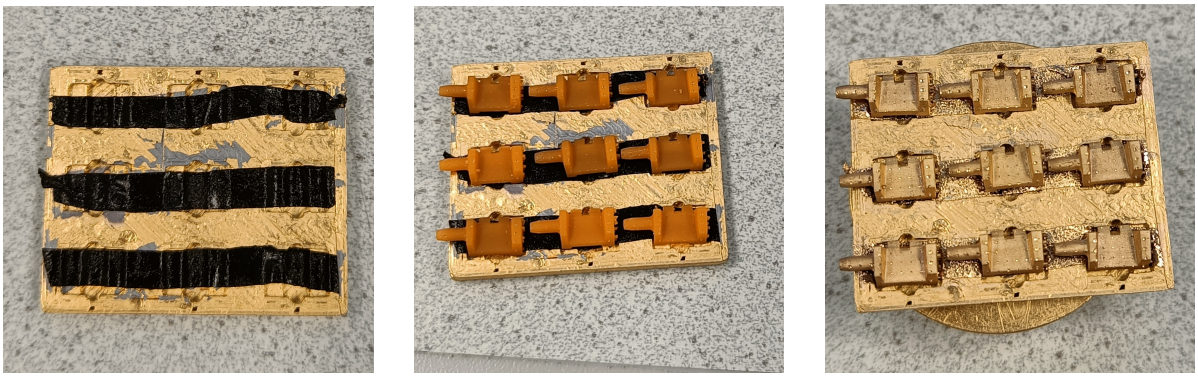

Figure C.2: Gold coating process. First an empty holder with small pieces of tape. Second, the cantilevers are placed on the holder with the mirror side up. Third the cantilevers are gold coated

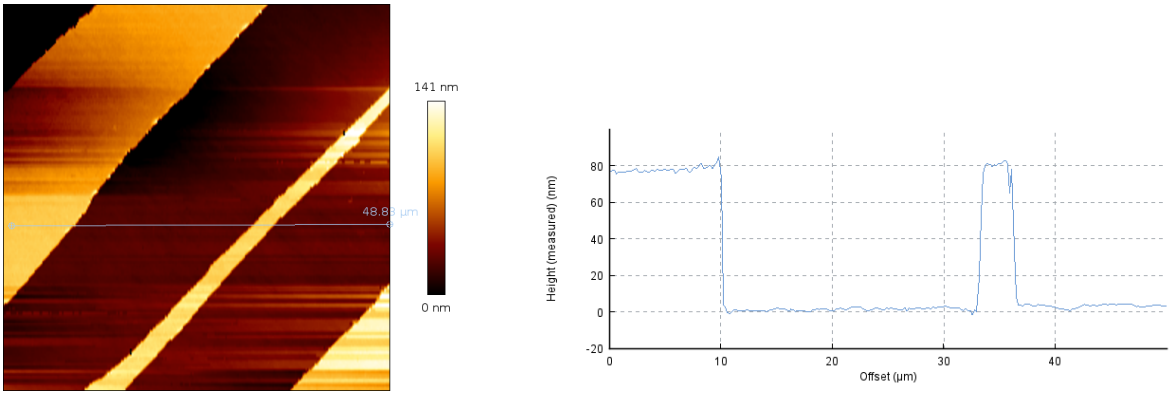

Figure C.3: AFM image of a microscope glass coated with gold, this is done with the JEOL sputter coater using the recipe used to coat the cantilever. The gold is partially removed with a razor blade. The top image shows the image, the second shows the histogram of the line. It shows that the gold layer is 80µm.

C.4. NANOSCRIBE

The cantilevers are printed with the NANOSCRIBE. The NANOSCRIBE(NANOSCRIBE Photonic Professional GT+, NANOSCRIBE GmbH & Co. KG)) is a state of the art 3d printer which uses the 3d print technique called two photon polymerisation(2PP), sometimes called direct laser writing. This technique uses a focused laser beam to polymerise a negative photoresist (resin). The photoresist is made only to polymerise if the light intensity is very high. This intensity is only reached in the most focused part of the laser, the voxel. This voxel can move in relation to the substrate and write lines of polymerised resin like that.

The size of the voxel is determined by the objective used, the higher the magnification of the objective the smaller the voxel size. For this project the highest resolution was desired so the largest available objective was used, the 63x objective. With this objective, a voxel size of roughly 300nm is

produced.

The resin used for the cantilever is IP-Dip(NANOSCRIBE GmbH & Co. KG). IP-Dip is a biocompatible, non-cytotoxic photoresist which can be used for submicrometer feature sizes [7]. The physical properties of the polymerised IP-Dip depend on the level of polymerisation.

C.4.1. Slicing

Before printing a CAD model needs to be translated into something a 3D printer can understand. This process is called slicing. For the NANOSCRIBE a proprietary slicer is used called DeScribe(V2.7, NANOSCRIBE)

For slicing with the Describe software, many terms are used. Below is a list of the most important terms and an explanation of their function.

Slicing The distance between printed lines

Hatching distance The distance between layers

hatching angle What angle following layers are in relation to eachother

contour Is a contour made, how many lines thick

Scanmode How the voxel is moved in the XY plane

- Piezo ==> The subtrate is moved by the piezo, slow but more complex movements of the voxel in the XYZ plane aere possible. It has a range of 300x300µm
- Galvo==> the voxel of the laser is moved in the xy plane by moving galvanic mirrors, quick and precise, only movement in XY plane are possible. For the 63x objective the voxel can be positioned precisely in a circle with a 150µm radius.

z-axis Which movement method is used for the z-direction, piezo or microscope z-drive.

- Piezo, piezos move the substrate in the z-direction. It has a range of 300µm.
- Microscope z-drive, the motors of the microscope are used to move the microcope in the z-direction, the full microscope range is roughly 11mm depending on the substrate position.

Hatch lines Are the hatch lines moved in alternating directions or the parallel direction, the parallel is more precise, and the alternating is quicker.

Exposure Variable/constant?

Z-direction is the print printed towards the microscope(Upwards +Z, most commonly used) or away from the microscope(downwards -Z, only relevant for printing in oil)

Write contour When is the contour written, First or last

Interface finder Is the interface finder software used in this print

Splitting mode Does the model need to be split into multiple smaller parts or not? This is necessary if the model is larger than the print range. The model can be split into rectangular blocks or Hexagonal blocks. The size and offset of the blocks can be given. The block width should be smaller than the maximum print area, this is dependent on the objective and the movement type used. The block size and position can be seen in the preview window, the preview is not always accurate so the block splitting should always be checked after slicing.

Block shear angle The angle of the side of each split block, the blocks are cut at an angle to get more contact area and better support.

Block overlap The overlap between neighbouring blocks, this is needed for the adhesion of the blocks.

Block order In which order are the blocks printed, multiple options available.

Avoid flying blocks Toggle switch, makes the software take into account flying, unsupported blocks. It is a bit hit or miss, if there is a mistake after slicing, this is one of the first things to change.

Group neighbouring blocks Toggle switch, this helps speed up the printing and overrides the block order.

After slicing all of these properties are saved in the .recipe file
General slicing process:

- A .stl file is loaded in the slicer.
- Load the parameters, parameters are saved in .recipe files, the recipe holds all the information about the properties described above.
- Make sure the model is aligned properly.
- Check the base name of the files.
- Check if all the settings are correct.
- Align the blocks in the block splitting if needed.
- Save the model

A few files are created, two .gwl files basename_job.gwl file and basename_data.gwl file and a few other files. The .gwl files are written in a proprietary programming language called NANOSCRIBE General Writing Language(GWL), which can be edited manually. The job file holds the final print settings with the laser power and such; this is the file that is loaded into the printer. The _data file holds information about the alignment of the blocks and the interface finder. There are a few more files that hold the precise print parameters only understood by the printer. The final settings used in the slicer are shown in Table C.4.
The most important terms in the GWL which are used in this project are:

InvertZAxis Determines the printing direction and therefore how the XYZ axis are aligned.

GalvoScanMode Determines that the galvanic mirrors are used for the XY movement of the laser.

PiezeScanMode Determines that the piezos are used for the XY movement of the laser.

ContinuousMode Determines that the laser is used continuously and not in pulses.

PiezoSettlingTime How long the piezo rests after each movement, this is needed to increase precision and compensate for hysteresis.

GalvoAcceleration How quickly the galvanic mirrors accelerate, this is a good parameter to play with in order to speed up print speeds.

StageVelocity How fast does the stage move when the laser is not used

XOffset Standard offset in the X direction.

YOffset Standard offset in the Y direction.

ZOffset Standard offset in the Z direction.

PowerScaling Is a multiplier for the overall laser power, generally set to 1.0.

MoveStageX Makes the stage move a distance in µm in the X direction.

MoveStageY Makes the stage move a distance in µm in the Y direction.

var Used to declare a variable.

$contourLaserPower The laser power used for drawing the contours, if they are used, given in a percentage.

$contourScanSpeed The scan speed, the movement speed of the laser while drawing the contours.

$solidLaserPower The laser power used for the solids, given in a percentage, basically everything that isn't the contour or the base.

$solidScanSpeed The movement speed of the laser in the solids µm/s?.

$interfaceLocation A variable which determines how far from the alignment position the surface height must be found, the print is usually aligned over the laser-drilled channel, finding the surface there is challenging therefore, a different spot is used.

$interfacePos The start position of the the print in relation to the surface given in µm. To get good adhesion between the print and the substrate the print is started below the surface, generaly 0.5µm for smooth surface, 8-15µm for rough surfaces like 3d prints.

For the slicing for the cantilever, these steps need to be taken:

- The three parts, the dome, the neck and the tip, need to be sliced with their respective recipe as in section...
- Remove the initial positions, the MoveStageX and MoveStageY lines, from the _data files
- Add /interfacepos to the dome_data as seen in
- Combine the properties of the three job files in a single file as seen in
- Make sure they are printed in the correct order.
- Align the three models in the software by changing the AddZDrivePosition MoveStageX and MoveStageY parameters and checking the results in the 3D preview window. (Alignment can be made easier by using the ctrl 1 to 5 keyboard shortcuts)
- Check that all galvoaccelerations and laser powers are correct.

NANOSCRIBE print code A custom job file is created to combine the three separately sliced parts. The MoveStage values need to be changed if the model is changed.

```
% File generated by DeScribe 2.7

% System initialization
InvertZAxis 1

% Writing configuration
GalvoScanMode
ContinuousMode
PiezoSettlingTime 10
GalvoAcceleration 1
StageVelocity 200

% Scan field offsets
XOffset 0
YOffset 0
ZOffset 0

% Writing parameters
PowerScaling 1.0

% dome:
GalvoAcceleration 6

% Compensating for microscope offset
```

Table C.4: The NANOSCRIBE print settings, for the different parts of the cantilever

	Dome	Neck	Tip
Laser Power[%]	75	45	50
Scanspeed[µm/s]	90000	40000	50000
Galvo acceleration [V/ms2]	6	6	1
ContourLaserPower[%]	80		
ContourScanspeed[µm/s]	900000		
Slicing mode	Fixed	Fixed	Adaptive
Slicing distance[µm]	0.35	0.2	0.3
Minimum slicing distance[µm]			0.05
Hatching distance[µm]	0.25	0.2	0.15
Contour count	3	0	0
Contour distance[µm]	0.15		
Hatching angle[degree]	Auto	90*	Auto
Scan mode	Galvo	Galvo	Galvo
Z-Axis	Piezo	Piezo	Microscope Z-drive
Hatch lines	paralel	paralel	paralel
Exposure	Variable	Variable	Variable
Configuration	DiLL	DiLL	DiLL
Z-direction	Z	Z	Z
Write contour	First	First	First
Interface finder	Execute	Skip	Skip
Splitting mode	None	Rectangular	None
Block size X[µm]		300	
Block size Y[µm]		4	
Block size Z[µm]		87	
Block offset X[µm]		-80	
Block offset Y[µm]		-6	
Block offset Z[µm]		0	
Block shear angle[degree]		45	
Block overlap[µm]		2	

*The cantilever is aligned with the Y-axis

```
MoveStageX 15
MoveStageY -15

% Contour writing parameters
var $contourLaserPower = 80
var $contourScanSpeed = 90000

% Solid hatch lines writing parameters
var $solidLaserPower = 75
var $solidScanSpeed = 90000

%the distance from the dome where the interface is found
var $interfaceLocation = 120
var $interfacePos = 8


% Include slicer output
include dome_data.gwl
```

```
% Neck:
GalvoAcceleration 6


AddZDrivePosition 20.6
MoveStageX 39.75
MoveStageY 32


var $solidLaserPower = 50
var $solidScanSpeed = 40000

include neck_data.gwl

% tip:
MoveStageX -39.75
MoveStageY -7.2
AddZDrivePosition 82.5
%532.999
GalvoAcceleration 1
% Solid hatch lines writing parameters
var $solidLaserPower = 50
var $solidScanSpeed = 50000
include tip_data.gwl
```

C.4.2. Print process

Install the x63 lens, mount the felt protection ring and clean the lens with some air. Mount the samples in the 9x 25x25 holder,fixate the samples with a piece of tape, shown in Figure C.4a. Make sure to align the samples consistently with respect to the edges to make alignment easier, I used the bottom left corner. Put a droplet of IP-dip photoresist on the print spots. Quickly mount the holder in the NANOSCRIBE before the resin can flow away from the print positions.

Start the nanowrite software on the PC, turn on the lights and start the internal camera. To get the best image quality it is recommended to set the Exposure Time to 50ms, the gain to 5 and auto contrast on. Move the sample to a rough sample position using a prepared script: StageGoToX -6826 StageGoToY 6200 AddZDrivePosition -9000 .This also moves the microscope closer to the surface. The NANOSCRIBE often has trouble finding 3D-printed surfaces, so it helps to do the approach manually. On the camera view, you should see the surface, if you can't see the surface, manually focus on the surface, it generally is at 11.2mm. Then turn on the alignment lines in the nanowrite software. Move the stage until the centre of the alignment marks is slightly down to the left of the centre of the laser-drilled hole. Sometimes finding the right spot might take some time. Manually focus the camera on the surface and write down the coordinates. Next, load the print file and start the print. If the surface is found automatically check that the z value is where it should be, sometimes surface defects make it hard to find the right surface. If the surface is not found, the print will start at the last z-value where the NANOSCRIBE tried to find the surface. Often this will be the position the objective was focussed on before the print started.

If it is incorrect abort the print

C.4.3. Development

The NANOSCRIBE print needs to be developed before it can be used. This process removes all the excess and unpolymerised resin from the print. The development consists of a few steps. First, the sample is put in PGMEA for at least 25 minutes to remove most of the resin then it is cleaned in a bath of IPA for five minutes to remove the PGMEA and lastly the print is put in a bath of Novec 7100™ for 3 minutes to clear out the small channels. For the best results during development, a syringe should be used to push the development fluids through the channels of the cantilever, this should be done at every step. Between each development step, it is advised to blow dry the prints very carefully. To securely put 2 holders in a small beaker during development I designed and 3d printed a " basket" to

hold them,

C.4.4. Closing the exit hole

Closing the hole The fluid interface has an exit hole which helps with the development of the cantilever, this hole needs to be plugged to use the cantilevers. Use a syringe with a small needle to add a tiny droplet of resin to the exit hole, just enough to cover it. As is semonstrated in Figure C.4b A 32 gauge tip is used. The same resin is used as for the resin used in the fluid interface to ensure good adhesion, the Prusament Tough Orange resin. To prevent the resin from clogging the whole channel, the other end of the fluidic interface is plugged with a closed-off tube. After adding the resin, it is cured in the curing station for four minutes.

(a) Fluid interfaces mounted in the Nanoscribe sample holder, ready for printing.

(b) FLuid interfaces plugged and the exit holes filled with a droplet of resin, the resin is applied with the syringe.

D

Measurements

D.1. Adhesion measurements

More adhesion measurements have been done on PCA-3 cells, but the resulting force curves were not always useable, and example of a strange force distance curve is seen in Figure D.1a. Also adhesion tests are done on hydrogel spheroids and solid ip dip spheres. In these measurements the cantilever detached from the sample before the sample detached from the substrate, the correspongin force distance curves are seen in Figure D.1b for the hydrogel and Figure D.1c for the IP-DIP sample. A clear peak is seen where the cantilever detached, why this peak is so large is unclear.

D.2. Comsol model

A finite element model of the cantilever is made to model its properties. Figures of the model are found in Figure D.2. There is a figure of the cantilever bending under a load the deflection is monitored, from which the stiffness is calculated using the Hertz model. The second figure shows the modelling of the eigenfrequency. The cantilever properties found in the COMSOL and beam theory model are shown in Table **??**.

	Beam Theory	**COMSOL**
Stiffness [N/m]	0,61	0,64
Natural frequency [Hz]	27100	21500

D.3. Microrheology

The multifunctional cantilever is also tested with microrheology, the results are shown in Figure D.3. Microrheology is a nanoindentation method where the tip vibrates for some time while indented. This gives much information about the viscoelastic properties of the material, shown in Figure D.1. The technique is tested on an endothelial cell. Microrheology with the multifunctional cantilever is possible, but more measurements are needed to verify the accuracy.

D.4. Material tests

D.4.1. Cytotoxicity prusa resin

The cytotoxicity of the Prusatough resin is tested by adding the cured material to live HeLa cells for 12 hours at 37 degrees celsius and checking their survival. No changes in the cell culture were observed so the material was deemed safe to use with cells.

D.4.2. Print settings

To find the optimal print settings of the NANOSCRIBE dose tests have been done where many different parameters are tested. An example of such a test is shown in Figure D.4a. In this image a grid is made

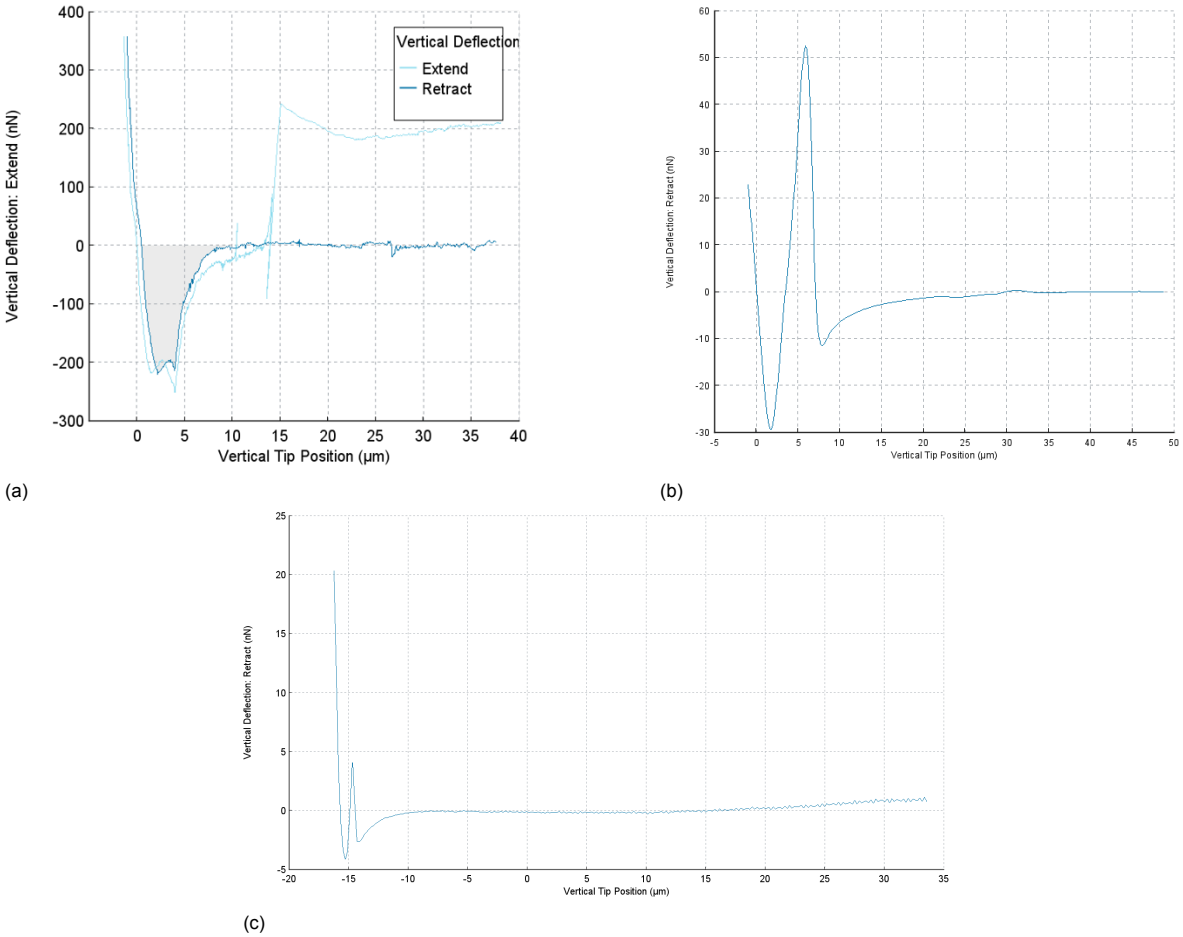

Figure D.1: Adhesion force-distance curves. (a) Successful removal of PCA cell from the substrate, a large jump is seen from the pump that was turned on during extension. (b) Unsuccessful, removal of hydrogel spheroid. (c) Unsuccessful removal of IP-DIP sample.

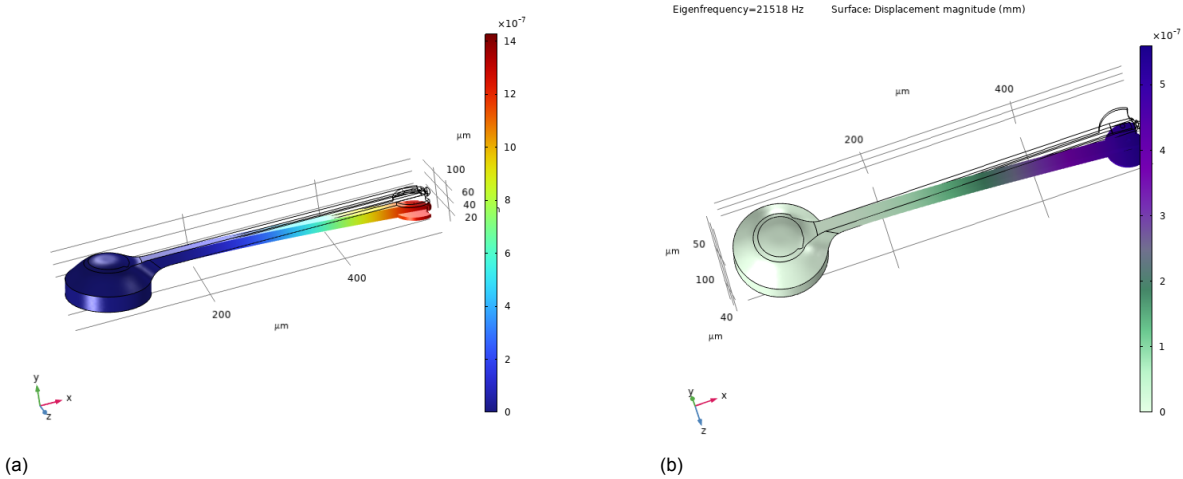

Figure D.2: Figures (a) and (b) show the modelled cantilever in COMSOL Multiphysics. Figure(a) shows the deflection in the FEM model used to find the cantilever stiffness. Figure(b) shows the natural vibrations modelled in FEM, the first eigenmode in vacuum at 25kHz.

where the scan speed(x axis) and laser power are varied(y axis). The green squares are exposed properly, the blue ones are underexposed and did not print adn the red ones are overexposed and

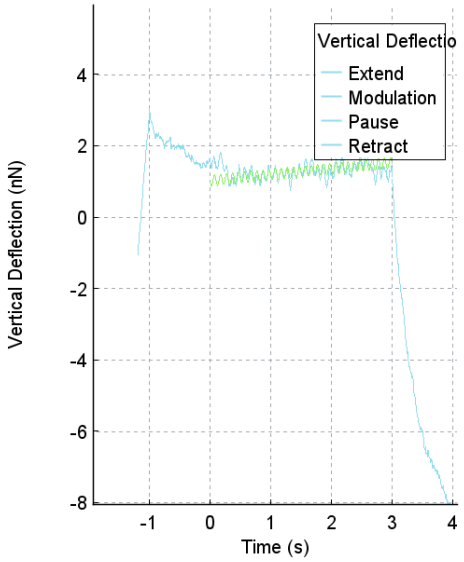

Figure D.3: Microrheology force-time curve, done on endothelial cells

Microrheology		
Property	**Value**	**Unit**
Frequency	10	Hz
Force Amplitude	154	pN
Force Phase	13,35	deg
Indentation amplitude	9,731	nm
Indentation Phase	-1,237	deg
Phase offset	0	deg
Phase Delta	14,59	deg
Young's Modulus	14,64	kPa
Storage Modulus E'	14,17	kPa
Loss Modulus E'	3,687	kPa
Shear Storage	4,722	kPa
Shear Loss G"	1,229	kPa
Loss Tangent	0,2602	
Drag Correction	0	Pa

Table D.1: Microrheology results on endothelial cells

bubbles formed during printing.

To find the smallest possible channel and wall size of the cantilever a cantilever with an incrementally smaller channel is printed and the clogging positions are observed, as seen in Figure D.4b.

The effect of the printing angle of the cantilever on surface quality is tested with test samples like the one in Figure D.4c. This is done with the goal to remove the ridges seen in Figure D.4d.

D.4.3. IP-Dip properties

To verify the assumed material properties of the IP-Dip in the cantilever the found cantilever stiffness with the AFM can be used in combination Equation D.1, which is a rewritten Equation 4.4, to calculate the Young's modulus.

$$Estimation\ of\ the\ Young's\ modulus\ of\ IP-Dip$$
$$E_{found} = \frac{k_{found} L^3}{3 I_z} \tag{D.1}$$

Where E_{found} is the Young's modulus of the IP-Dip, $k_{measured}$ is the found stiffness of the cantilever, L is the length and I_z is the second moment of area of the cantilever respectively.

The found stiffness values of the cantilever, **??**,are used to further define the Young's modulus of the IP-DIP using Equation D.1, to verify the accuracy of Equation D.1 it has been tested with cantilevers of multiple lengths, a linear relation between cantilever length and stiffness is found which verifies the usability of the equation. For the final printing recipe, a Young's modulus of 3,1GPa is found.

D.5. Photonic crystals

Photonic crystals are structures made of materials with different reflective indexes which are ordered. These materials can have amazing optical properties, such as high reflectance mirrors and colour-changing materials like butterfly wings and car paints.

For this project, I looked into photonic crystal reflectors to see if they would be viable to use as a reflector in a 3D-printed AFM cantilever. Photonic crystals have been fabricated using 2PP [8][9] [10]. Photonic crystals can be categorised into 3 types, one, two and three-dimensional, depending on how the materials are positioned.

A one-dimensional photonic crystal is an alternating stack of multiple materials, by tuning the thickness of the materials to a specific wavelength high reflection or high absorption can be achieved. A

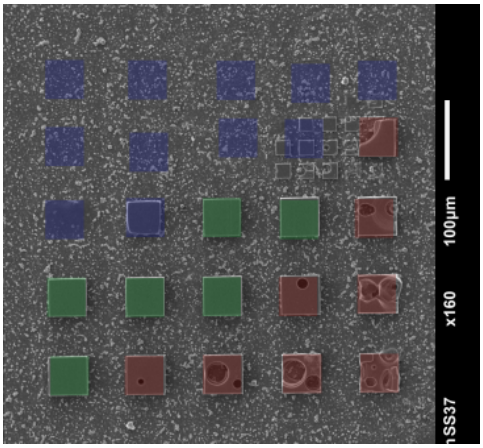

(a)

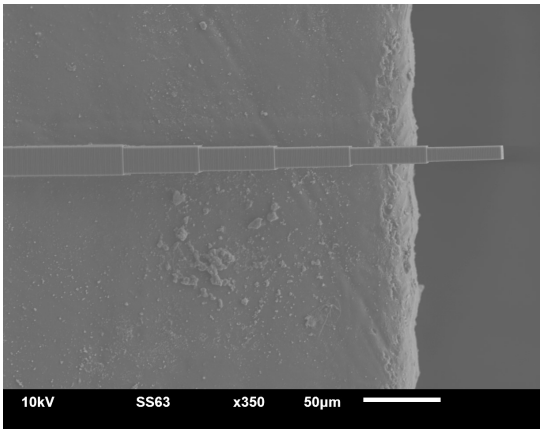

(b)

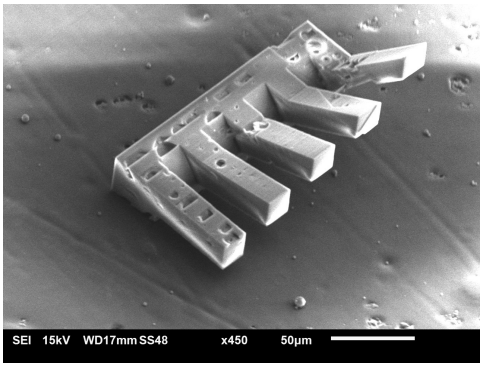

(c)

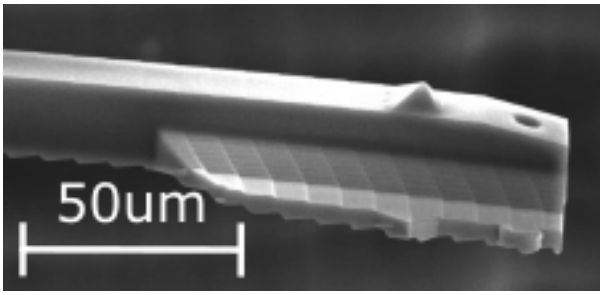

(d)

Figure D.4: Material tests for IP Dip printing

mirror of alternating layers of material is called a Bragg reflector [11][12]. These reflectors have been fabricated with 2PP [13], but the current design is too bulky for an AFM cantilever (50x50x50µm).

Two-dimensional photonic crystals have their material laid out in a 2d plane, like a checkerboard pattern. Ultra-thin 2d mirrors exist but have never been fabricated using 3d-printing techniques [14]. These mirrors could be used in AFM cantilevers.

Three-dimensional photonic crystals are structures such as ”wood stacks” that can have interesting properties but are not generally used as reflectors. Also, they are by definition large in three dimensions, making them less useful for AFM cantilevers which are generally very thin.

Printed photonic crystals use a combination of print material and air for the photonic effects. AFM cantilevers for biological applications work submerged in water or cell medium. Research needs to be done on the effects of the water on the cavities in the photonic crystal, will they be filled or stay open? This is important for the functionality of the crystal.

Photonic crystals have potential as a 3d printed AFM mirror, but much research needs to be done. Two-dimensional mirrors have the most potential.

Bibliography

[1] John E. Sader, James W. M. Chon, and Paul Mulvaney. “Calibration of rectangular atomic force microscope cantilevers”. In: *Review of Scientific Instruments* 70.10 (Oct. 1999), pp. 3967–3969.

[2] John Elie Sader. “Frequency response of cantilever beams immersed in viscous fluids with applications to the atomic force microscope”. In: *Journal of Applied Physics* 84.1 (July 1998), pp. 64–76.

[3] Jeffrey L. Hutter and John Bechhoefer. “Calibration of atomic-force microscope tips”. In: *Review of Scientific Instruments* 64 (July 1993). ADS Bibcode: 1993RScI...64.1868H, pp. 1868–1873.

[4] JPK Instruments AG. *Nanowizard AFM Handbook Version 6.0*. JPK, 2018.

[5] *Original Prusa SL1S SPEED 3D printer | Original Prusa 3D printers directly from Josef Prusa*. en.

[6] M.B. Blankespoor. “Liquid dosing on the micro-scale”. MA thesis. Delft University of Technology, 2022.

[7] *Nanoscribe photoresins specifically designed for Two-Photon Polymerization*. en-GB.

[8] Mikhail V. Rybin et al. “Band Structure of Photonic Crystals Fabricated by Two-Photon Polymerization”. en. In: *Crystals* 5.1 (Mar. 2015), pp. 61–73.

[9] David Lowell et al. “Flexible Holographic Fabrication of 3D Photonic Crystal Templates with Polarization Control through a 3D Printed Reflective Optical Element”. en. In: *Micromachines* 7.7 (July 2016), p. 128.

[10] R Houbertz et al. “Investigations on the generation of photonic crystals using two-photon polymerization (2PP) of inorganic–organic hybrid polymers with ultra-short laser pulses”. In: *physica status solidi (a)* 204.11 (2007), pp. 3662–3675.

[11] Dr Rüdiger Paschotta. *Bragg Mirrors*. en.

[12] P. V. Braun, S. A. Rinne, and F. García-Santamaría. “Introducing Defects in 3D Photonic Crystals: State of the Art”. en. In: *Advanced Materials* 18.20 (2006), pp. 2665–2678.

[13] Y. Li et al. “High-contrast infrared polymer photonic crystals fabricated by direct laser writing”. EN. In: *Optics Letters* 43.19 (Oct. 2018), pp. 4711–4714.

[14] João P Moura et al. “Centimeter-scale suspended photonic crystal mirrors”. In: *Optics express* 26.2 (2018), pp. 1895–1909.